BNWL-654

DECLASSIFIED by CG-NMP-2, 9/00 and
Approved for Public Release
Name/Date BU22 Hammon 5/13/03
Name/Date W.F. Nicaise, 5-14-03
ORG: PNNL NSAT
JE Sawyer 5-20-03 JA Thurow 6/3/03

[redacted]

BNWL-654

UC-80, Reactor
Technology
Special Distribution

UNCLASSIFIED

PLUTONIUM UTILIZATION PROGRAM
TECHNICAL ACTIVITIES QUARTERLY REPORT

September, October, November, 1967

By

Staff of Battelle-Northwest
Program Leader: F. G. Dawson

BEST AVAILABLE
REPRODUCED COPY

February 1968

LEGAL NOTICE

This report was prepared as an account of Government sponsored work. Neither the United States, nor the Commission, nor any person acting on behalf of the Commission:

A. Makes any warranty or representation, expressed or implied, with respect to the accuracy, completeness, or usefulness of the information contained in this report, or that the use of any information, apparatus, method, or process disclosed in this report may not infringe privately owned rights; or

B. Assumes any liabilities with respect to the use of, or for damages resulting from the use of any information, apparatus, method, or process disclosed in this report.

As used in the above, "person acting on behalf of the Commission" includes any employee or contractor of the Commission, or employee of such contractor, to the extent that such employee or contractor of the Commission, or employee of such contractor prepares, disseminates, or provides access to, any information pursuant to his employment or contract with the Commission, or his employment with such contractor.

PACIFIC NORTHWEST LABORATORY
RICHLAND, WASHINGTON

[redacted]

UNCLASSIFIED

DISTRIBUTION OF THIS DOCUMENT IS UNLIMITED
To Government Agencies and Contractors

Printed in the United States of America
Available from
Clearinghouse for Federal Scientific and Technical Information
National Bureau of Standards, U.S. Department of Commerce
Springfield, Virginia 22151
Price: Printed Copy 3.00, Microfiche $0.65

PLUTONIUM UTILIZATION PROGRAM
TECHNICAL ACTIVITIES QUARTERLY REPORT
SEPTEMBER, OCTOBER, NOVEMBER, 1967

FOREWORD

This report is the first in a series of Plutonium Utilization Program Technical Activities Quarterly Reports.

The Plutonium Utilization Program is conducted by the Pacific Northwest Laboratory for the USAEC. The objective of the Technical Activities Quarterly Report is to inform the scientific community in a timely manner of the technical progress made on the program. The report contains brief technical discussions of accomplishments in all areas where significant progress has been made during the quarter. The results presented should be considered preliminary, and do not constitute final publication of the work. A list of publications and papers is given in the report. Anyone wishing to obtain additional information on the work presented is encouraged to contact the author directly.

TABLE OF CONTENTS

LIST OF FIGURES

LIST OF TABLES

PLUTONIUM UTILIZATION PROGRAM
TECHNICAL ACTIVITIES QUARTERLY REPORT
SEPTEMBER, OCTOBER, NOVEMBER, 1967

1.0 SUMMARY

FUELS DEVELOPMENT

Vibrationally compacted UO_2–2 wt% PuO_2 HPD elements are performing satisfactorily in the Plutonium Recycle Test Reactor (PRTR). The present average element burnup is 3100 MWd/tonne with peak rod powers of approximately 20 kW/ft. Under PRTR operating conditions, onset of melting in these HPD fuel rods has been determined to occur at a linear heat rating of 20.5 ± 0.5 kW/ft. Two commercially designed and fabricated 19-rod cluster elements containing hot-pressed UO_2–1.94 wt% PuO_2 pellets are being irradiated in PRTR. The first of three commercially fabricated fuel rods, which contain cold pressed and sintered UO_2-PuO_2 pellets, is operating at a rod power of about 19 kW/ft.

Pressure buildup and gas plenum temperatures in vibrationally compacted mixed oxide fuel rods are being measured as part of the Batch Core Experiment in the PRTR. Preliminary results for the exposures experienced to date indicate that 13% of the gases formed are released in rods operating at 9.5 kW/ft (volumetric averaged fuel temperature of 700 °C) and 25% of the gases formed are being released in rods operating at 16.5 kW/ft (volumetric averaged fuel temperature of 1250 °C).

An intentionally defected, vibrationally compacted, UO_2 element was successfully irradiated in the ETR P-7 loop under molten core conditions. Activity release to the coolant caused no operational problems during irradiation. Postirradiation examination is being conducted.

Irradiation proof tests on EBWR rods and capsules were completed and the data from the highest burnup capsules and production-run rods are being analyzed. Isotopic data indicate that burnups as high as 30,000 MWd/tonne were successfully attained.

High speed motion pictures of three vibrationally compacted UO_2 fuel rods undergoing transient irradiations were obtained. One rod developed an as yet unexplained high temperature band about 1/8 in. long near the bottom of the fuel column during the transient irradiations.

Fission product migration characteristics in vibrationally compacted UO_2-PuO_2 fuel rods are being studied. Some fission products such as ^{137}Cs migrate considerably from their point of formation. The fission product distribution is affected by the shape of the temperature profile within the fuel.

A seven-rod cluster containing low density fuel (71% TD cold pressed unsintered pellets) was successfully

irradiated in the ETR to 600 MWd/tonne at a linear heat rating of 16 kW/ft. A second experiment is now underway in which a similar element will be irradiated to ∿10,000 MWd/tonne.

Neutron dose rates of 0.2 mrad/hr at 1 ft and gamma dose rates of 110 mrad/hr at 1 ft were measured for stacks of Al–20 wt% Pu plates fabricated from high exposure plutonium. The gamma dose rate is due mainly to low energy gamma rays which are relatively easy to shield.

Dissolution processes are being developed to provide techniques for chemically decontaminating reactors that use ceramic fuel materials. Work during the past quarter has been centered on preparing equipment to study the effects of reactor exposure and operation on ceramic fuel dissolution behavior.

REACTOR PHYSICS

The first series of interim critical tests have been performed in the PRTR with the Batch Core loading of 2 wt% UO_2–PuO_2 elements.

The physics characteristics of reduced density plutonium fuel loadings in the PRTR have been investigated.

Analytical correlations of measured temperature coefficients in UO_2-PuO_2-H_2O lattices have been made.

A set of 17 rods from the Experimental Boiling Water Reactor (EBWR) at the Argonne National Laboratory have been gamma scanned at the Pacific Northwest Laboratory Gamma Scan Facility.

The first series of reactor application experiments have begun in the Plutonium Recycle Critical Facility in a joint program between the USAEC and Comitato Nazionale Per L'Energia Nucleare, Rome, Italy.

Measurements have been made in the PCTR utilizing 0.9 wt% PuO_2 rods in a 1.0 in. square lattice moderated by light water. Foil activation measurements were obtained to be utilized in the determination of the infinite medium neutron multiplication factor by both the null reactivity technique and the adjoint weighted excess neutron production cross section measurements. Null reactivity measurements were made with boric acid mixed with water as the neutron absorber.

Light water moderated experiments with 2 wt% PuO_2–UO_2 fuel rods and various PuO_2 particle sizes have been started for comparison with previous measurements in graphite moderator.

Based on the Placzek Moment Theorems, an improved short time approximation for evaluating the Egelstaff-Schofield Scattering Law was devised.

PLUTONIUM UTILIZATION STUDIES

Studies are in progress to determine if plutonium enrichment can be used to improve performance of thermal, light water reactors. The incentive of shaping the axial power distribution in the core by grading the enrichment is being evaluated.

Economic incentives of utilizing low density, cold-pressed PuO_2-UO_2 fuel pellets are being evaluated.

It appears that this type of fuel can be fabricated at a considerable reduction in cost.

PRTR OPERATION

The PRTR has operated with two coolants: previously with pH-10 LiOH (D_2O) and currently at neutral pH. Tests are in progress to evaluate and compare the corrosion rates of zirconium alloys in the two environments.

Systematic shutdown radiation measurements are made on the PRTR to determine radioactivity buildup rates. Recent emphasis has been placed on comparing buildup rates in the PRTR primary system operating with a neutral pH coolant to those encountered during earlier reactor operating periods with pH-10 coolant.

Analyses and experiments were performed to determine the adequacy of the normal air cooling system used with FERTF during fuel charge–discharge operations. Alternate cooling methods were also investigated. Also studies were performed to reevaluate the adequacy of the emergency cooling system for FERTF.

PRTR pressure tube evaluation continues as neutron exposure increases with reactor operation. Recently, studies have been concerned with the effect of hydrides on pressure tube fracture.

The PRTR operated to 55 MW to produce 2163 MWd during September, October, and November, 1967. Reactor power continues to be limited by the 5% rod power difference reported in July.

The PRTR has accumulated 5226 MWd since beginning the batch core experiment, with the central 55 fuel elements (batch core) accumulating 4278 MWd. Interim critical tests for the first burnup step of the batch core were conducted when the reactor achieved 3369 MWd. The results showed that the reactivity of the core had decreased from an initial excess reactivity of 262 to 228 mk. The batch core life was extrapolated to 22,300 MWd.

The Fuel Element Rupture Test Facility in-reactor loop was removed from service in September so the interim critical tests could be conducted and returned to service in November. A commercially fabricated, 19-rod, 2 wt% PuO_2–UO_2 fuel element was irradiated in the in-reactor loop position. FERTF operation produced higher than usual oxygen concentration in the coolant, and several periods of single-pass operation were required to satisfy oxygen control requirements.

The corrosion and process tube surveillance program continued to indicate that there is no significant corrosion, crud deposition, or fretting corrosion problems occurring in PRTR systems. However, the leaks found in the primary treatment heat exchanger (HX-5) may indicate a condition that will limit the life of the heat exchanger.

Radiation measurements of the PRTR piping systems continue to be favorable. Slight increases in moderator piping radioactivity was traced to ^{60}Co.

2.0 FUELS DEVELOPMENT

HIGH POWER DENSITY FUEL IRRADIATIONS IN THE PRTR

M. D. Freshley and T. B. Burley

The Batch Core Experiment in the PRTR is providing statistically significant irradiation behavior data on UO_2-PuO_2 fuel elements operated at power generations greater than those currently employed in commercial power reactors. These High Power Density (HPD) fuel elements are generating as much as 20 kW/ft with maximum fuel temperatures near melting. Goal element average burnups are greater than 13,000 MWd/tonne, and peak burnups near 20,000 MWd/tonne are expected. The status of the present core loading is summarized in Table 2.I. Two vibrationally compacted UO_2-PuO_2 elements containing four rods instrumented to measure plenum gas temperature and pressure are included in the Batch Core loading. A similarly instrumented vibrationally compacted ThO_2-PuO_2 element will be charged into the reactor in the near future.

Vibrationally compacted UO_2–2 wt% PuO_2 HPD elements in the Batch Core have reached average burnups as high as 3100 MWd/tonne. Nondestructive and destructive examinations of selected fuel rods indicate that performance is satisfactory. No fuel element failures have occurred thus far in the program. A transverse cross-section of a vibrationally compacted UO_2–2 wt% PuO_2 fuel rod irradiated in PRTR at approximately 20 kW/ft is shown in Figure 2.1.

Destructive examination of HPD fuel rods have shown that a thin (0.0002 in. thick) ZrO_2 layer forms on the inside surfaces of the Zircaloy cladding after only two days irradiation (Figure 2.2). The ZrO_2 layer builds up to a thickness of about 0.0006 in. after a burnup of approximately 7600 MWd/tonne. A similar layer is formed during the preassembly autoclaving of commercially fabricated pellet rods (Figure 2.3). These oxide layers are probably formed from moisture and excess oxygen in vibrationally compacted, pneumatically impacted UO_2-PuO_2 fuels. The effects of the layer on fuel element performance will be evaluated as irradiation progresses.

Irradiation of some UO_2 and UO_2-PuO_2 fuel elements (pre-High Power Density vintage) containing 0.5 to 2.0 wt% PuO_2 is continuing in fringe positions of the PRTR during the Batch Core Experiment. These elements and their current burnup status are listed in Table 2.I.

The fringe elements contain both pneumatically impacted and mechanically mixed (incrementally loaded) UO_2-PuO_2 fuel material. One of the first mechanically mixed UO_2-PuO_2 elements charged into the PRTR has attained the highest burnup (greater than 11,000 MWd/tonne). Periodic underwater examination of these elements indicates that their performance continues to be satisfactory. Irradiation of these elements will continue for the duration of the Batch Core Experiment.

TABLE 2.I. PRTR Core Loading Status (11/15/67)

Element Type(a)	No. of Elements	Max. Rod Power Gen. kW/ft	Element Average Burnup, MWd/tonne
Batch Core Experiment:			
Vipac PI(b) UO_2–2 wt% PuO_2 (Batch Core Experiment Elements)	65	20	3,100
Hot Pressed Pellet UO_2–1.94 wt% PuO_2	2	21.5	2,700
Fringe Position Tests:			
Vipac PI UO_2–2 wt% PuO_2 (Pilot HPD Elements)	6	20	6,000
Swaged PI UO_2–2 wt% PuO_2	1	20	3,700
Swaged PI UO_2–1 wt% PuO_2	1	17	8,500
Vipac PI UO_2–1 wt% PuO_2	2	15	6,500
Vipac MM(c) UO_2–0.5 wt% PuO_2	1	16	11,000
Swaged MM UO_2–0.5 wt% PuO_2	2	13	10,400
Swaged UO_2	1	14	9,500

(a) *PRTR elements are 19-rod clusters of 0.565 OD Zircaloy-clad rods with active fuel lengths of 58.5 and 88.5 in.*
(b) *PI = High-energy-rate pneumatically impacted fuel.*
(c) *MM = Mechanically mixed fuel.*

Among the first fuel irradiations to be performed in the PRTR during the Batch Core Experiment were tests to determine the maximum reactor power level attainable while maintaining maximum fuel temperatures just below melting (∿2790 °C). Thirteen fuel rods were metallographically examined, and maximum temperatures attained were deduced from the fuel structures formed during irradiation. These experiments indicated that under PRTR operating conditions, the onset of melting in vibrationally compacted UO_2–2 wt% PuO_2 fuel rods occurs at a heat rating of 20.5 ± 0.5 kW/ft. (This value will be refined as more data are acquired.) This power to produce melting is equivalent to an $\int_0^{T_M} k\,dT$ value of about 68 W/cm.

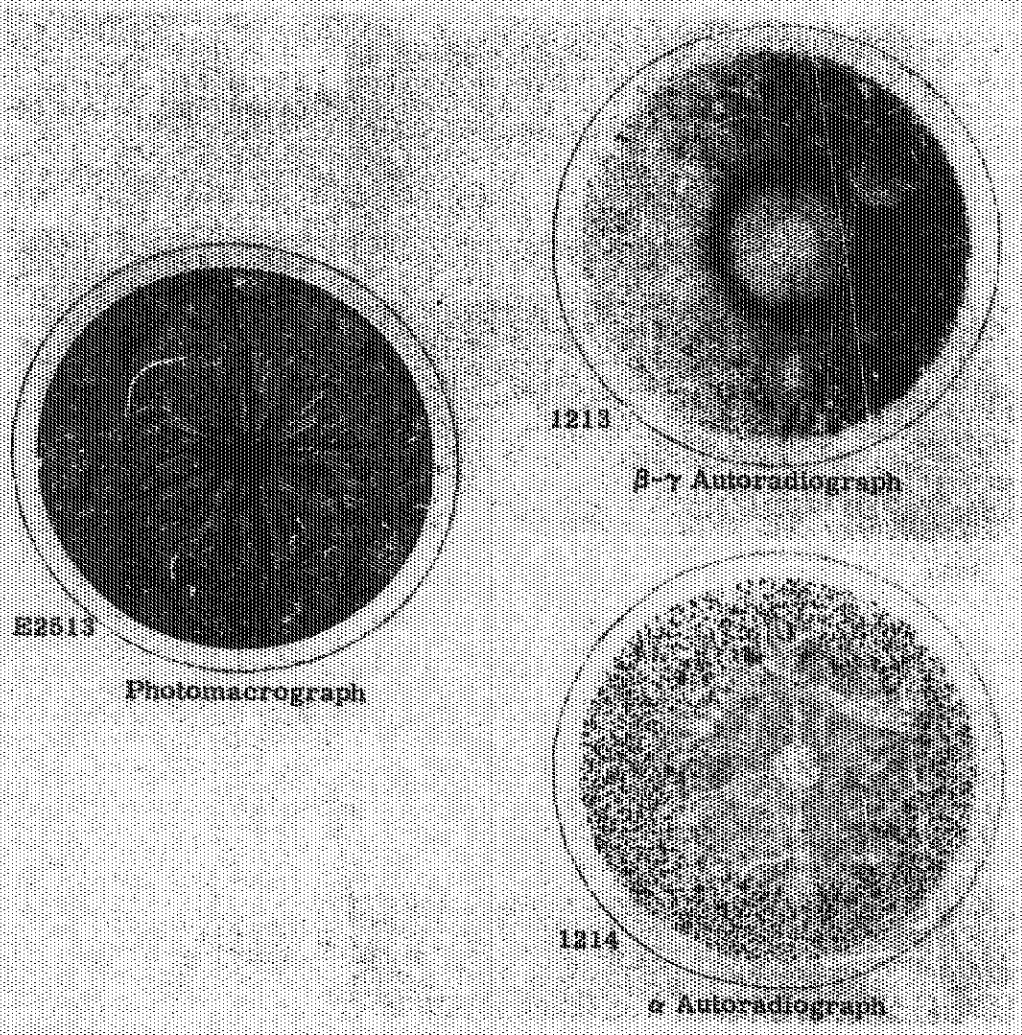

Neg 6873184-1

FIGURE 2.1. Transverse Section of a Vibrationally Compacted UO_2-8 wt% PuO_2 Fuel Rod Irradiated Under the Maximum High Power Density Conditions in FFTF, i.e., 20 kW/ft with Maximum Fuel Temperatures near Melting.

Results of these examinations also show that:

1) The temperature at which columnar grain growth begins is approximately 2000 °C for irradiation times to 80 hr.
2) Ceramographic evidence of typical once-molten fuel structures formed during irradiation are erased by time-temperature dependent diffusion phenomena in less than 72 hr irradiation under nonmolten, but high-temperature conditions.
3) Fission product distribution patterns typical of molten fuel operation, as indicated on beta-gamma autoradiographs, are not

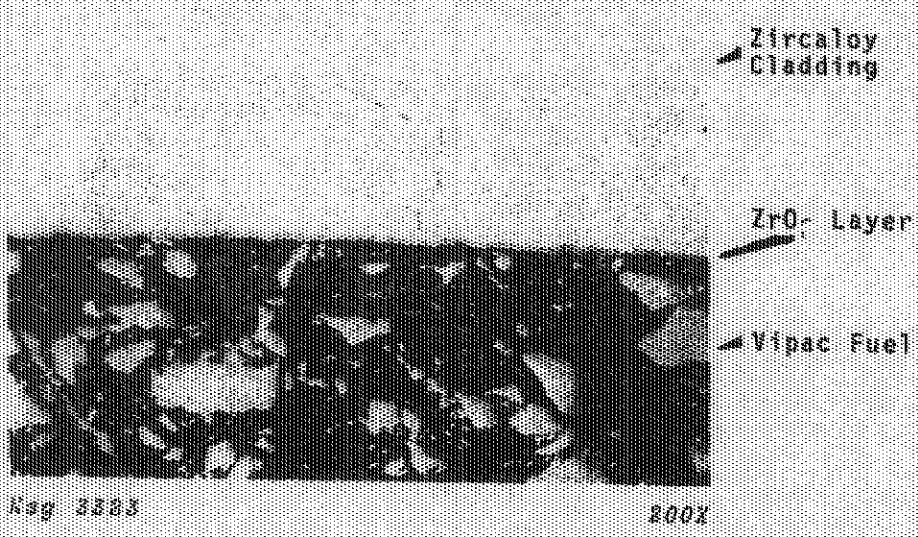

FIGURE 2.2. ZrO_2 Layer Forms on the Inner Cladding Surface of a Vibrationally Compacted UO_2–PuO_2 PRTR Fuel Rod after 2 Days Irradiation at a Peak Rod Power of 18.6 kW/ft.

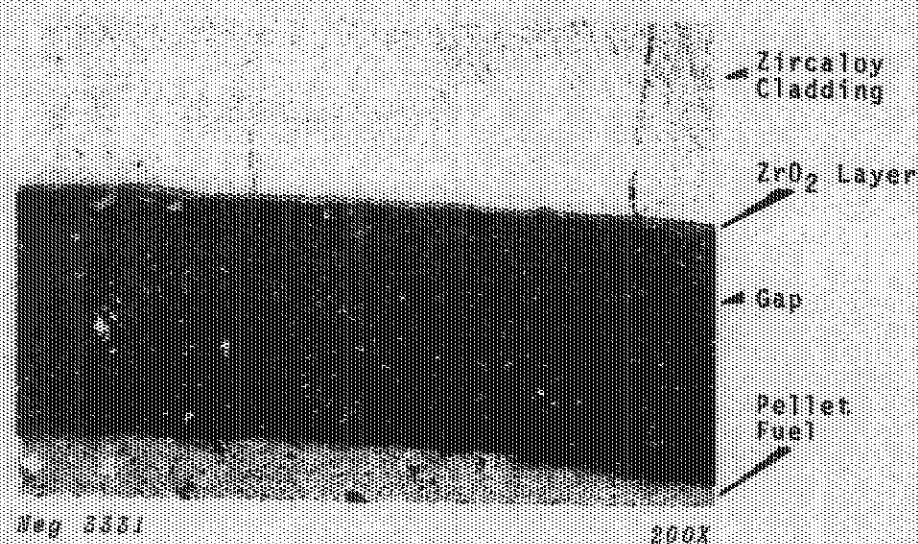

FIGURE 2.3. ZrO_2 Layer on the Inner Cladding Surface of a PRTR Fuel Rod Containing Hot-Pressed UO_2–PuO_2 Pellets. Tubing was autoclaved before loading.

completely eradicated during 72 hr of subsequent nonmolten irradiation.

4) Fuel structures formed in different rods irradiated under the same nonmolten conditions are comparable.
5) Structural equilibrium is reached more rapidly at higher power generations.

Fuel melting occurred in two of the vibrationally compacted rods examined. Fuel in one of the rods melted to approximately 10% of the radius (Figure 2.4) and to approximately 33% of the radius in the other. Both rods were presumably irradiated under the same conditions. The reason for the difference in the

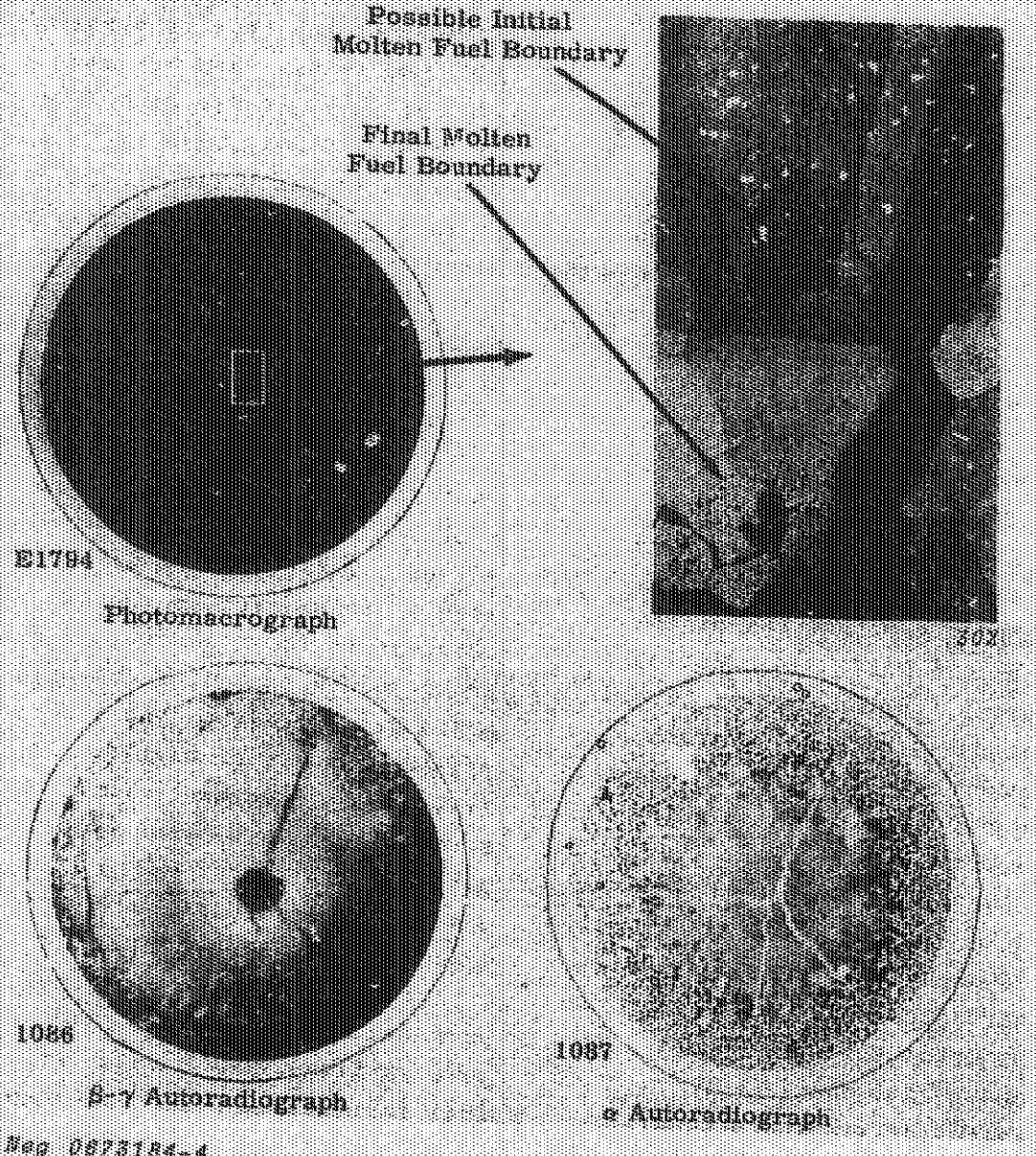

FIGURE 2.4. Transverse Section of a Vibrationally Compacted UO_2-2 wt% PuO_2 Fuel Rod Irradiated in PRTR at a Maximum Linear Power Generation of 21 kW/ft.

indicated melt radius is being investigated. A region of subgrain structure in the center of the fuel specimen is thought to represent fuel that was molten at the time of shutdown. The extent of the central dark region on the beta-gamma autoradiograph corresponds to the subgrain region on the micrographs. Alpha autoradiographs of once-molten mixed-oxide fuel specimens show a centrally located dark region which extends beyond the region containing high density grains. This dark region is interpreted as representing the molten fuel boundary at the start of the irradiation. It is hypothesized that this boundary recedes as the fuel sinters and the effective thermal conductivity improves.

In conjunction with the irradiations to establish the maximum allowable PRTR power level, autoradiographs were obtained for some irradiated UO_2-PuO_2 fuel specimens within 48 hr after shutdown of the reactor (Figure 2.5). In addition to the normal fission product distribution patterns, high concentrations were observed on the inner surfaces of cracks and large grain surfaces located equidistant from the thermal center. The fission product concentrated in these areas is apparently one with a high vapor pressure and a short half life. A second autoradiograph taken six weeks after fuel discharge did not detect concentrations of fission products in these areas.

An important part of the Plutonium Utilization Program Fuel Development studies is to procure and test plutonium-containing fuel rods designed and fabricated by commercial fuel vendors. One 19-rod cluster of commercially designed and fabricated fuel rods containing hot-pressed UO_2–1.94 wt% PuO_2 pellets is being irradiated in the Fuel Element Rupture Test Facility (FERTF) at a maximum linear rod power of 21.2 ± 1.0 kW/ft to an average element burnup that is presently 2700 MWd/tonne. Another similar element is being irradiated in a core position. Examination of one of the elements in the basin indicates that it is performing satisfactorily; no adverse effects of irradiation have been observed. Postirradiation examination of one rod from the element indicates that incipient fuel melting occurred (Figure 2.6). Structures typical of those found in irradiated cold pressed and sintered pellet fuel rods were observed. The structure is characterized by an unaffected region adjacent to the cladding, an equiaxed grain growth region, a columnar grain growth region, and a central region composed of high density pore-free grains. Ceramographic examination and the beta-gamma autoradiograph indicate that molten fuel was extruded into radial cracks that apparently existed during irradiation.

Three fuel rods containing cold pressed and sintered UO_2-PuO_2 pellets were obtained from a commercial fuel fabricator. The performance of these rods will be investigated and will be compared to that of the hot pressed pellet rods and to packed-powder fuel rods designed and

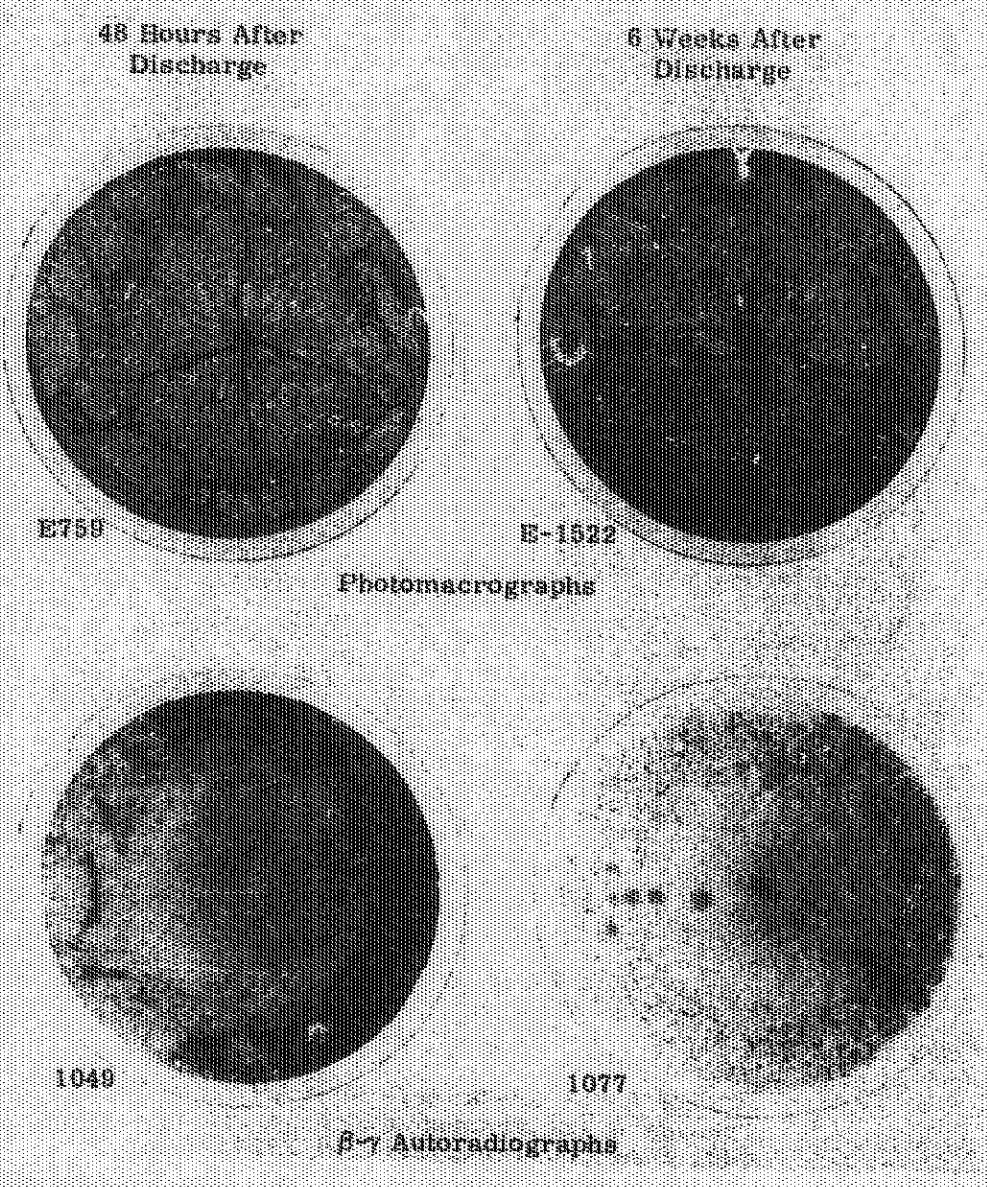

FIGURE 2.5. Transverse Section of a Vibrationally Compacted UO_2–2 wt% PuO_2 Fuel Rod Irradiated 45 hr in PRTR at a Linear Power Generation of 18.2 kW/ft.

fabricated at the Pacific Northwest Laboratory. The first of these rods is now being irradiated at about 19 KW/ft.

The effects of specific power and burnup on the defect behavior of pellet and packed-powder fuel will be studied by irradiating elements in the PRTR Fuel Element Rupture Test Facility (FERTF). An eight-rod element (Figure 2.7) has been designed and built for defect testing in the FERTF. This element comprises a protective sleeve assembly surrounding a rack that supports an eight-rod ring of fuel rods. The

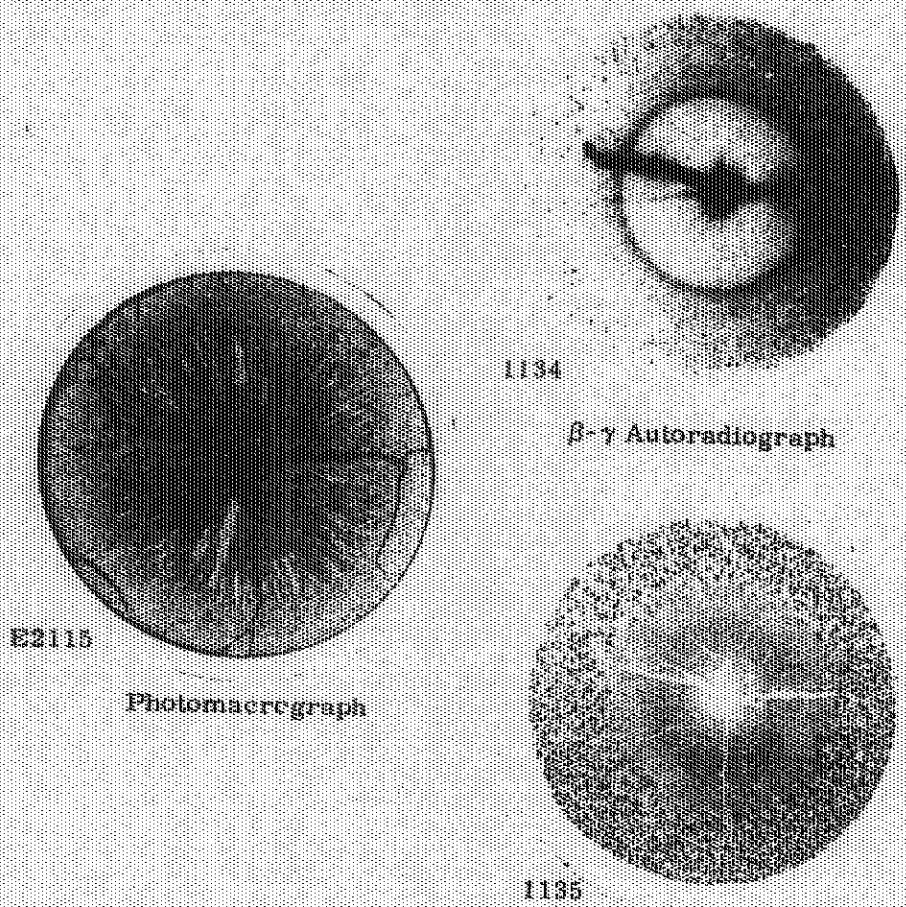

FIGURE 2.6. Transverse Section Through a Hot Pressed UO_2–1.94 wt% PuO_2 Fuel Rod Irradiated in PERTP at a Linear Power Generation of 21.1 ± 1.0 kW/ft.

sleeve assembly provides protection for the surrounding Zircaloy pressure tube. The fuel rod rack assembly can be removed from the sleeve assembly as an integral unit to facilitate rod manipulations. The fuel rods are suspended from the top of the rack assembly and are free to expand or contract independently. Four circumferential strip bands secure the rods to the rack assembly. The power generation of fuel rods irradiated in the PERTP can be changed by using various sleeve and insert materials in the assembly.

Vibrationally compacted UO_2–PuO_2 fuel rods, pellet UO_2-PuO_2 fuel rods, and vibrationally compacted enriched UO_2 fuel rods will be irradiated in the PERTP Test Element at linear heat ratings to 20 kW/ft. This test

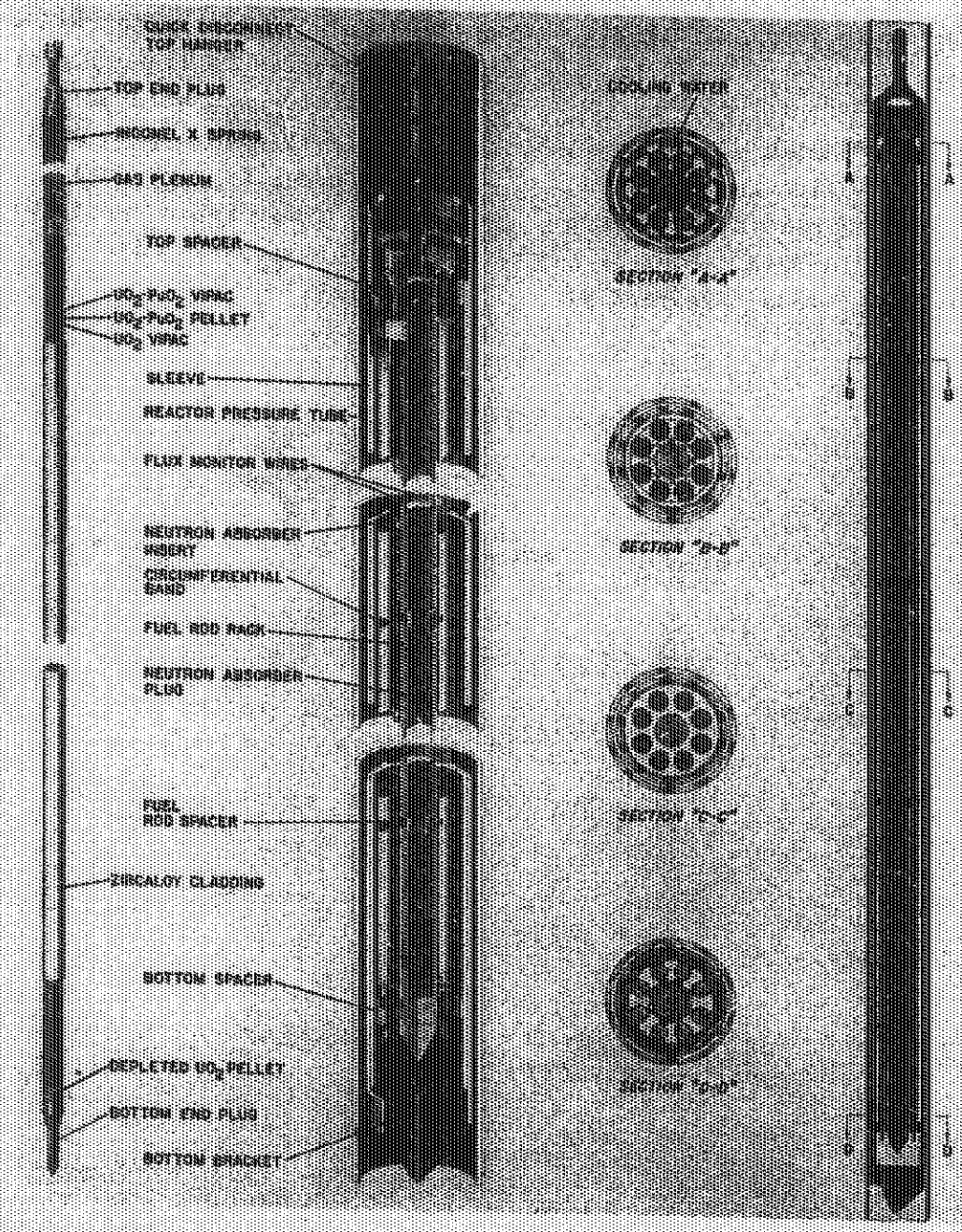

Neg 0871861

FIGURE 2.7. Eight Rod PBRTF Test Element.

series will require approximately nine irradiation periods. Subsequent test series will include linear heat ratings to 28 kW/ft. Testing will include irradiation of both nondefected and deliberately defected fuel rods.

GAS PRESSURE MEASURING EXPERIMENTS

T. B. Burley

Pressure buildup in vibrationally compacted mixed-oxide fuel rods is being measured as part of the Batch Core Experiment in PRTR. Four instrumented fuel rods (Figure 2.8) presently operating in PRTR contain thermocouples to measure plenum gas temperatures and null-balance pressure transducers to measure internal gas pressures during irradiation. These measurements will be made to burnups as high as 15,000 MWd/tonne.

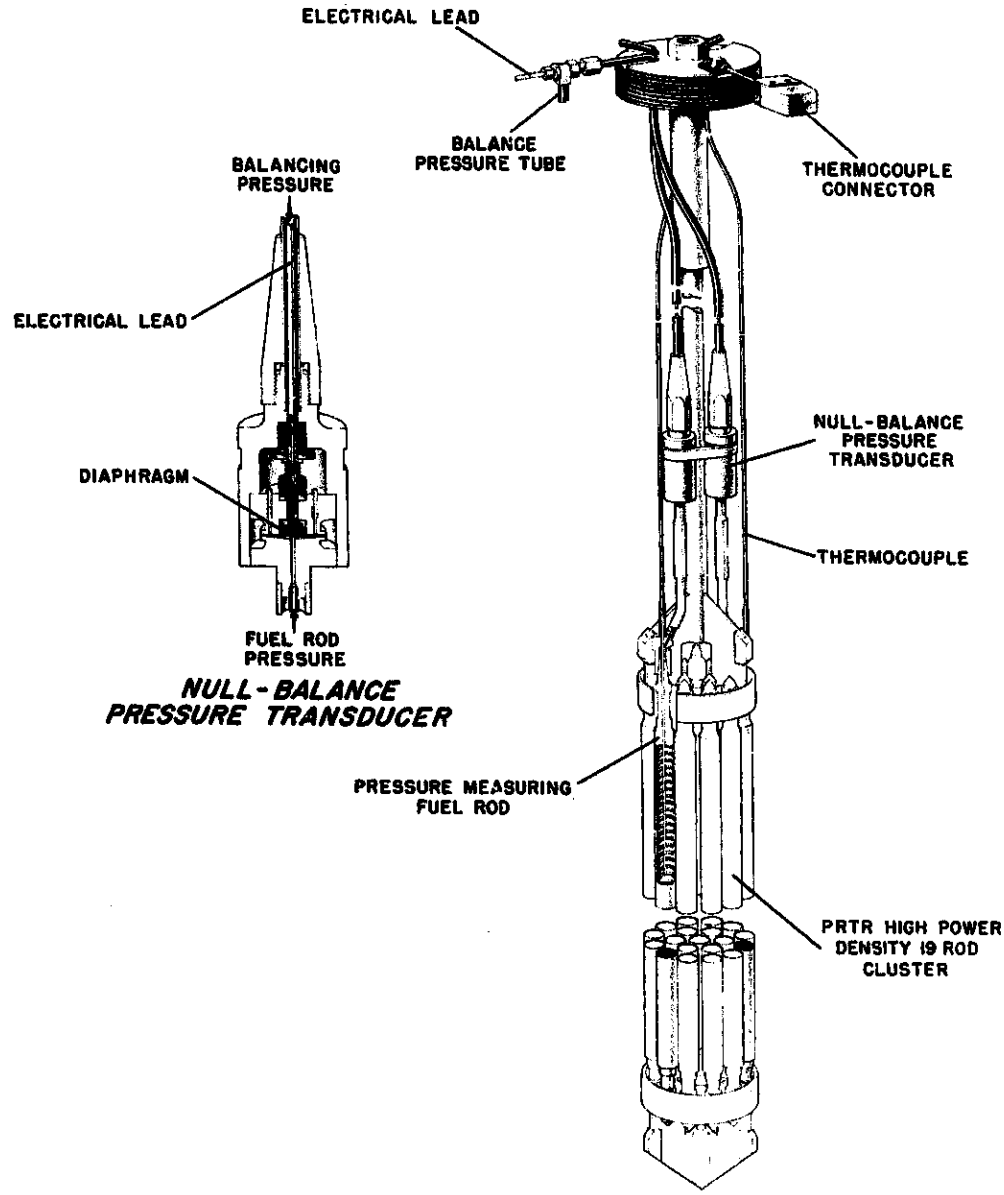

Neg 0670955

FIGURE 2.8. *PRTR In-Reactor Fuel Rod Pressure Measuring Element.*

Two of the instrumented rods operated at peak powers of nominally 9.5 kW/ft, and the other two rods operated at peak powers of nominally 16.5 kW/ft.

As shown in Figures 2.9 and 2.10, the pressure exerted by the sorbed gases and moisture in the fuel (the pressure at zero burnup) was less than calculated if 100% release of these gases is assumed. However, the rates of pressure increase are consistent with rates predicted from fission gas release measurements previously made for similar fuel.[1] This comparison indicates that approximately 13% of the gases are being released from the low power fuel (volumetric averaged fuel temperature of 700 °C) and about 25% of the gases formed are being released from the high power fuel (volumetric averaged fuel temperature of 1250 °C). After about 1000 MWd/tonne exposure, the two high power fuel rods operated for a short time (approximately 5 hr) at a peak linear heat rating of 20 kW/ft and fuel temperatures above melting. No unusual gas release was noted. The rate of pressure increase in the high power fuel rods was lower during recent operation than during the first 1000 MWd/tonne because peak linear heat ratings, and hence fuel temperatures, were lower.

The gas release rates are approximately constant over the exposure range tested and are apparently directly proportional to volumetric average fuel temperature. In the high power fuel rods the pressure increased in a step manner during reactor power cycles. The pressure was generally higher after a shutdown and startup than before the shutdown. A pressure increase was also noted when the power level was increased after long periods of steady-state operation.

The pressure increases with burnup were much less in the low power fuel rods than in the high power fuel rods. The step increases during power cycles were small and in many cases could not be detected. Pressure increases in the low temperature fuel were more dependent on coolant temperature than on fuel temperature. A power cycle occurred at about 1100 MWd/tonne, (See Figure 2.10) during which the peak linear heat rating was lowered from 8.2 to 6.4 kW/ft and the coolant outlet temperature remained constant. No significant change in gas pressure was noted during this power cycle.

Plenum temperatures have been measured in all of the instrumented fuel rods. As shown in Figure 2.11, plenum temperatures are primarily a function of coolant outlet temperature; fuel temperatures have an insignificant effect on plenum temperatures. A 0.5 in. long depleted pellet at the end of the fuel column acts as an effective thermal insulator. At no time during operation (maximum fuel temperatures 200 °C to melting and maximum coolant temperatures of 270 °C) did the measured plenum temperatures exceed the coolant outlet temperatures by more than 13 °C.

The plenum thermocouples, which are positioned at the axial midpoint of the 7 in. long plenum are now

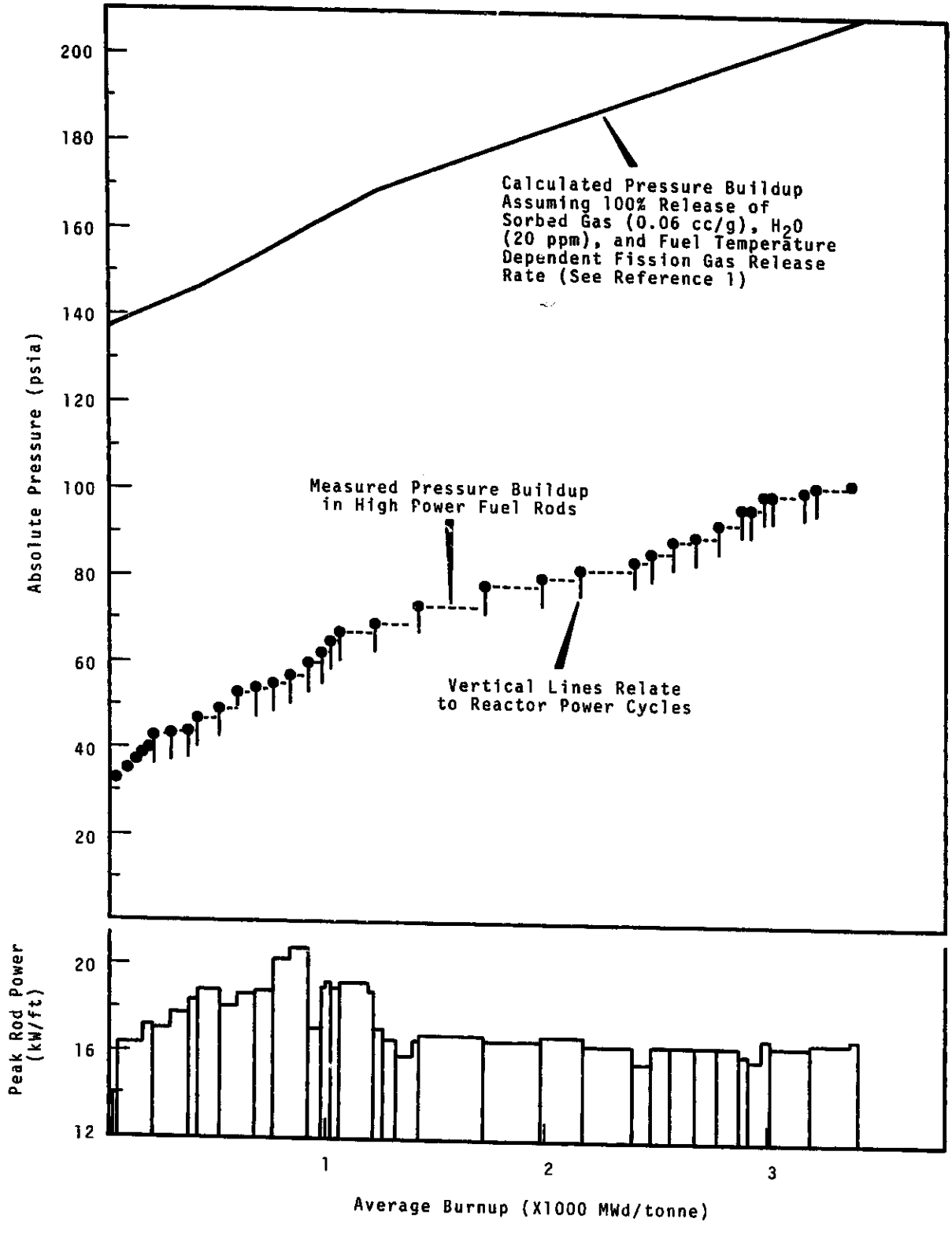

FIGURE 2.9. Pressure Buildup in High Power PRTR Fuel Rods.

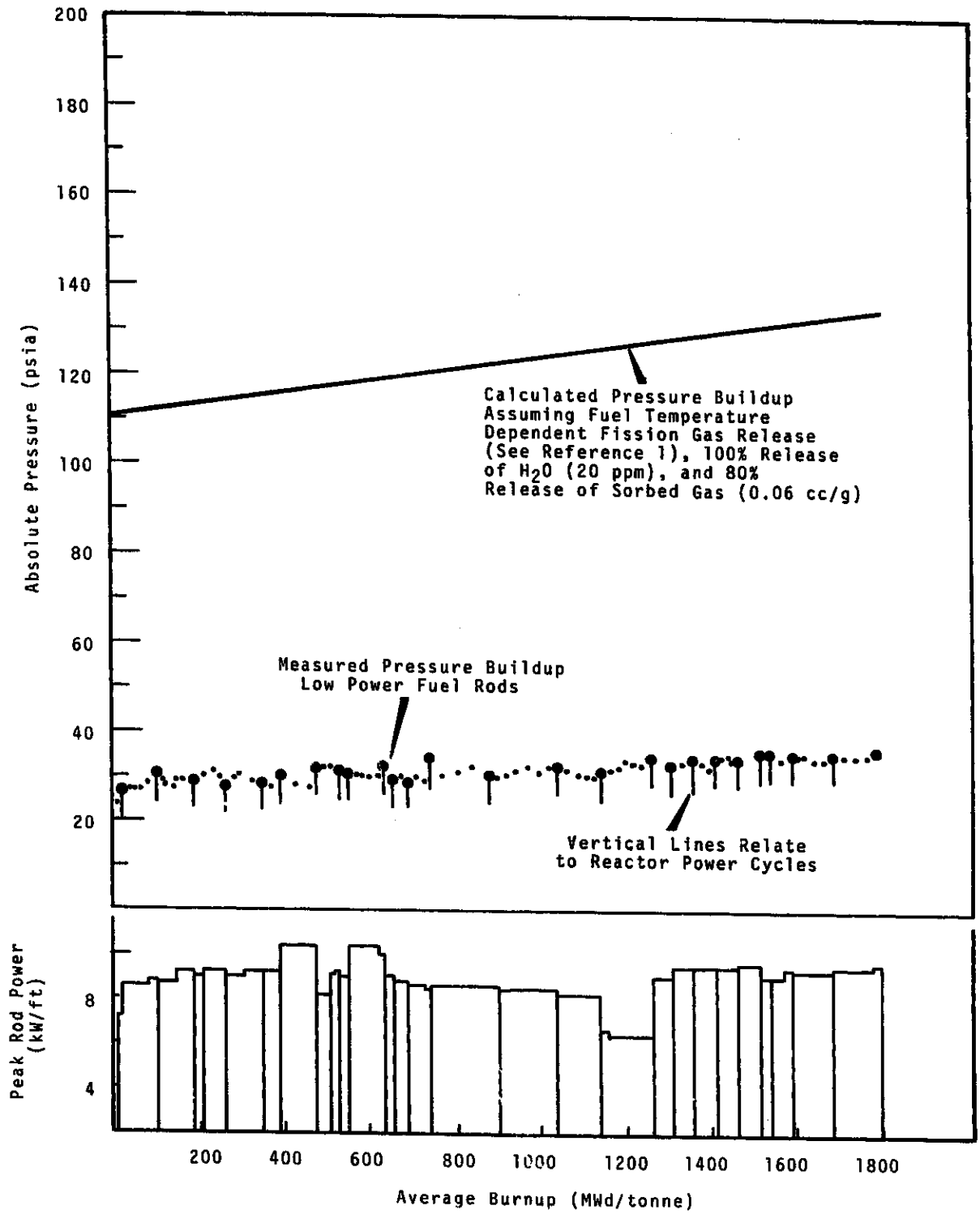

FIGURE 2.10. Pressure Buildup in Low Power PRTR Fuel Rods.

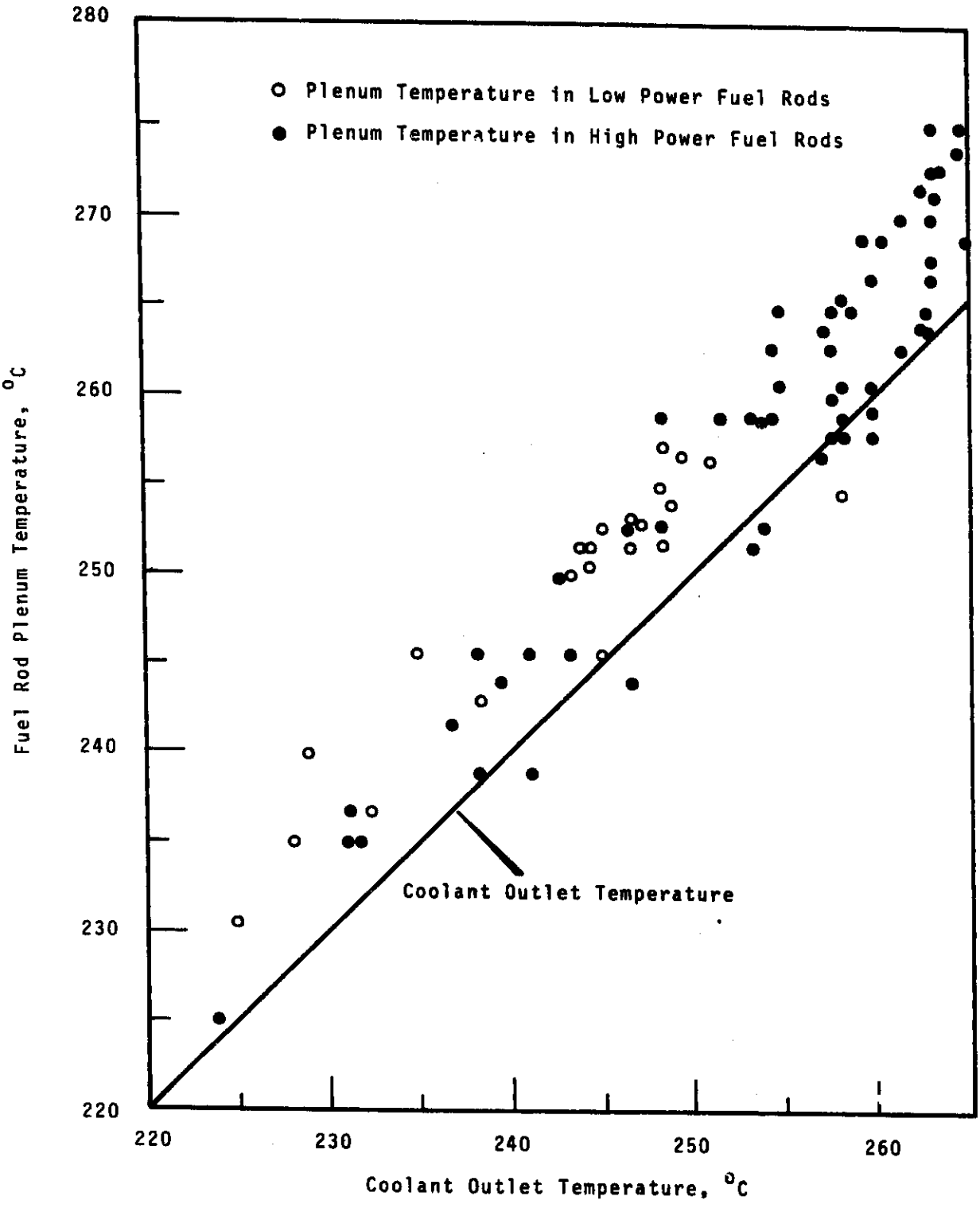

FIGURE 2.11. Measured Plenum Temperature Versus Coolant Outlet Temperature.

operating in only the low power fuel rods. The thermocouples in the high power fuel rods were damaged beyond repair after three months of operation.

References

1. *M. D. Freshley and F. E. Panisko. The Irradiation Behavior of UO_2-PuO_2 Fuels in PRTR, BNWL-366 Pacific Northwest Laboratory, Richland, Washington.*

DEFECT TESTING

M. D. Freshley

Investigation of the defect behavior of both vibrationally compacted and pelleted UO_2-PuO_2 fuels operating under high performance conditions is an important part of the Plutonium Utilization Program. An intentionally defected 7-rod cluster was irradiated under molten core conditions in the ETR P-7 high pressure loop as the first of a series of defect tests.

The prototypic PRTR element was a Zircaloy-clad 7-rod cluster with an active fuel length of approximately 30 in. The fuel column was vibrationally compacted, pneumatically impacted, UO_2 enriched to 2.6% ^{235}U. A 2.75 in. long gas plenum was provided at the top of the fuel column. One rod was defected with a 0.060 in. diameter hole through the cladding at the peak power position.

The element was irradiated for nine effective full power days at a maximum linear rod power of 28 to 29 kW/ft. Calculations indicate that for this linear rod power generation, fuel melting should have occurred to approximately 60 to 65% of the radius at the plane of the defect.

Activity release to the coolant caused no operational problems during the irradiation. Activity bursts occurred at the start of power level increases. One small burst occurred during steady-state full-power operation. Increases in reactor power and coolant temperature caused activity bursts which decreased to low equilibrium values during continued steady-state operation. During its residence time in the reactor, the defected element was subjected to three programmed power increases, two of which were from zero power.

The element was also subjected to one scram recovery, which included a very rapid power increase (3 min) from 1 to 50% of full power. Although the activity release to the loop piping was quite high during the scram recovery, modest amounts of activity were released during the programmed power increases.

Postirradiation examination of the defected rod and nondefected rods from the element is in progress. Some of the preliminary results of the examination are:

1) There was no change in the external appearance of the defect as a result of irradiation. There were no measurable changes in the dimensions of the rod, even in the immediate vicinity of the defect (Figure 2.12).
2) Molten fuel, as indicated by the centrally located porous fuel structure, was present to about 22% of the radius at the

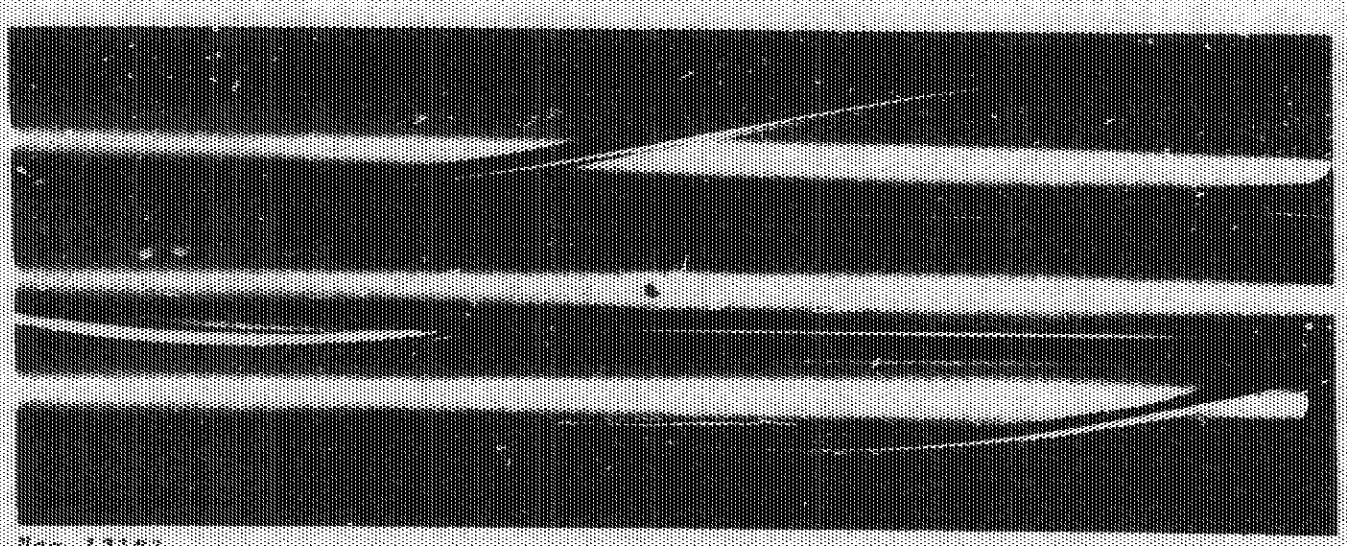

Neg 17193

FIGURE 2.18. Defected Zircaloy-Clad Fuel Rod Containing Vibrationally Compacted UO_2 after Irradiation for 9 Effective Full Power Days in the ETR P-7 High Pressure Loop. Peak Power Generation at the Plane of the Defect was Approximately 28 kw/ft.

plane of the defect at the time of shutdown (Figure 2.13). Autoradiographs indicate that initial fuel melting occurred to approximately 67% of the radius as planned. The molten fuel region was displaced away from the defect and the shape of the molten zone was affected by the presence of the defect.

3) A small amount (approximately 5.5% of the cross-sectional area) of fuel washout occurred in the immediate vicinity of the defect. The washout was limited to the unsintered fuel in the peripheral region of the rod.
4) There was no metallographic evidence of increased hydrogen concentration in the cladding in the vicinity of the defect.
5) A thin ZrO_2 layer about 0.0002 in. thick formed on the inner surface of the Zircaloy cladding in the defected rod.

Examination of these rods is continuing.

IRRADIATION TESTING OF EBWR PROTOTYPE FUEL RODS

W. J. Bailey

The Experimental Boiling Water Reactor (EBWR) at Argonne National Laboratory (ANL) was shut down on June 30, 1967 after successful operation at 70 MWt to fuel exposures as high as 3000 MWd/tonne. The reactor was fueled with 1296 mixed oxide fuel rods that were fabricated by Pacific Northwest Laboratory (PNL). The vibrationally compacted, Zircaloy-clad rods (1.07 cm OD by 148 cm long) each contained 830 g of pneumatically impacted UO_2-1.5 wt%

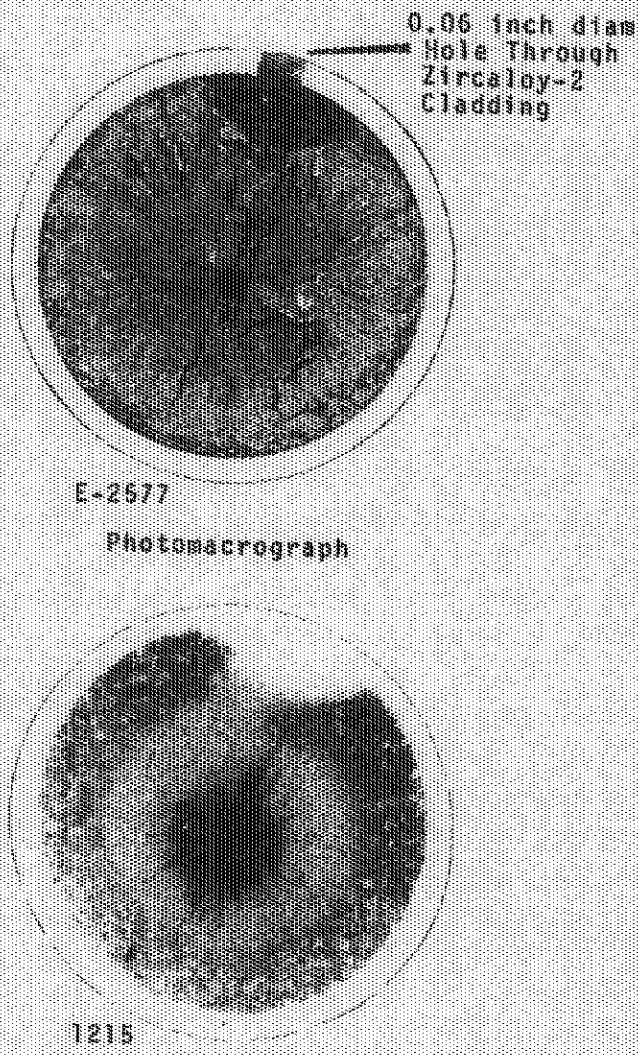

FIGURE 2.13. Transverse Section of a Defected Vibrationally Compacted UO_2 Fuel Rod. Peak power generation was approximately 20 kW/ft with fuel melting to about 33% of the radius at the time of shutdown.

PuO_2. Fuel rods from this cooperative PNL-ANL Plutonium Recycle Demonstration Experiment in EBWR were removed for PNL physics measurements[1]. These included:

1) 17 rods with a burnup of 1300 MWd/tonne
2) 17 rods with a burnup of 2200 MWd/tonne
3) 72 rods with a burnup of 2500 to 3000 MWd/tonne

Recent PNL data[1] indicate that the burnup is slightly lower than that previously reported (3000 MWd/tonne) by ANL.[2] Gamma scanning of some of the rods indicated that the maximum flux position in the EBWR occurred about 28 cm or about 23% (and not ~40% as previously reported) from the bottom of the fuel column.

Successful completion of irradiation proof tests of prototypic EBWR rods and capsules have demonstrated that these fuel elements could operate to exposures of 10,000 to 30,000 MWd/tonne. Table 2.II shows isotopic data for the two highest burnup capsules. The highest burnup specimen contains plutonium with nearly 20% ^{242}Pu. Information on the concentrations of other isotopes (e.g., ^{236}Pu, ^{238}Pu, ^{244}Cm) is being obtained. Analytical data on americium and curium isotopes from these capsules are shown in Table 2.III. The ^{244}Cm isotope is of possible interest as a heat source. The last capsule in Table 2.II (18,300 MWd/tonne exposure) contains 0.9 mg of ^{244}Cm in the 52.7 g of fuel.

References

1. *R. C. Liikala to W. J. Bailey, Personal Communication, November 1, 1967.*
2. *C. H. Bean, R. C. Sharp, and W. J. Bailey. "The EBWR Plutonium Recycle Demonstration Experiment," a paper presented at the AIME, 1967 Nuclear Metallurgy Symposium on Plutonium Fuels Technology held in Phoenix, Arizona, during the period October 4-6, 1967.*

TABLE 2.II. Burnup and Isotopic Data for UO_2–1.5 wt% PuO_2 Fuel Irradiated in the Materials Testing Reactor (MTR). Mass Spectrographic Data[a]

Burnup		At.% Plutonium					
Mwd/tonne of fuel	10^{20} fiss/cm^3	236	238	239	240	241	242
0	0			91.53	7.75	0.69	0.03
4,290	1.1		(b)	72.94	22.90	3.67	0.484
12,560	3.1	1.8×10^{-7}	0.231[c]	47.28	37.22	9.24	6.03
18,300	4.5	5.0×10^{-7}	0.416[c]	38.87	38.22	11.74	10.76
~26,400[e]	~6.5[e]	(b)	0.605	36.1	35.3	11.27	16.75
~30,000[e]	~7.4[e]	(b)	0.574	35.4	33.8	10.40	19.8

Burnup		At.% Uranium			
MWd/tonne of fuel	10^{20} fiss/cm^3	234	235	236	238
0	0	<0.001	~0.22	<0.002	99.78
4,290	1.1	0.0024	0.122	0.0095	99.868
12,560	3.1	ND[d]	0.0376	0.0214	99.941
18,300	4.5	ND	0.0234	0.0240	99.953
~26,400[e]	~6.5[e]	(b)	0.011	0.026	99.964
~30,000[e]	~7.4[e]	(b)	0.0050	0.024	99.971

(a) *Typical uncertainties (at the 95% confidence level) are: for ^{238}Pu, ± 0.003 to 0.006; ^{239}Pu and ^{240}Pu, ± 0.1 to 0.2; for ^{241}Pu, ± 0.02 to 0.1; for ^{242}Pu, ± 0.002 to 0.1; for ^{234}U, 5 ppm (detection limit) to ± 0.009; for ^{235}U, ± 0.0007 to 0.002; for ^{236}U, ± 0.0004 to 0.009; and for ^{238}U, ± 0.0008 to 0.003.*
(b) *Analysis currently in progress.*
(c) *Value obtained by alpha energy analysis.*
(d) *ND = Not Detected.*
(e) *More detailed analysis in progress.*

TABLE 2.III. Concentrations of ^{241}Am, ^{243}Am, ^{242}Cm, and ^{244}Cm (UO_2–1.5 wt% PuO_2 Capsules Irradiated in the MTR).

Burnup	Weight Ratios			
MWd/tonne of fuel	$^{241}Am/^{243}Am$	$\left[^{241}Am/U\right]\times10^{-4}$	$\left[^{242}Cm/U\right]\times10^{-4}$	$\left[^{244}Cm/U\right]\times10^{-4}$
12,560	3.00-3.06	1.59	0.00819	0.0462
16,300	1.83-1.88	(a)	(a)	(a)
18,300	0.856-0.882	1.42	0.0711	0.189

(a) *Not available*

TRANSIENT TESTS ON THERMAL REACTOR OXIDE FUELS

R. L. Gulley

High speed motion pictures of vibrationally compacted UO_2 fuel rods undergoing transient irradiations were obtained as part of a joint BNW-ANL* investigation. These experiments were performed in the Transient Reactor Test Facility (TREAT). Each nonirradiated fuel rod (Figure 2.14) was irradiated under the conditions shown in Table 2.IV while submerged in ambient temperature stagnant water.

One fuel rod (Experiment 237T) developed a high temperature band about 1/8 in. long, near the bottom of the fuel column. Except for a low temperature region immediately above

* *Contributors to the cooperative investigation include staff members of the Chemical Engineering Division of ANL, the TREAT Facility, and BNW.*

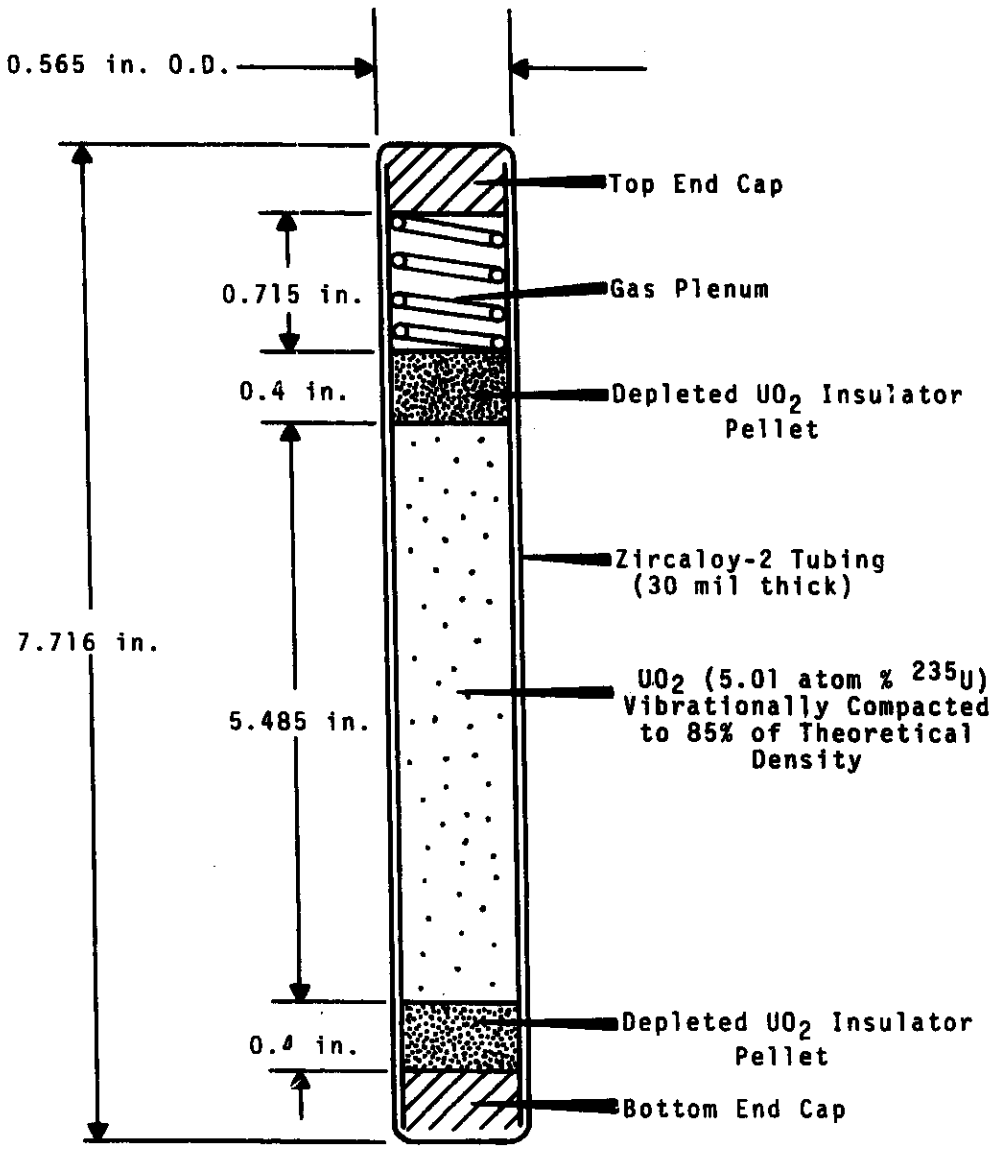

FIGURE 2.14. Transient Irradiation Test Rod

TABLE 2.IV. Summary of Transient Experiments with Zircaloy-2-Clad Vibrationally Compacted UO_2 Fuel in Transparent Autoclaves

Reactor Characteristics	Experiment Number		
	235T	236T	237T
Integrated Power, MW sec	354	338	392
Peak Power, MW	1297	1118	1430
Period, msec	71	75	67
Fission Energy Input, cal/g UO_2	236	223	259

Fuel Appearance After Transient

235T	Cladding bulged near the bottom of the fuel column but did not rupture. The fuel rod bowed about 1/8 in.
236T	Cladding bulged near the bottom of the fuel column but did not rupture.
237T	Cladding bulged and blistered near the top and bottom of the fuel column but did not rupture.

the high temperature band, the remainder of the fuel rod achieved a uniform temperature. In the other two fuel rods (Experiments 235T and 236T), only the upper half of each fuel rod was visible because steam formed between the inner and center transparent autoclaves during the initial part of the transients. Detailed study of the results is continuing. Further irradiations utilizing the transparent autoclave are planned to better define the transient behavior of both pellet and powder thermal reactor oxide fuel rods.

FISSION PRODUCT MIGRATION IN MIXED OXIDE FUEL

R. Shimanuki and M. D. Freshley

Migration of fission products in vibrationally compacted UO_2-PuO_2 fuel rods irradiated in the Batch Core in PRTR is being studied. Self-shielding effects within the 19-rod cluster PRTR fuel elements result in a nonsymmetric radial power generation and hence a nonsymmetric fission product formation within each rod in the outer 12-rod ring of the elements. In addition, the resulting radial displacement (as much as 0.6 mm) of the thermal center in the rods causes the fission products to migrate in a nonsymmetric manner.

Fission product migration studies are being conducted on a vibrationally compacted UO_2–2 wt% PuO_2 fuel specimen that was irradiated at a rod power of about 20 kW/ft to a burnup of approximately 0.9×10^{19} fissions/cm^3. This power generation caused fuel to be molten to approximately 10% of the radius at the time of reactor shutdown. Analytical samples were

obtained by drilling at selected locations on the surface of a cross-section of the specimen (Figure 2.15). The nonsymmetric structure formation and fission product distribution patterns are evident on the photograph and autoradiographs. Microdensitometer scanning of the beta-gamma autoradiograph in the radial direction (with respect to the fuel cluster) also illustrates the nonsymmetric fission product distribution (Figure 2.16). Scanning in the tangential direction (with respect to the fuel cluster) revealed a symmetric fission product distribution about a line that extends from the center of the fuel cluster through the center of the fuel rod.

Analytically determined fission product distributions are compared with the distributions alculated by computer codes THERMOS, HRG, ALTHEA, PROGRAM S-XIII, and LEARN in Figure 2.16. The deviation from the calculated distribution is determined by the migration characteristics of the particular fission product species, the thermal conditions within the specimen, and microstructural changes that occur. Preliminary results for ^{137}Cs, which has migrated considerably in the specimen under study, are shown in Figure 2.17. A higher concentration of volatile cesium has occurred on the side of the rod with the steeper temperature gradient away from the center of the element than on the side closest to the center.

Similar studies of other fission products and uranium and plutonium isotopes are in progress.

LOW DENSITY OXIDE FUELS

G. R. Horn and R. L. Gulley

Substantial reductions in the cost of fabricating plutonium-bearing oxide fuels may be possible by simply cold-pressing pellets and then loading them into the cladding. In this manner, costs associated with powder preparation, sintering, and grinding can be reduced.

Preliminary investigations indicate that satisfactory inexpensive pellets of adequate density (~70% TD) and quality can be made by pressing as-received "high-fired" UO_2* at 80 to 100 tons/in.^{2} with no subsequent sintering. Vacuum outgassing of the pellets at 600 °C should reduce the sorbed gas and moisture contents so that the pellets can be successfully irradiated to high exposures under normal power reactor operating conditions.

Irradiation experiments are currently being conducted to demonstrate the feasibility of operating low density mixed oxide fuels. A 7-rod cluster experimental fuel element was irradiation tested in the ETR to a maximum burnup of ~660 MWd/tonne at a linear heat rating of ~16 kW/ft. Each rod in the cluster contained 0.50 in. diameter UO_2–0.5 wt% PuO_2 pellets densified to 71% TD. It was anticipated that gross fuel movement or relocation might result from using low density fuel; therefore, fuel movement restrictors were included in the element to prevent gross

* *High-fired UO_2 is UO_2 that was reduced at 900 °C instead of the more normal 650 °C.*

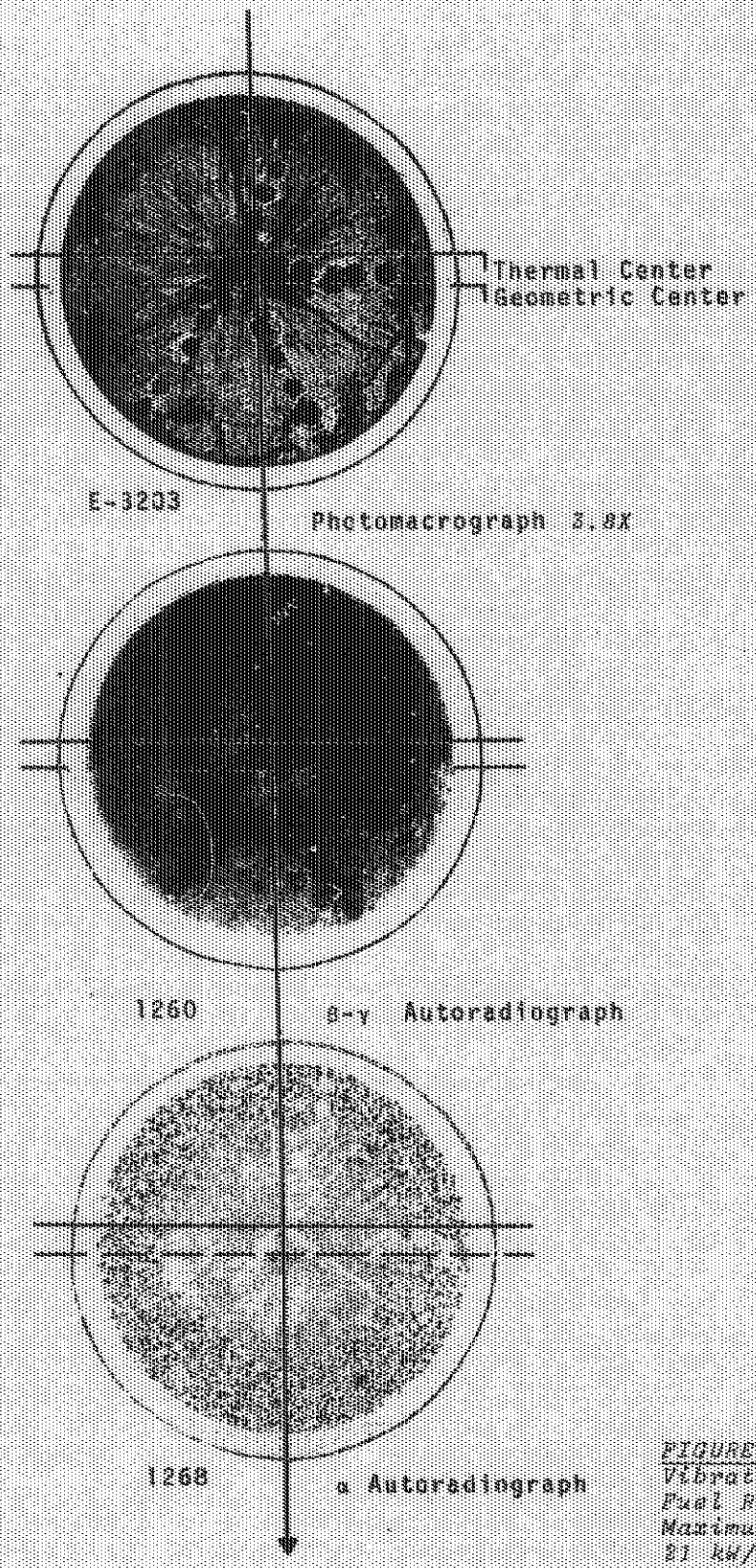

FIGURE 2.16. Transverse Section of a Vibrationally Compacted UO_2-2 wt% PuO_2 Fuel Rod Irradiated in PNPR at a Maximum Linear Power Generation of 21 kW/ft to 0.9 x 10^{19} fissions/cm^3. Location of Micro-Drilled Analytical Samples Is Shown.

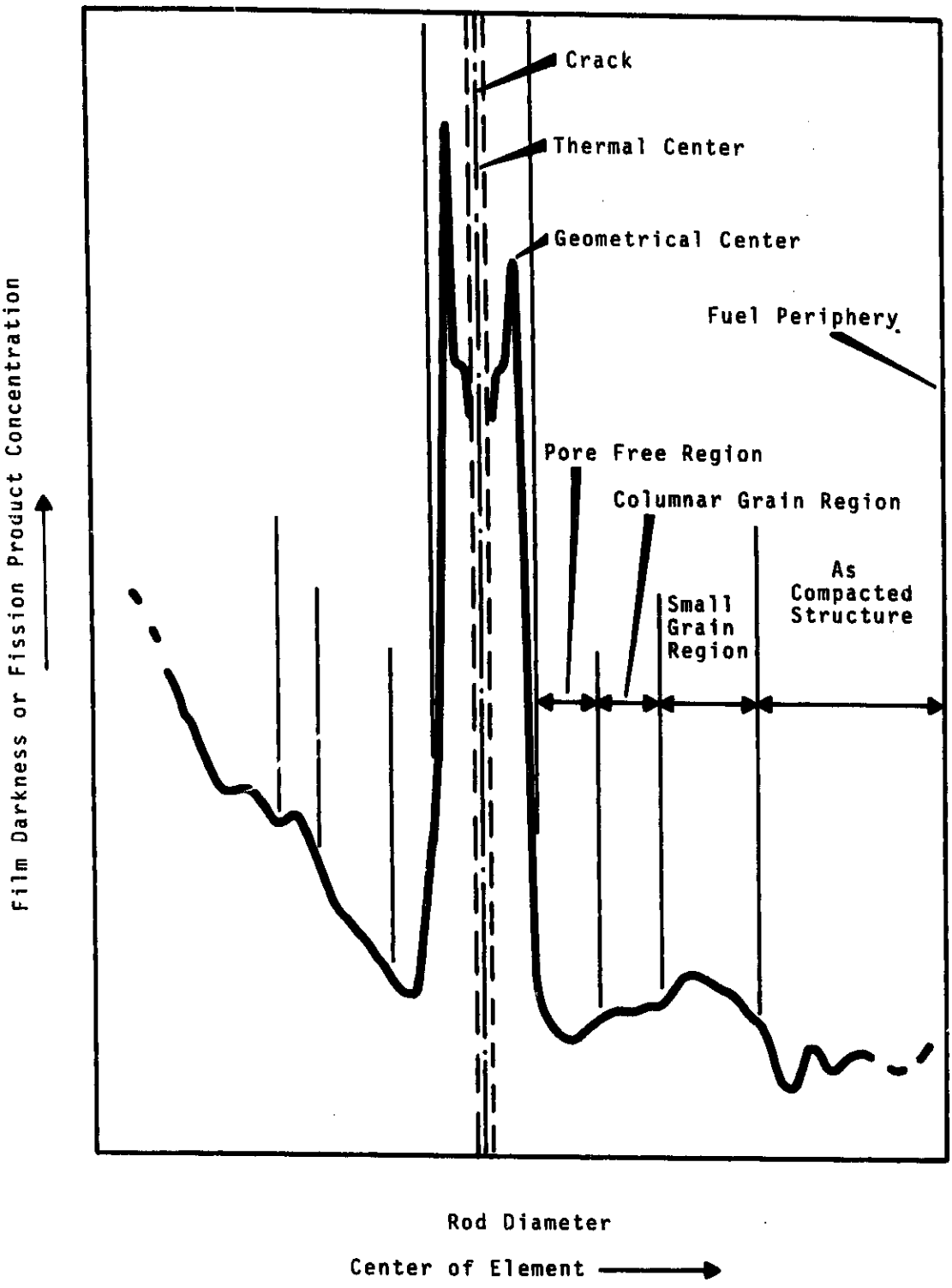

FIGURE 2.16. Micro-Densitometer Scan of the Beta-Gamma Autoradiograph. Direction is Radial with Respect to the Center of the Cluster.

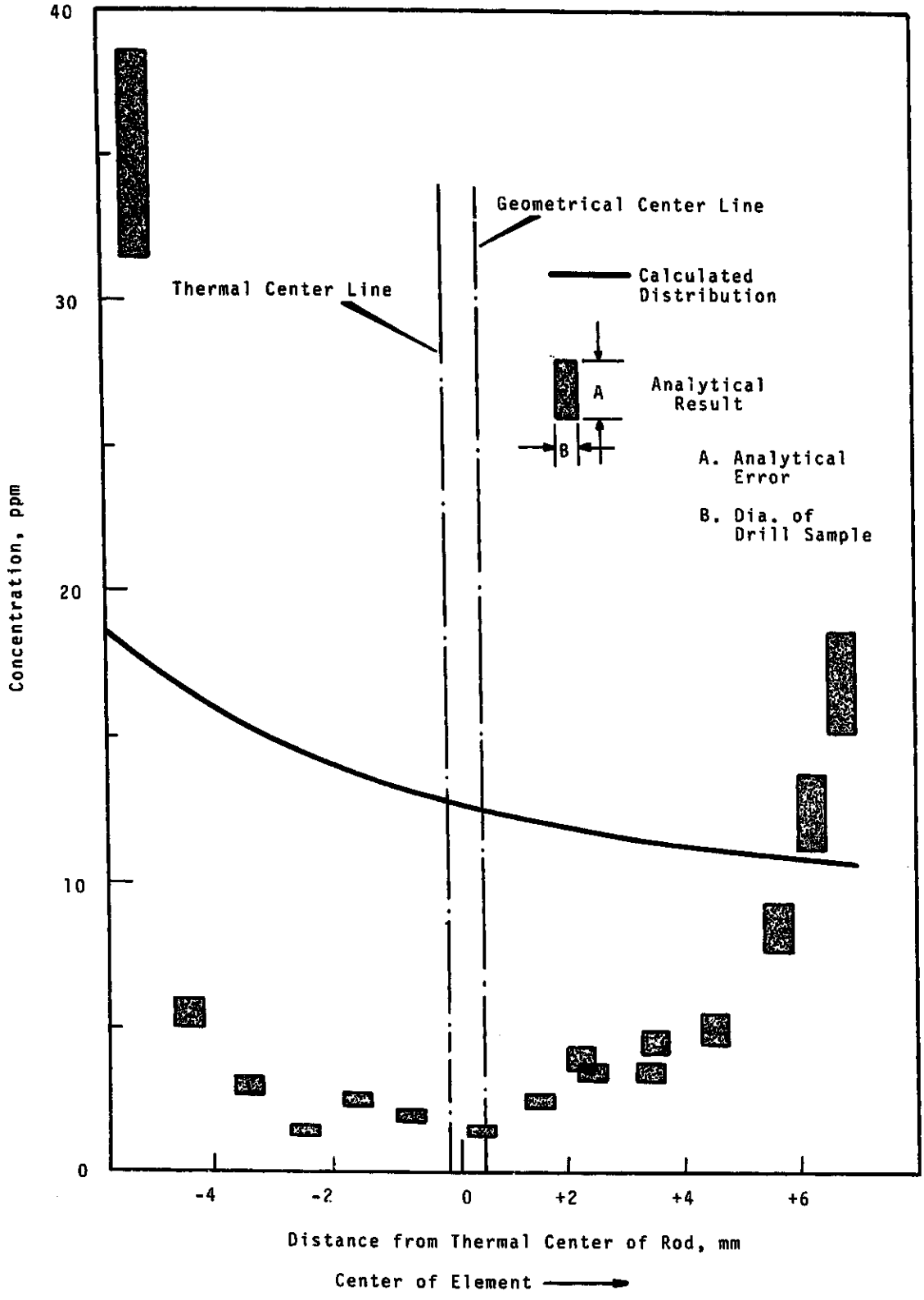

FIGURE 2.17. *^{137}Cs Distribution in an Irradiated UO_2–2 wt% PuO_2 Fuel Rod. The direction is radial with respect to the center of the element.*

axial relocation. Three types of restrictors were tested: 0.400 in. thick depleted UO_2 sintered pellets, 0.038 in. thick tungsten wafers, and 0.058 in. thick tungsten wafers. Although the element has not been subjected to destructive post-irradiation examination, the irradiation does indicate that a low density fuel element can operate satisfactorily under prototypic power reactor conditions including heat ratings to 16 kW/ft, coolant temperatures to 450 °F, and external pressures as high as 2500 psi.* A second experiment is now underway in which a similar fuel element will be irradiated to 10,000 MWd/tonne.

HIGH EXPOSURE PLUTONIUM STUDIES

R. C. Smith, L. G. Faust, and H. H. VanTuyl

Neutron and gamma dose rates and resultant personnel exposure problems can be significant when handling chemically separate plutonium that has been irradiated to the exposures now recommended for power reactors. The objective of the High Exposure Plutonium Study is to measure the dose rates from this type of plutonium.

Gamma and neutron dose rates increase as plutonium exposure increases. The increase in gamma and X-rays comes mainly from the increased amounts of ^{238}Pu and the daughters of ^{236}Pu and ^{241}Pu. The increase in neutrons comes mainly from the even numbered plutonium isotopes (^{238}Pu, ^{240}Pu, and ^{242}Pu). In addition, (α,n) reactions contribute significant additional neutrons.

The neutron energy spectrum from a 925 g sample of high exposure PuO_2 was measured and compared to similar values from a PuF_4 sample used as a standard at PNL. A plot of the two spectra (Figure 2.18) shows a marked difference in the average neutron energy of the samples. The PuF_4 sample emitted neutrons having an $\bar{E}$ of about 0.87 MeV, while the $\bar{E}$ of the neutrons emitted from the high exposure PuO_2 sample was nearly 2 MeV. Also, the spectrum from the oxide had a long fission tail which is probably due to the marked difference in isotopic composition of the high exposure PuO_2 sample compared to the PuF_4 sample. The isotopic content of the Pu in the PuO_2 sample was 22% ^{240}Pu, 4% ^{241}Pu, and 0.1% ^{238}Pu.

Aluminum–20 wt% plutonium fuel plates were recently fabricated at PNL from high exposure plutonium obtained from Shippingport Reactor. Spontaneous fissions and (α,n) reactions in the plutonium caused significant neutron dose rates from the fuel plates. Each plate, which contains an Al–20 wt% Pu core about 0.040 in. thick by 2.5 in. by 23 in. long clad in 0.020 in. of Al, read about 1200 counts/min (0.2 mrad/hr) when measured with a long counter at a distance of 1.7 ft. Stacking plates together increased the dose rate linearly with the number of plates; ten stacked plates had a dose rate of approximately 2 mrad/hr at 1.7 ft.

---

* *The test element was irradiated in 1600 psi flowing water but was inadvertently subjected to a static pressure of 2500 psi after irradiation.*

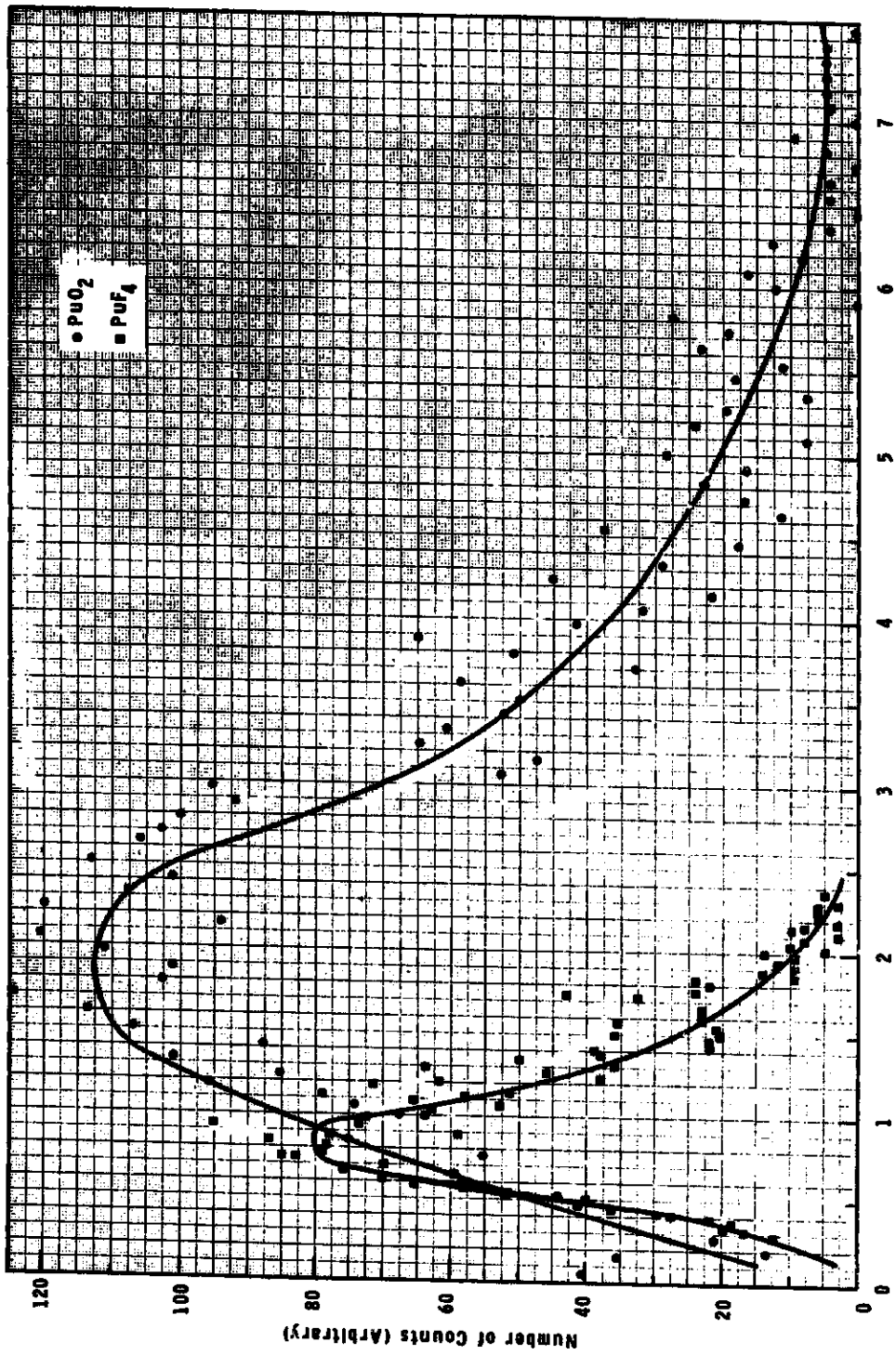

Neg 0673568

FIGURE 2.18. PuO_2 and PuF_4 Neutron Energy Spectra.

The gamma dose rates for these plates were 2.24 to 2.37 rad/hr at the surface of the aluminum cladding and dropped to 98 mrad/hr at 1 ft. When five plates were stacked together, the dose rate at 1 ft was approximately 110 mrad/hr, but stacking of additional plates did not increase the dose rate measurably. With the fuel plates on edge, nine plates spaced 3/16 in. apart measure 50 mrad/hr at 1 ft. The maximum gamma dose rate for any number of these plates in any configuration would, therefore, be 110 mrad/hr at 1 ft.

Dose rate attentuations by neoprene and lead loaded gloves were measured. With 50 mils of lead loaded glove material, attenuations of only 32% to 37% were obtained. Most of the soft energy gammas were attenuated within the source due to self absorption in the plates and cladding. A small amount of ^{106}Rh impurity, which contributed higher energy gamma photons, was detected in the plutonium.

Surface dose rate measurements were continued on PuO_2 sources from three Shippingport and one Dresden fuel samples to determine the surface dose rate buildup with time due to plutonium daughter products. Present measurements confirm previous results which showed that high exposure plutonium containing 6 1/2% to 8% ^{241}Pu is expected to double its gamma surface dose rate within the first 250 days.

Computer codes for evaluating the dosimetry data are being developed. The PEAK code now in use estimates the gamma photopeak energy and provides an integrated count of the area beneath the photopeak, but does not correct for background. Both a tabulated and graphical readout are obtained. The SAMPO code, which is now being debugged, adds to the PEAK code information a background correction, detector efficiency, best fit graphical, and a continuous energy shift (linearity) correction.

Dose rate attenuation by various materials was measured for three PuO_2 samples including Shippingport and Dresden high exposure plutonium and a "B" sample of intermediate exposure (88% ^{239}Pu). Figure 2.19 shows the attenuation provided by each of these materials. The gamma rays from the highest exposure sample (Shippingport PuO_2) were attenuated the most in the various materials studied. This confirms the thesis that the major portion of the dose rate from high exposure PuO_2 is due to low energy gamma rays, which are relatively easy to shield. It can be seen from the graph that 1/8 in. of lead will provide an attenuation factor of about 125 for the Shippingport PuO_2 sample.

A computer code for calculating surface dose rates from a plutonium source was developed based on the attenuation measurements made in the high exposure plutonium study. The plutonium sources for which calculations were made were in the form of oxide samples 60 to 100 g in size and bagged in three layers (33 mils) of vinyl plastic shielded with materials placed between the source and the detector window. Calculated data agree well with empirical results.

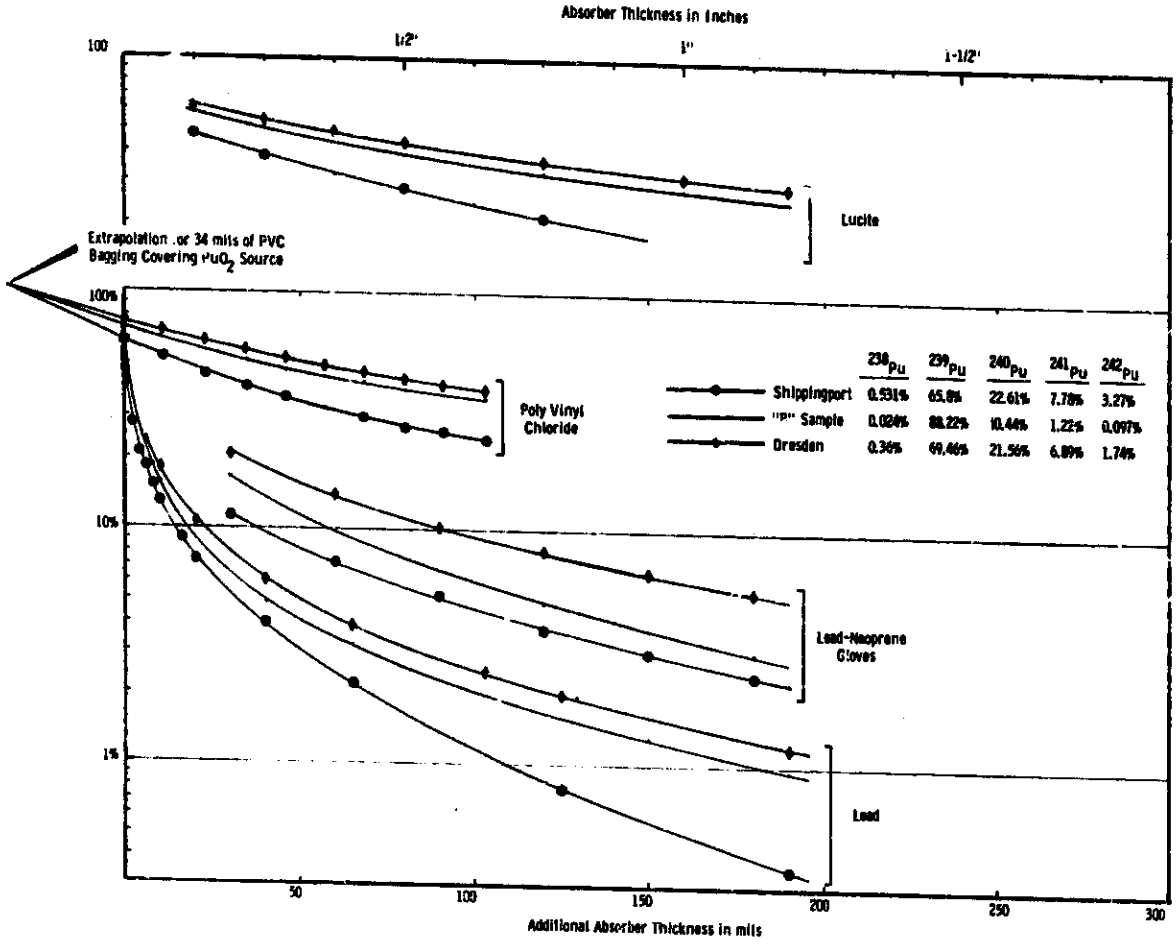

FIGURE 2.19. Reduction of Photon Dose Rate from PuO_2

The code was based upon a hemispherical rather than cylindrical source geometry to simplify the calculations. This induced only minor errors in the calculation, since the source was relatively large.

The program considers 13 nuclides associated with a plutonium source. These include the six isotopes of plutonium (236, 238, 239, 240, 241, and 242), the two daughters of ^{241}Pu (^{241}Am and ^{237}U), and the five daughters of ^{236}Pu (^{232}U, ^{228}Th, ^{224}Ra, ^{212}Pb, and ^{212}Bi). The dose rate of a pure isotope is calculated first, and the program is then supplied with the isotopic composition of the plutonium of interest. The program then calculates the dose rate as a function of time after chemical separation. Up to 30 different shielding configurations can be used with up to 6 different materials in each shield. At present, calculations have been made for Shippingport plutonium (the ^{239}Pu content varies from 65% to 46%, which is equivalent to exposures of 10,000 to 27,000 MWd/tonne), Dresden plutonium (69% ^{239}Pu, estimated equivalent to 20,000 MWd/tonne exposure), Yankee plutonium (from 87%

^{239}Pu to 56% ^{239}Pu, equivalent to exposures of 8000 to 38,000 MWd/tonne) and type "B" plutonium (approximately 88% ^{239}Pu). Shielding materials including PVC, Lucite, leaded gloves, steel, and lead, and plutonium ages of 1, 2, 5, 10, 20, 50, 100, and 200 days and 1, 2, 5, 10, and 20 years were used. The program indicates dose rates to be expected and will be a great help in defining future work needed in this study. The code will be modified and refined if warranted by additional empirical data.

CERAMIC FUEL DISSOLUTION STUDIES

L. D. Perrigo

Ceramic fuel dissolution processes are being developed to provide techniques for chemically decontaminating reactors that use ceramic fuel materials. Work during the past quarter has been centered on preparing equipment to study the effects of reactor exposure and operation on ceramic fuel dissolution behavior.

Current plans call for candidate dissolution procedures to be used on UO_2-PuO_2 fuel that has been exposed in the PRTR. Suitable specimens of this irradiated fuel will be placed in the IRP loop at 242-B Building, will be exposed to dissolution reagents, and the effectiveness will be measured. Use of the IRP for this work has required minor system modification and a thorough corrosion evaluation of the IRP loop, since this system has been used for about 40 fuel element rupture studies with accompanying chemical decontaminations. Preliminary data indicate no significant corrosion attack on the main loop system. Stress corrosion attack was found on a few tubing fittings, so all of these fittings will be replaced before further operation. Experimental operation is expected during the next quarter after fitting changes and modifications are completed.

3.0 REACTOR PHYSICS

PRTR BATCH CORE INTERIM CRITICAL TESTS - SERIES 1

J. W. Kutcher, R. E. Harris, and W. P. Stinson

The first series of interim critical tests have been performed in the Plutonium Recycle Test Reactor (PRTR) with the batch core loading.[1] The tests were run at a reactor burnup of 3369 MWd, which corresponds to an exposure of 2813 MWd or 1693 MWd/tonne for the 55 elements of the batch core. The tests began five days after reactor shutdown from power operation at 44 MW and were performed with the basic 55 element batch core configuration. The core is moderated and cooled with D_2O. The primary coolant system was cold and depressurized, with the primary coolant circulating on low flow.

The primary purpose of the first interim critical test was to determine the excess reactivity of the batch core loading of UO_2–2 wt% PuO_2 fuel elements for the first fuel burnup step. The reactivity worth of an individual batch core fuel element as a function of burnup was also of interest, along with changes in the boron coefficient of reactivity.

Experiments which were performed during the first series of batch core interim critical tests were Reactivity Worth of a Ring Three Element, Boron Worth and Concentration for the Cold and Xenon-free Loadings, and Spectral Density Measurements using Reactor Noise Techniques.

Reactivity Worth of a Ring Three Element

The exposure of fuel elements in ring three of the batch core is approximately the same as the average exposure for the basic 55 elements of the batch core. Measurement of the reactivity worth of a ring three element at each burnup step provides an additional means of determining reactivity changes in the batch core.

The reactivity worth of FE 6069, relative to the D_2O filled channel located in PC-1748, was determined during the initial batch core critical tests. In the first series of batch core interim critical tests, the reactivity worth of this element was again determined. In addition, the reactivity worth of FE 6506, which had zero burnup, was also determined in PC-1748. The results of these measurements are listed in Table 3.I. As expected, the reactivity worth of FE 6069 has decreased due to its burnup, while the reactivity worth of a clean element has increased relative to the core, due to the burnup of the core.

Boron Worth and Concentration for the Cold and Xenon-Free Loading

The primary means for determining batch core excess reactivity as a function of burnup is the measurement of the boron concentration associated with standard critical moderator heights of 90, 95, and 100 in. for each of the batch core

TABLE 3.I. Reactivity Worth of a Fuel Element

Batch Core Burnup, MWd/tonne	^{10}B in Moderator, wppm	Fuel Element	FE Exposure, MWd/tonne	FE Worth, mk*
0	19.24	6069	0	6.7
1693	16.71	6069	1930	6.0
1693	16.71	6506	0	7.1

* *All reactivities in this report are relative to an effective delayed neutron fraction of 3.08 x 10-3.*

burnup steps. The critical height was determined by an approach-to-critical measurement and the boron concentration was determined by analysis of a moderator sample in the Thermal Test Reactor. In Table 3.II are listed results from the initial batch core critical tests, along with results of the first series of interim critical tests. These results indicate a net reactivity loss of 34 mk during the batch core burnup of 1693 MWd/tonne.

TABLE 3.II. Characteristics of the Cold and Xenon-free Loading

Critical Height, in.	^{10}B in Moderator, ppm	Excess Reactivity, mk
Initial Critical Tests		
85.30	18.89	264
91.10	19.89	262
93.05	20.18	261
95.70	20.43	261
98.30	20.98	264
	Average =	262
First Interim Critical Tests		
90.67	16.32	228
95.75	16.80	226
100.52	17.30	229
	Average =	228

Spectral Density Measurements

Measurements of spectral density were made at four degrees of subcriticality, with 17.64 W ppm ^{10}B in the moderator. The first level was very slightly subcritical, the second was 0.27 mk subcritical, the third was 0.55 mk subcritical and the fourth was 0.94 mk subcritical. The moderator was at a high level in an attempt to remove from the spectrum a resonance which was believed to be caused by moderator level fluctuations.

The resonance was removed but an extraneous white noise contribution to the frequency spectrum was predominant. The power in the low frequency part of the frequency spectrum increases at the rate of 20 dB per decade from where the reactor break frequency was expected to occur, increasing toward the lower frequencies. The white noise could probably be reduced by cross correlating the spectral signals. However, future measurements will

probably be made at critical and the resonance reduced in intensity but not removed completely.

Reference

1. *J. W. Kutcher and J. H. Lauby. "Batch Core Critical Tests in the PRTR," Reactor Physics Department Technical Activities Quarterly Report, October, November, December, 1966, BNWL-400, Pacific Northwest Laboratory, Richland, Washington. April, 1967.*

PHYSICS CHARACTERISTICS OF REDUCED DENSITY UO_2-PuO_2 LOADINGS IN THE PRTR

U. P. Jenquin and T. M. Traver

There appears to be an economic incentive associated with the use of reduced density plutonium fuels in power reactors. The Plutonium Recycle Test Reactor (PRTR) would probably be utilized as a test bed for investigating the characteristics of these fuels. Survey calculations are being performed to determine the physics characteristics of reduced density UO_2-PuO_2 fuels in the PRTR. A summary of some of the results are given here.

The isotopic composition of the plutonium was assumed as 92% ^{239}Pu and 8% ^{240}Pu with the uranium being natural. The operating temperatures assumed for these PRTR loadings are: 58 °C for the moderator, 265 °C for the coolant, and 1000 °C for the fuel. The calculations are performed using the codes HRG,[1] THERMOS,[2] TEMPEST,[3] HFN,[4] and ZODIAC(2+2).[5]

The reactivity and effective multiplication was determined for fuel densities of 88, 70, 60, and 50% of theoretical density (TD) while keeping the PuO_2 density constant at 0.193 g/cm^3. The results are shown in Table 3.III. As expected, the reactivity increases as UO_2 density decreases. The 88% TD fuel is identical to the batch core fuel.[6] The effect of plutonium content on reactivity is shown in Table 3.IV. The results given in these two tables show that the reactivity varies considerably with the density and the plutonium content. Thus, considerable leeway is afforded in the physics design of these fuels in the PRTR.

Moderator, coolant, and fuel temperature coefficients of reactivity were calculated for fuel densities of 88 and 50% of theoretical. Preliminary results are listed in Table 3.V.

TABLE 3.III. Variation of Reactivity and Effective Multiplication of 55 Element PRTR Loadings for Plutonium Density of 0.193 g/cm^3

% TD	Reactivity, k_∞		Effective Multiplication, keff	
	Room Temp.	Operating Temp.	Room Temp.	Operating Temp.
88	1.404	1.368	1.213	1.202
70	1.456	1.421	1.252	1.241
60	1.488	1.452	1.276	1.265
50	1.522	1.486	1.301	1.291

The coefficients are all negative in sign and change significantly with the change in fuel density. The reactivity invested in the sum of moderator, coolant, and fuel heating is about 3% Δk/k for both types of fuel.

A burnup calculation was performed for a two-region PRTR core containing 19 irradiated batch core fuel elements surrounded by 66 UO_2-PuO_2 fuel elements at 50% TD. The 19 irradiated elements were assumed to have received an average exposure of 13,000 MWd/tonne (megawatt days per metric ton of UO_2-PuO_2). The core lifetime was calculated to be 19,000 MWd, thus increasing the average exposure on the batch core fuel elements by approximately 5000 MWd/tonne.

TABLE 3.IV. Variation of Reactivity with Plutonium Content at Room Temperature

Density of PuO_2, g/cm^3	Reactivity, k_∞	
	88% TD	50% TD
0.097	1.335	1.461
0.193	1.404	1.522
0.290	1.434	1.539

References

1. *J. L. Carter, Jr. "Computer Code Abstracts, Computer Code-HRG," Reactor Physics Department Technical Activities Quarterly Report, July, August, September, 1966, BNWL-340, Pacific Northwest Laboratory, Richland, Washington. October 15, 1966.*

2. *H. C. Honeck. THERMOS - A Thermalization Transport Theory Code for Reactor Lattice Calculations, BNWL-5826. Brookhaven National Laboratory.*

3. *F. H. Shudde and J. Dyer. "TEMPEST - A Neutron Thermalization Code," NAA Program Description, North American Aviation Corp. 1960.*

4. *J. R. Lilley. Computer Code HFN-Multigroup, Multiregion Neutron Diffusion Theory in One Space Dimension, HW-71545. General Electric Company, Richland, Washington. November, 1961.*

5. *R. H. Holeman and D. D. Matsumoto. ZODIAC(2+2): A Rev. to ZODIAC 2, BNWL-459. Pacific Northwest Laboratory, Richland, Washington. May 1967.*

6. *M. D. Freshley, F. E. Ianisko and R. E. Skavdahl. "Irradiation of UO2-PuO2 High Power Density Fuel Elements in PRTR," Trans. Am. Nucl. Soc., vol. 8, p. 365. 1965.*

TABLE 3.V. Average Temperature Coefficients of Reactivity

Type of Coefficient	Temperature Range, °C	Avg. Temp. Coeff., $\frac{1}{k_\infty}\frac{dk_\infty}{dT}$ (10^{-3}/°C)	
		88% TD	50% TD
Moderator	20-58	-0.101	-0.134
Coolant	20-265	-0.007	-0.004
Fuel (Doppler)	20-1000	-0.020	-0.017

TEMPERATURE COEFFICIENTS OF PuO_2-UO_2-H_2O LATTICES

V. O. Uotinen, S. Kobayashi, and U. P. Jenquin

Temperature coefficients of reactivity have been calculated for several PuO_2-UO_2-H_2O lattices and compared to experimental values. The calculations were performed using a model consisting of the codes THERMOS, HRG, and HFN, with four neutron energy groups. Calculated temperature coefficients for two lattices containing UO_2–2 wt% PuO_2 fuel rods[1] agree quite well with measured results. Calculated results for a lattice of UO_2–1.5 wt% PuO_2 fuel rods[2] do not agree as well with measured results. Reasons for this disagreement are being explored.

The temperature coefficient of reactivity is an integral quantity that is composed of many separate components. We have separated the calculated temperature coefficient into the contributions of various basic parameters by differentiating the two-group equation

$$k_{eff} = \frac{\bar{\eta}f_1 (1 - P_1)}{1 + \tau B^2} + \frac{\bar{\eta}f_2 P_1}{(1 + \tau B^2)(1 + L^2 B^2)} \qquad (1)$$

with respect to temperature. Upon differentiating Equation (1) we obtain

$$\frac{dk_{eff}}{dT} = \frac{\partial k_{eff}}{\partial \bar{\eta}f_1}\frac{\partial \bar{\eta}f_1}{\partial T} + \frac{\partial k_{eff}}{\partial P_1}\frac{\partial P_1}{\partial T} + \frac{\partial k_{eff}}{\partial \bar{\eta}f_2}\frac{\partial \bar{\eta}f_2}{\partial T} + \frac{\partial k_{eff}}{\partial \tau}\frac{\partial \tau}{\partial T} + \frac{\partial k_{eff}}{\partial L^2}\frac{\partial L^2}{\partial T} + \frac{\partial k_{eff}}{\partial B^2}\frac{\partial B^2}{\partial T} \qquad (2)$$

The contributions due to changes in the leakage parameters τ and L^2 are proportional to the buckling. In the small cores that were studied, these contributions as well as the contribution due to the buckling are quite large. An example of the relative importance of the various contributions is given in Table 3.VI.

A study was made to determine the importance of various assumptions which are made in the calculational model. It was found that it is very important to include (1) a temperature-dependent scattering kernel for water, which includes a correction for anisotropic scattering, (2) the

TABLE 3.VI. Contributions to Total Temperature Coefficient (at 55 °C) in Two Cores of UO_2–2 wt% PuO_2, V_M/V_F = 1.83

Parameter	Contribution to Temp. Coeff., 10^{-5}/°C: 8% ^{240}Pu	24% ^{240}Pu
$\bar{\eta}f_1$	-0.2	-0.1
P_1	-9.7	-10.3
$\bar{\eta}f_2$	+1.0	+5.2
τ	-18.3	-14.5
L^2	-3.6	-2.1
B^2	+10.7	+7.5

temperature-dependence of the H_2O-reflector, and (3) thermal expansion of lattice plates.

In general, the accuracy of calculated temperature coefficients for these high-leakage cores depends largely on how accurately the leakage is calculated. It appears advisable to measure temperature coefficients in low-leakage cores to minimize the contributions of the leakage terms. Likewise, it appears necessary to investigate the accuracy with which the leakage can be computed for these cores.

References

1. *V. O. Uotinen and L. D. Williams. "Experiments and Calculations for H_2O-Moderated Assemblies Containing UO_2–2 wt% PuO_2 Fuel Rods," Trans. Am. Nuc. Soc., vol. 10, p. 186. June 1967.*

2. *L. C. Schmid, et al. "Critical Masses and Bucklings of PuO_2-UO_2-H_2O Systems," Trans. Am. Nuc. Soc., vol. 7, no. 2, p. 216. 1964.*

BURNUP DATA FROM GAMMA SCANNING

D. E. Christensen, D. S. Murphy,* and G. Manca**

A set of seventeen rods from the Experimental Boiling Water Reactor (EBWR) at the Argonne National Laboratory have been gamma scanned at the Pacific Northwest Laboratory Gamma Scan Facility.[1] The rod identification numbers and fuel compositions are tabulated in Table 3.VII. The intensity of all fission product gamma rays above 675 keV was measured at several points along each rod to determine the relative fuel burnup of the rods and power distribution of the region of the core the rods were taken from. Also, gamma ray energy spectra using a NaI(Tl) detector and a Ge(Li) detector were obtained for each fuel composition. A complete report of the results is being readied for publication.

Typical of the data taken is that shown in Figure 3.1 which shows data for five standard UO_2-PuO_2 rods.

TABLE 3.VII. Fuel Composition of 17 Rods from the EBWR

Rod Number	Serial Number	Fuel Composition
1	EP98	UO_2-PuO_2 (8% 240)
2	EL67	UO_2-PuO_2 (8% 240)
3	E016	UO_2-PuO_2 (8% 240)
4	EV71	UO_2-PuO_2 (8% 240)
5	EX42	UO_2-PuO_2 (8% 240)
6	EY22	UO_2-PuO_2 (8% 240)
7	EY32	UO_2-PuO_2 (8% 240)
8	EI16	UO_2-PuO_2 (8% 240)
9	ET54	UO_2-PuO_2 (8% 240)
10	EQ51	UO_2-PuO_2 (8% 240)
11	EH24	UO_2-PuO_2 (8% 240)
12	EX89	UO_2-PuO_2 (8% 240)
13	EX01	UO_2-PuO_2 (20% 240)
14	EX55	UO_2-PuO_2 (26% 240)
15	EU07	Al-Pu (8% 240)
16	EU10	Al-Pu (26% 240)
17	EX65	Natural UO_2

* *Presently with the Physics Department, Central Washington State College, Ellensburg, Washington.*

** *On Assignment from the National Committee for Nuclear Energy, Rome, Italy.*

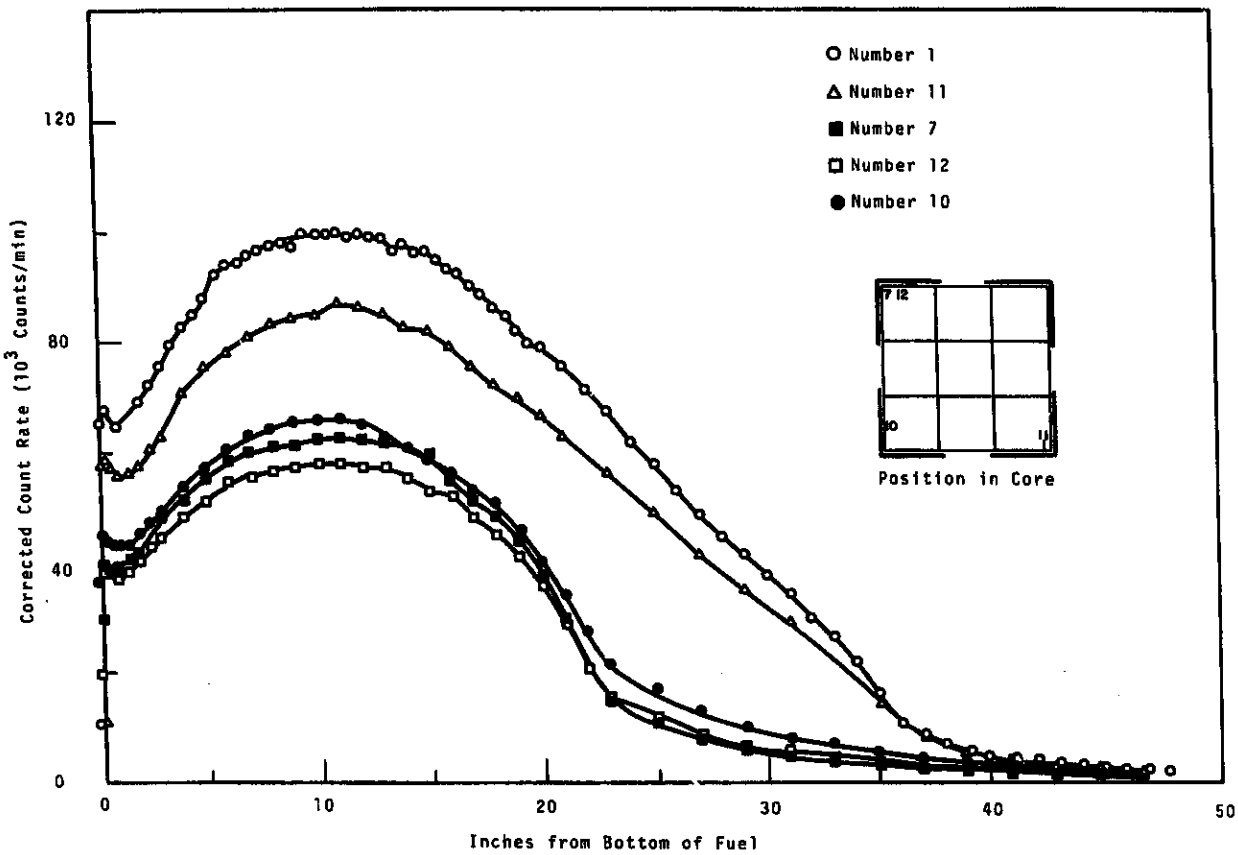

FIGURE 3.1. Gamma Scans of Fuel Rods Numbers 1, 11, 7, 12, and 10

The rods are from the plutonium region (see Figure 3.2) of the EBWR core which had reached an average exposure of 1300 MWd/tonne UO_2-PuO_2 before the rods were removed. They were taken from the upper left-hand quadrant (Zone 1) of the plutonium region and rod Number 1 was located at the center of the core. The insert in Figure 3.1 indicates the position of the five rods from Zone 1. The peak in gamma activity occurs approximately 11 in. from the bottom of the fuel, and there is very little burnup in the top of the fuel. This asymmetrical burnup pattern results from an increase in moderator voids at the top of the EBWR core and from the effect of the control rods which are active near the top of the core. It is evident from Figure 3.1 that the active portion of the center control rod ended 35 in. above the bottom of the fuel, while the active portion of the control rods adjacent to fuel rod numbers 7, 12, and 10 ended about 23 in. above the bottom of the fuel.

A second set of seventeen rods from the lower left-hand quadrant (Zone 2) of the plutonium region in the EBWR core have also been scanned. These rods were removed after the plutonium region reached

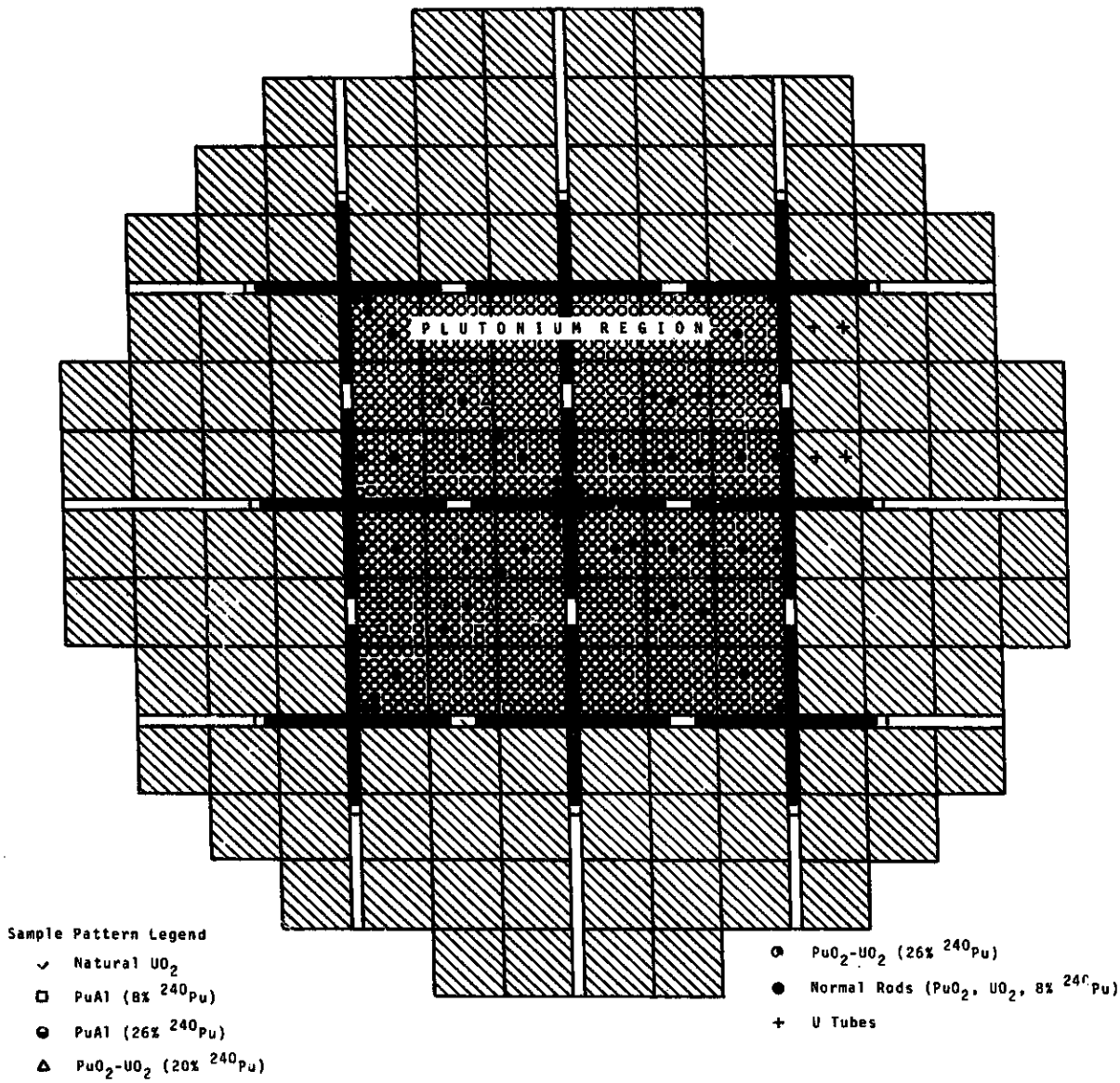

FIGURE 3.2. Plutonium Region of the EBWR Core

an average exposure of 2300 MWd/tonne UO_2-PuO_2. The data taken are yet to be summarized.

In addition to the rods from EBWR, two cermet fuel pins irradiated in EBR-II and one rod irradiated in the PRTR have been scanned during this reporting period.

References

1. *D. E. Christensen. "Gamma Scan Facility to Acquire Burnup Data by a Nondestructive Method," Reactor Physics Department Technical Activities Quarterly Report, October, November, December, 1966. BNWL-400, Pacific Northwest Laboratory, Richland, Washington. April, 1967.*

REACTOR APPLICATIONS EXPERIMENTS

L. D. Williams and R. Martinelli*

Experiments are in progress at the Plutonium Recycle Critical Facility as part of a cooperative program established between the USAEC and Italian Comitato Nazionale Per L'Energia Nucleare. The first series of reactivity measurements and power distributions have been measured in a H_2O-moderated core fueled with rods containing 1128 g of UO_2–2 wt% PuO_2 (8 at.% ^{240}Pu). The fuel, 0.508 in. diameter and 36 in. long, is clad with 0.030 in. Zircaloy-2. The rods are loaded at a 0.75 in. square lattice pitch. A fully reflected 19 x 19 square array of 361 rods was determined to have an excess reactivity of 14.5 ± 0.5 mk. A nearly cylindrical loading (the square array, but with 10 rods removed from each corner) was critical with 320.5 ± 0.5 fuel rods. This value agrees with the value measured at the Westinghouse Reactor Evaluation Center for an experiment[1] using the same fuel and lattice pitch.

Moderator reactivity coefficients and safety system worths were measured in preparation for reactivity and power distributions measurements. Moderator level calibrations were made down to a level 8 1/4 in. below the top of the fuel. The top reflector worth was determined to be 2.35 ± 0.02 mk. The safety system worths are listed in Table 3.VIII. An absolute accuracy of better than 10% is not expected for the worths since they were determined approximately from rod drop measurements.

Reactivity worths and power peaking due to water gaps were measured by gamma scanning fuel rods for various configurations of the nearly cylindrical loading. The configurations studied are shown in Table 3.IX and include, in addition to the uniform lattice

- A water hole (center rod removed),

TABLE 3.VIII. Safety System Worth

	Worth, mk	
	Cylindrical Loading	19 x 19 Square
Rod No. 7	6.0	5.2
Sheet No. 8	4.8	5.0
Total System (4 sheets + 2 rods)	38.8	35.6

* *On assignment from Comitato Nazionale Per L'Energia Nucleare, Rome, Italy.*

TABLE 3.IX. Configurations of the Nearly Cylindrical Core

Configuration	Shape	Number of Rods	Excess Reactivity, mk
Regular		321	+0.2 ± 0.1
Water Hole		320	+1.5 ± 0.2
Water Slot		309	+6.6 ± 0.5
Water Cross		284	+7.6 ± 0.5
9 x 9 Array		257	+8.2 ± 0.5
9 x 9 Array 25% super void		289	-0.6 ± 0.1
7 x 7 Array		249	+3.1 ± 0.2

- A water slot (all rods in a central row removed),
- A water cross (a second central row of rods removed perpendicular to the water slot,
- A 9 x 9 simulated element (rows of rods removed from around the center 9 x 9 array), and
- A 7 x 7 simulated element.

Analysis of the power distributions are in progress and results of the excess reactivity for the various configurations are listed in Table 3.IX. All reactivity values are for a delayed neutron fraction of 3.80×10^{-3}.

References

1. *R. D. Leamer, et al. PuO_2-UO_2 Fueled Critical Experiment, WCAP-3726-1. 1967.*

WATER MODERATED TEST LATTICES IN PCTR

D. F. Newman, D. R. Oden, W. P. Walsh, and A. D. Vaughn

The Physical Constants Testing Reactor (PCTR) technique has been extended[1] to include measurements of k_∞ and other neutronic parameters in light water moderated lattices by the development and use of the PCTR

water tank. This facility is especially valuable in the current particle size experiments where determination of the reactivity effect of changing the size of PuO_2 particles in fuel mixtures of PuO_2-UO_2 can be compared for both the graphite moderated and water moderated systems.

Measurements in the PCTR utilizing 0.9 wt% PuO_2 rods in a 1.0 in. square lattice moderated by light water have been made. Foil activation measurements were obtained to be used to determine the infinite medium neutron multiplication factor by both the null reactivity technique[2] and the adjoint weighted excess neutron production cross section measurements.[3,4] Null reactivity measurements were made with boric acid mixed with water as the neutron absorber.

Experiments with 2 wt% PuO_2-UO_2 fuel rods and varying PuO_2 particle sizes have been started for comparison with previous measurements in graphite moderator.

Description of the Tank[5]

A two region tank of ASTM-type 1100 aluminum was designed and fabricated to contain fuel rods in a water moderator with the assembly to fit inside the 37.5 in. PCTR test cavity (see Figure 3.3). The tank was constructed in two regions; the outer region is an annulus, 17-1/2 in. outside diameter and 12-1/4 in. inside diameter; the inner region of the tank is 11.5 in. in diameter. The tank was designed in these two regions so that possible extra buffers could be charged into the outer region if required, and also, so that the inner tank could fit into the Thermal Test Reactor (TTR).

For the initial experiments, the templates in the inner tank were designed to contain 108, 1/2 in. diameter fuel rods in a 1 in. square lattice pitch. Beneath the tank is an aluminum drip pan to contain any water in event of a leak.

Center Cell Description

Sixteen of the 1/2 in. diameter fuel elements and 1 gal of light water are contained in a 20 in. long and 4 in. wide square lucite container (see Figure 3.4) with front and rear buffers of the same geometry but short so that their combined length does not exceed the 37-1/2 in. limitation of the PCTR test cavity. This center cell is contained inside a 4-1/4 in. square zirconium can which extends the full length of the inner tank. The zirconium wall contains punched holes in a regular array and sealed with 0.004 in. thick mylar. Therefore, the center cell can be removed without the necessity of draining and refilling the inner tank.

Radial Buffer Region

The region of the inner tank bounded on the inside by the square zirconium can and on the outside by the inner region tank wall is referred to as the radial buffer

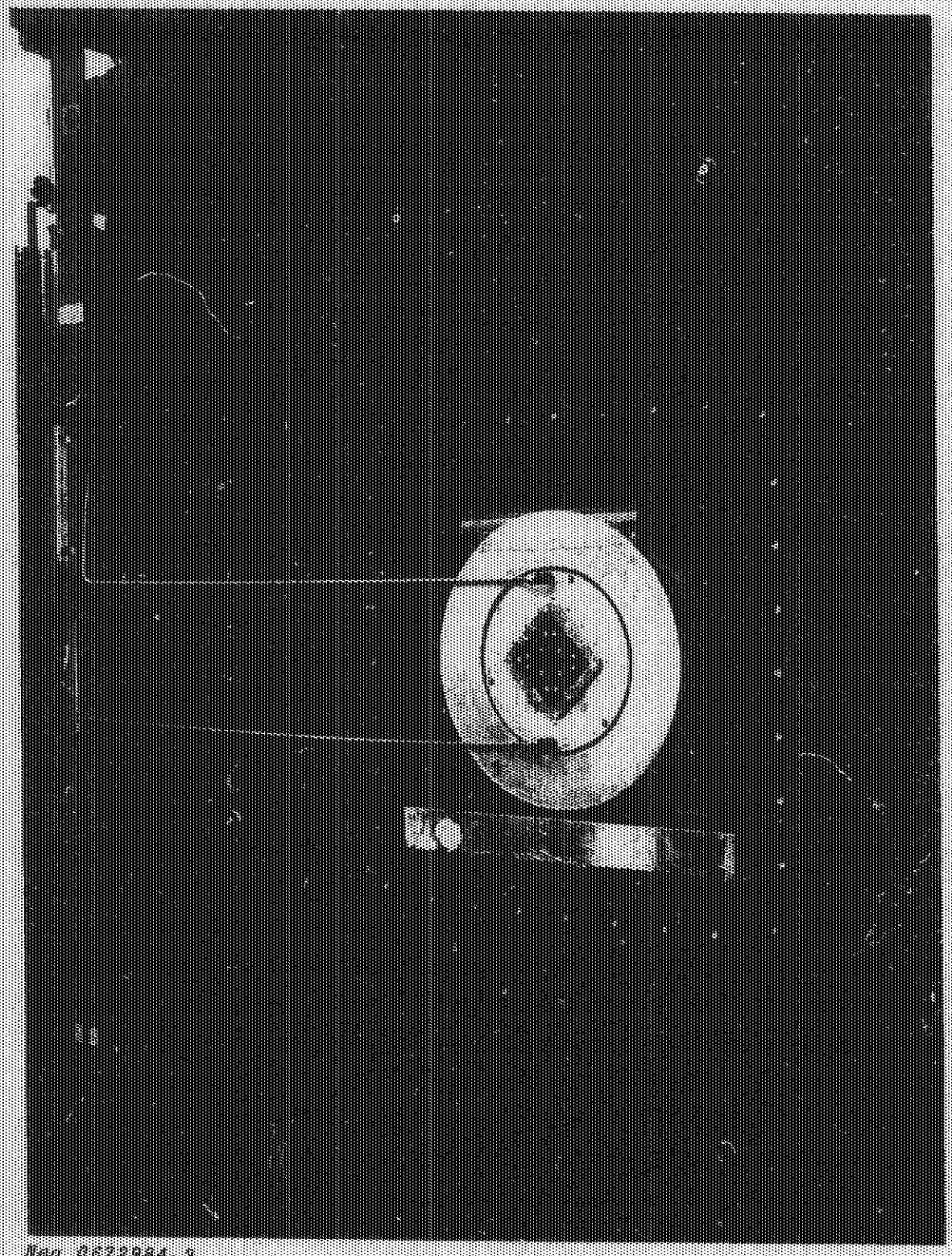

Neg 6672984-2

FIGURE 3.3. PCTR Test Cavity

FIGURE 3.4. Illustration of Square Inertia Container

region. This buffer region can contain 92 of the 108 total fuel elements in the inner tank cylinder (16 are contained in the center cell) plus 10.5 gal of light water.

Initial Loading and Critical Tests

Only the inner tank has been used in the initial fuel loading for PCTR tests: the outer region has remained empty of both water and fuel. The initial fuel loadings were done with mixed oxide fuel (PuO_2-UO_2) in the water tank and standard PCTR driver fuel in the surrounding graphite. The initial loading configuration is shown in Figure 3.5 and illustrates the nearest driver fuel 8-1/2 in. outside the PCTR cavity. Natural uranium fuel rods, 1/2 in. diameter, were placed between the cavity and the driver fuel to increase the average neutron energy incident on the water tank. Initial criticality was achieved with the water tank in the PCTR test cavity with the following fuel inventory:

108, 0.9 wt% PuO_2-UO_2 (8% ^{240}Pu) in the inner tank and center cell and water moderator
58, PCTR driver elements
128, natural uranium fuel rods in graphite surrounding the tank
outer tank empty

Reactivity Characteristics and Safety Specifications

With the water tank in the PCTR, the potential reactivity change due to water loss is of primary importance. Initial measurements of this effect indicated the change in reactivity to be continuously negative. In order to change the spectrum incident on the water tank, the 128 natural uranium rods were removed, criticality was reached with only 40 drivers, and the water loss reactivity was remeasured. The removal of 128 natural uranium fuel rods (total of four per channel) in the graphite moderator sufficiently altered the neutron spectrum incident on the water tank so that the reactivity change due to water loss increased the reactivity until 25% of the water had been removed; further water loss decreased the reactivity.

0.9 wt% PuO_2 Single Rod PCTR Experiment

Following the critical approach and safety parameter measurements, an experimental measurement of k_∞ was started with the 0.9 wt% PuO_2-UO_2 (8% ^{240}Pu) mixed oxide rods in the water tank, 1 in. square lattice, and light water moderator. The experimental procedure included the null reactivity technique, with boric acid dissolved in the water as a neutron absorber, and the adjoint weighted excess neutron production cross section measurements, which do not require the absorber in the cell during the experiment. The change in the procedures for this technique, specific to water tank measurements, are described below.

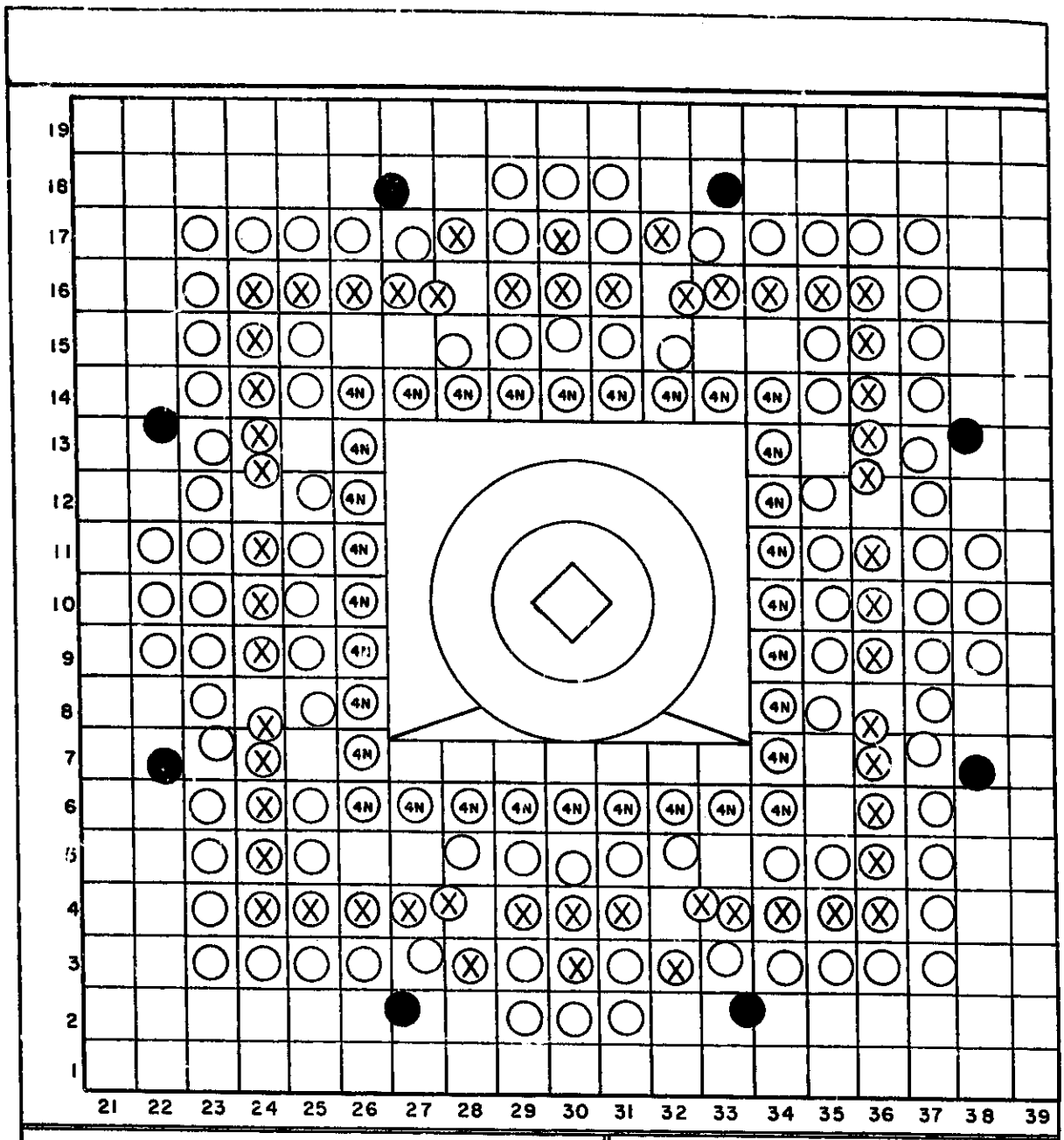

X - DRIVER
C - 6"Al - U FUEL
J - 8"Al - U FUEL
POISON USED - YES ☐ NO ☒
H - H TUBE
E - EMPTY
N - 0.5" NAT. U.
O - CONTROL ROD

LEVELING SLUG POSITIONS - INCHES OUT			
	INNER	MIDDLE	OUTER
FRONT	3.0"	3.0"	0.0"
REAR	3.0"	3.0"	0.0"

REMARKS: 0.9 wt% PuO_2/PuO_2-UO_2 single rods in 1" square pitch light water moderator.
128 natural uranium flux modifiers
108 .9% PuO_2 rods in core tank (16 in center container, 92 in inner tank).

FIGURE 3.5. PCTR Core Fuel Loading Diagram with Water Tank

Flux Matching

The measurement of k_∞ requires that the neutron energy distribution in the test cell be typical of that to be found in an infinite array of cells. Integral spectral indices are measured throughout the test cell and buffer regions in order to determine if the condition of an equilibrium spectrum has been achieved.

The cadmium ratio, obtained by placing bare and cadmium covered 0.020 in. diameter gold pins on the fuel cladding surfaces, was found to be sufficiently sensitive for this purpose. The pin locations for the cadmium ratio measurements are shown in Figure 3.6 and 3.7.

The radial traverse data (see Figure 3.8) indicates that 108 fuel elements in the inner container were more than adequate to achieve an equilibrium neutron spectrum across the center cell; however, equilibrium in the axial direction was not so easily attained.

Axial spectrum measurements indicated that level ring position has little effect on the spectral conditions in the center cell. In order

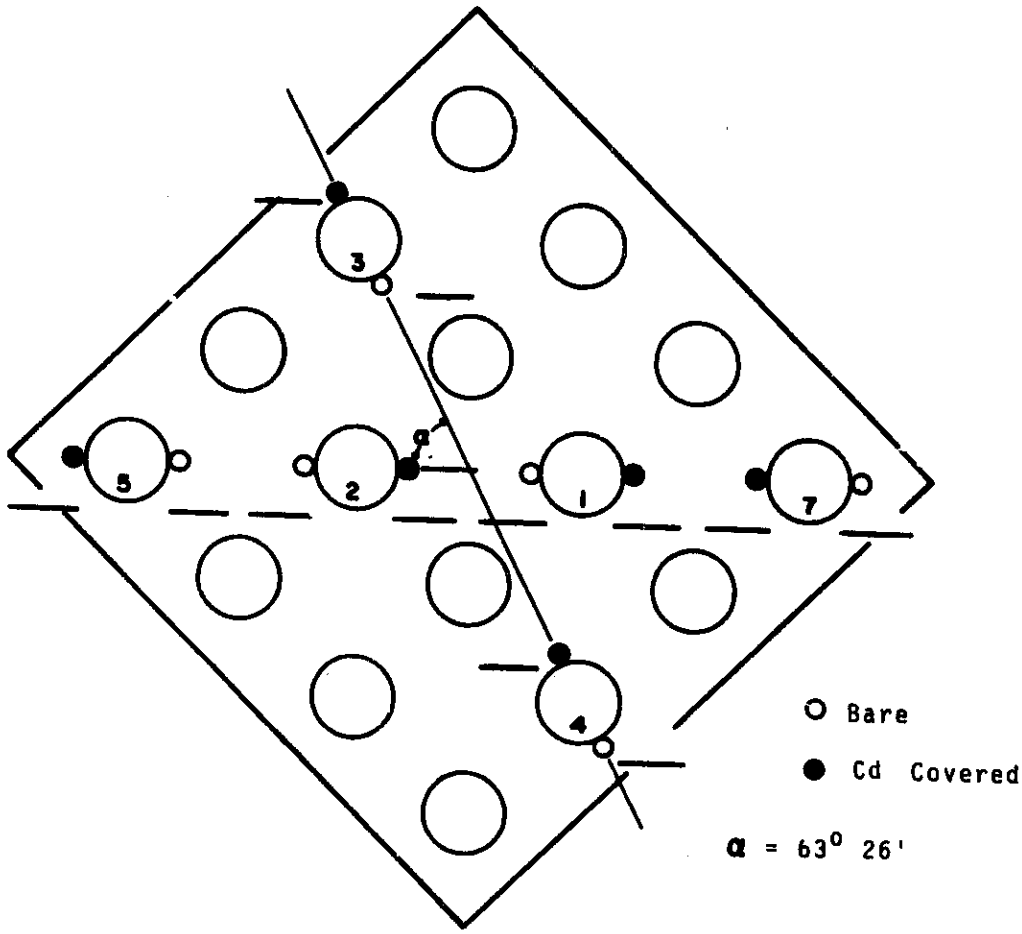

FIGURE 3.6. Pin Locations in Central Core Container

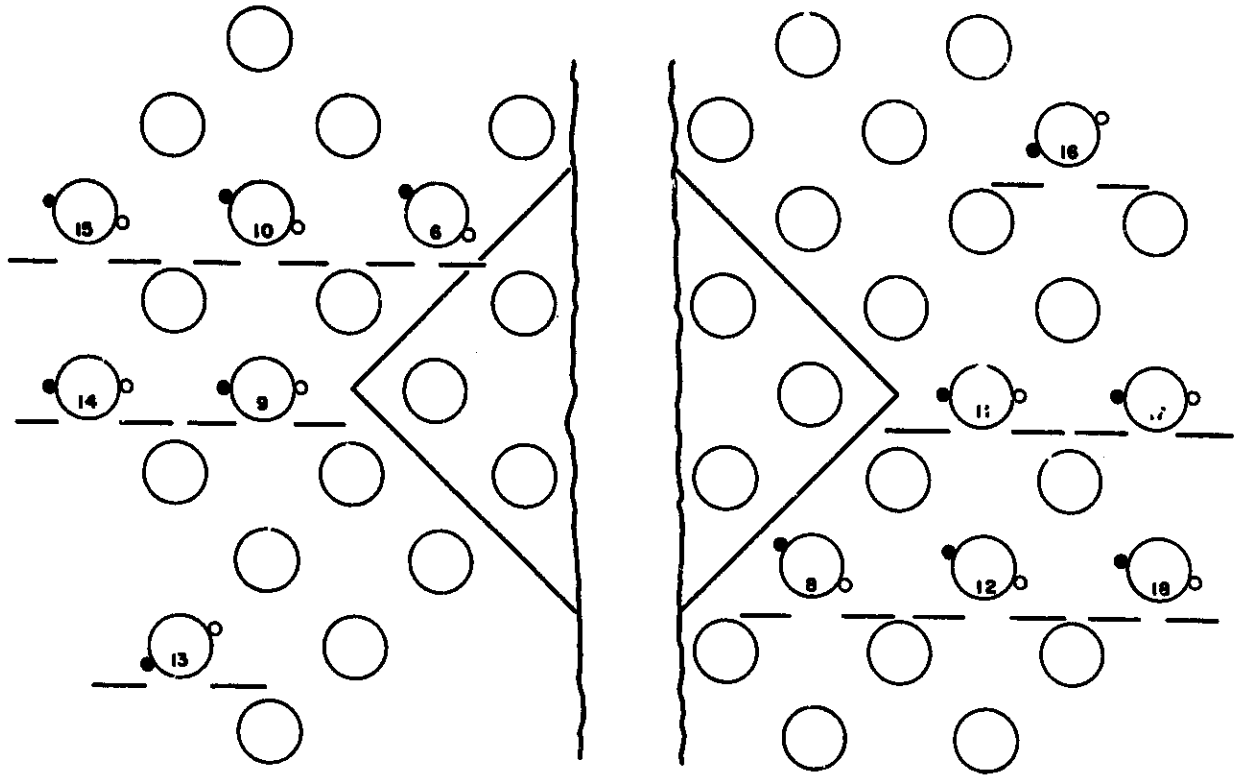

FIGURE 3.7. Pin Locations in Radial Buffer Tank

to prevent thermal flux peaking at the ends of the fuel elements due to moderation in the polyethylene and lucite container ends, it was sufficient to add cadmium discs (12 mils thick) and ^{235}U foil (2 mils thick) outside the ends of the center cell. The differences in the flux between these conditions are shown in Figure 3.9.

It should be noted that the neutronic parameters derived from the experiment are not as sensitive to these end effects in the axial traverse as Figure 3.9 seems to indicate. The preliminary results show that the maximum effect of end peaking is only 2% of the final measured value (k_∞ - 1).

Cell-In and Cell-Out Measurements

The measurement of the reactivity change between center cell-in and center cell-out conditions is essentially the same for the water tank as for graphite moderated systems and comparable accuracy could be attained.

Null Reactivity Technique

Additional data for the determination of k_∞ by the null reactivity technique was obtained for the 0.9 wt% PuO_2 rods with boric acid in the water. Reactivity measurements, made with several concentrations of boric acid in the water, indicate that the

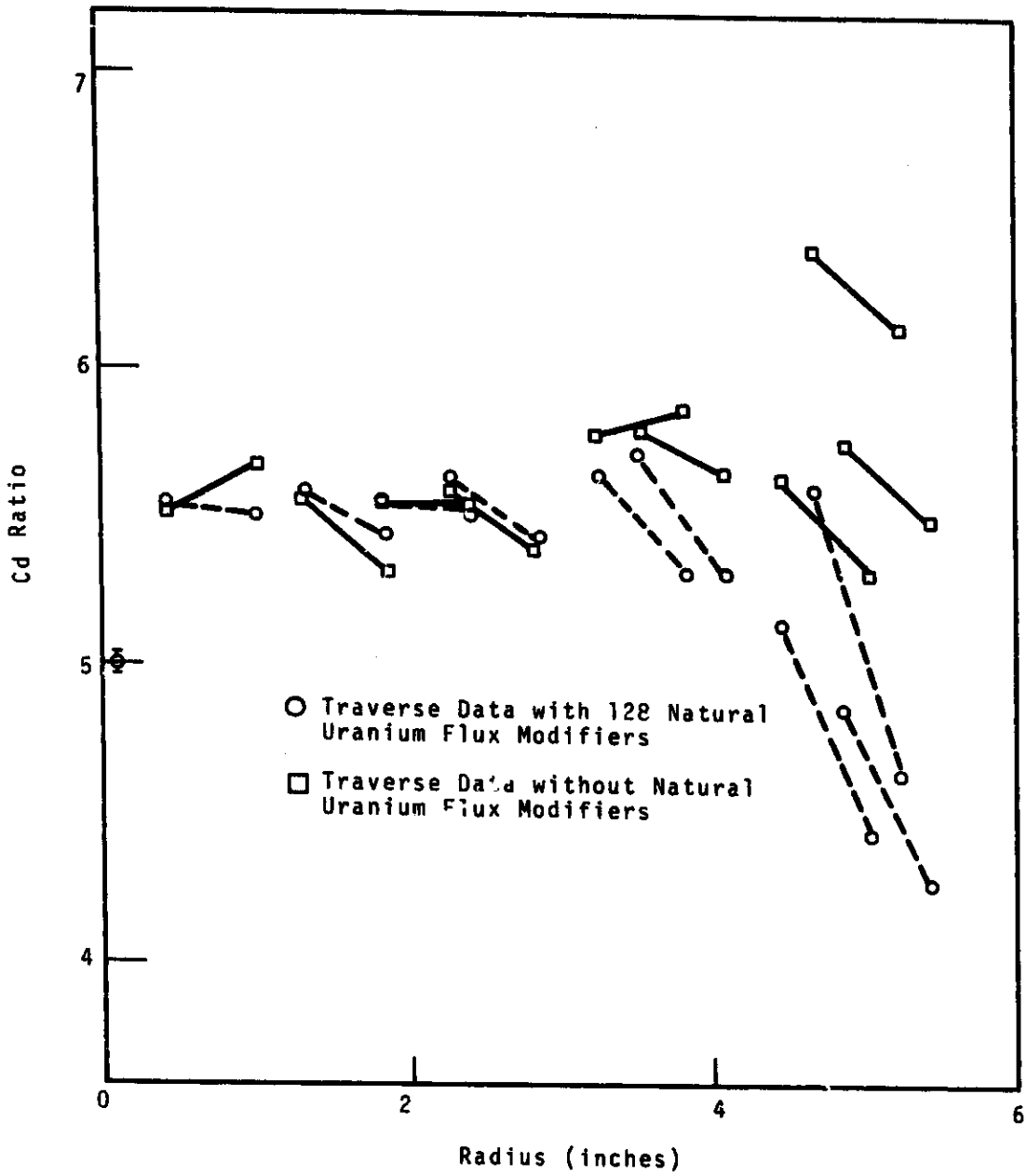

FIGURE 3.8. Radial Traverse Data

concentration of boron required to reduce k_∞ to unity is approximately 273 ppm by weight.

Foil Irradiations

Spatial distributions of the neutron reaction rates in each region of the test cell are required for determination of the neutron utilization in the lattice cell. The foil irradiations in the lattice, both with and without boron, have been made for the experiment with 0.9 wt% PuO_2 rods. However, only the foil irradiations in the lattice without boron have been made for the experiment with 2.0 wt% PuO_2 rods at the present time.

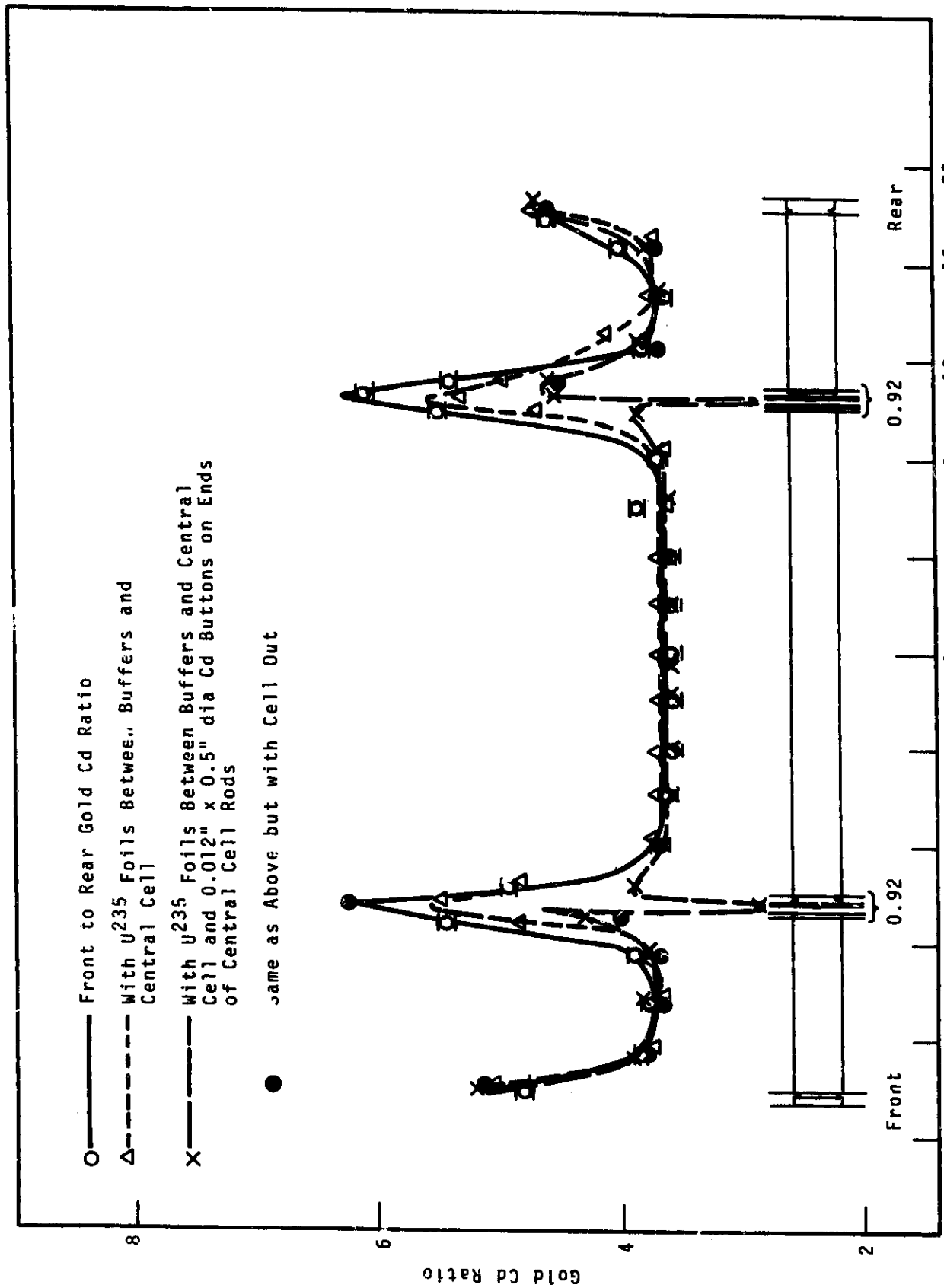

FIGURE 3.9. Axial Flux Traverse Data (36 2 wt% $Pu:O_2$–UO_2 Rods)

The spatial distribution of the reaction rates in the lattice are determined with copper foils and pins and fission foils strategically placed throughout the lattice in the fuel. These foils and their holders are of particular interest because of the detail they provide during the cell analysis and the unique way they are positioned in the water lattice. Therefore, a loading diagram is shown in Figure 3.10 which shows the positions of the copper pins and quadrants irradiated in the center cell.

The radial traverse through the moderator was taken with pins contained in a specially constructed lucite container. This assembly is illustrated in Figure 3.11.

Effects of Changing to 2 wt% PuO_2-UO_2 Rods in Water Tank

After the experiment with the 0.9 wt% fuel had been completed, sixteen of the central rods were replaced with 2 wt% PuO_2-UO_2 fuel rods (8% ^{240}Pu), and the PCTR drivers were reduced accordingly. The

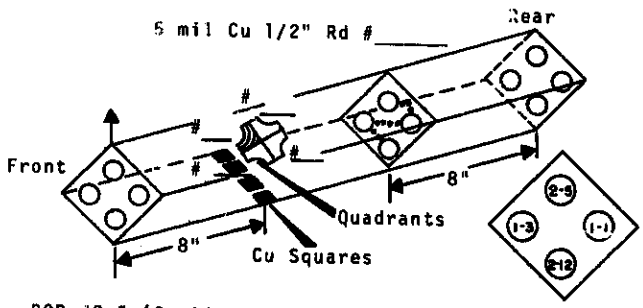

5 mil Cu Rd 1/2" dia #____
5 mil Cu Sq. 443" #____
36 mil dia Cu Pin 1/4" #____
10 mil Cu Quad #____
5 mil Cu Quad #____
3 mil Cu Quad #____
U^{235} 1/2" Rd #____
PuAl 1/2" Rd #____
Nat. U 1/2" Rd #____
Dep. U 1/2" Rd #____
1/2 mil Au 1/2" Rd #____

ROD #2-5 (Cu Pins Toward Open Side)

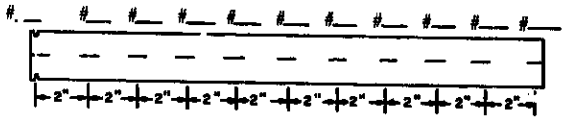

℄

ROD #1-1 — Packet #1 — ROD #1-2

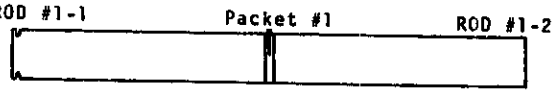

Packet #1
- PuAl #____
- 0.0005" Au #____
- 0.005" Cu #____
- UAl #____

*ROD #1-3 — Packet #2 — ROD #1-4

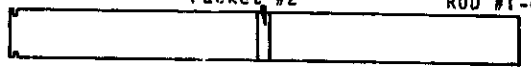

Packet #2
- Natural U #____
- Depleted U #____

UNIRRADIATED MONITORS
- Natural U #____
- Depleted U #____
- U^{235} Al #____
- PuAl #____

* Separable Rods have 0.005 inch end Caps at one End and are Held Together with an Aluminum Sleeve.

FIGURE 3.10. Center Cell Foil Loading Diagram

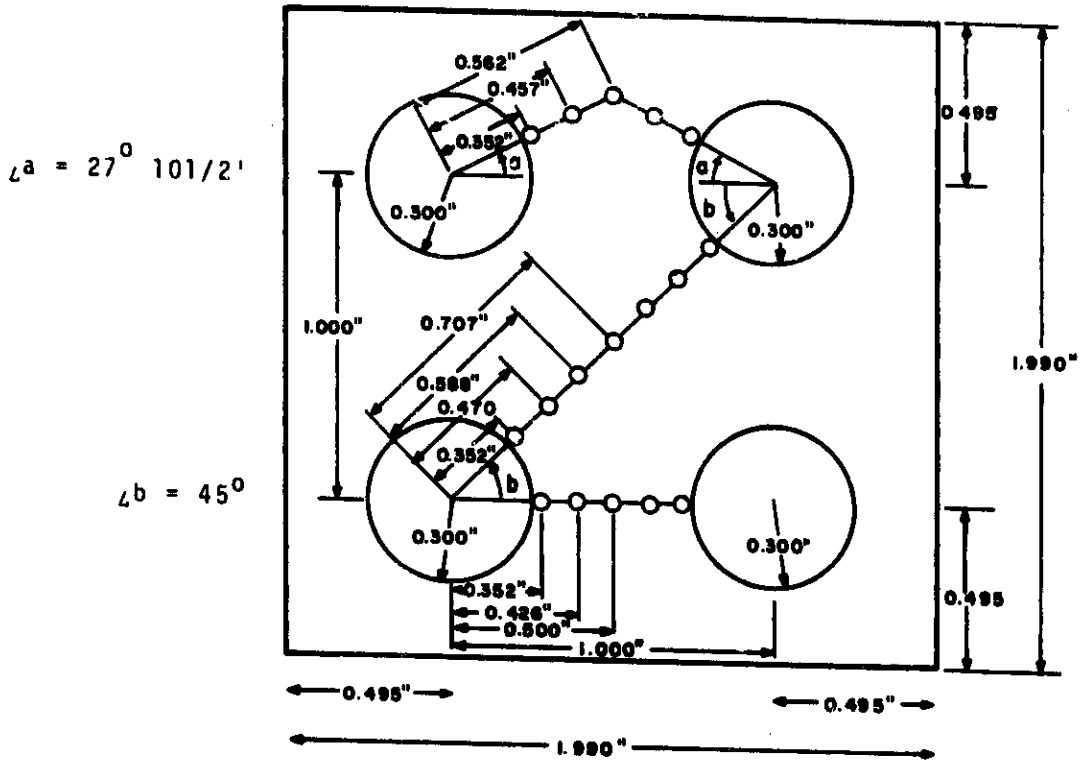

Small Pin Holes = 0.040" Bare, 0.082" Cd. Covered

Material: Lucite

1/16" Lucite Plate Thickness

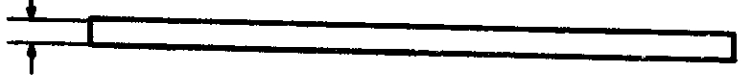

Drill Holes all the way Through

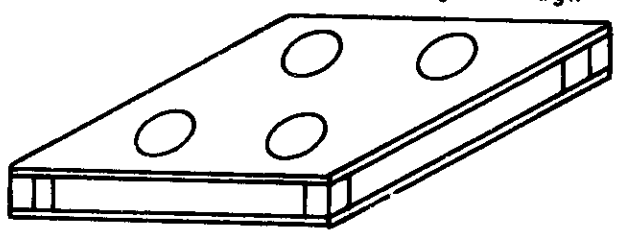

FIGURE 3.11. Lucite Pin Holders

radial and axial flux traverses were remeasured, followed by the replacement of twenty more of the 0.9 wt% fuel rods with the 2 wt% rods. The results of the successive axial traverse measurements are illustrated in Figure 3.12 and indicate that it was sufficient to change only 36 of the central rods to the 2 wt% fuel rods before attaining an equilibrium neutron spectrum across the cell. Thirty-four standard PCTR drivers were necessary to achieve critical with

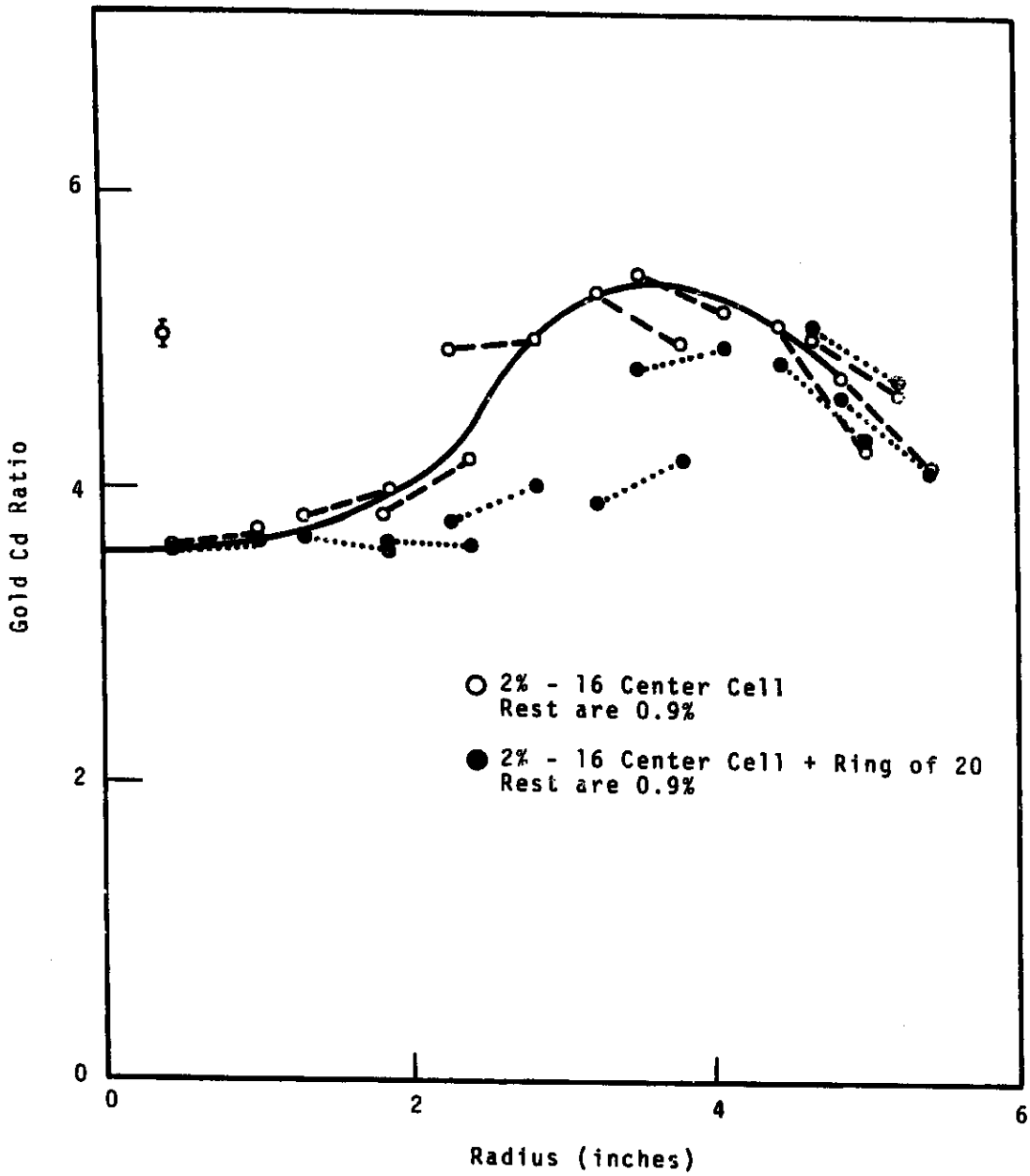

FIGURE 3.12. Radial Traverse with 2 wt% PuO_2-UO_2 Rods

36, 2 wt% PuO_2-UO_2 rods in the center, surrounded by 72, 0.9 wt% PuO_2-UO_2 fuel rods.

Particle Size Fuel Rods

Four sets of 2 wt% PuO_2-UO_2 rods (8% ^{240}Pu) were manufactured for the center cell. Each set of four 20 in. rods was made from different particle sizes so that reactivity differences due to PuO_2 particle sizes could be measured. These reactivity comparisons were previously measured in a graphite lattice with a 4 in. pitch. The reactivity of the

rods have now been measured in the water tank, and the data is currently being analyzed.

References

1. *H. L. Henry. "Authorization Letter, 67-11, Mixed Oxide Fuels in H_2O Moderated Tank." August 10, 1967.*

2. *D. J. Donahue, D. D. Lanning, R. A. Bennett, and R. E. Heineman. "Determination of k_∞ from Critical Experiments with the PCTR," Nucl. Sci. Eng., vol. 4, p. 297. 1958.*

3. *R. E. Heineman. Reactivity Measurements on Samples of Multiplying Media, BNWL-SA-263, Pacific Northwest Laboratory, Richland, Washington. November 14-18, 1965.*

4. *N. A. Hill, E. P. Lippincott, D. F. Newman, D. D. Lanning, and R. E. Heineman. "Comparison of PCTR Measurements Using Un-Poisoned and Poisoned Techniques on PuO_2-UO_2 Graphite Systems," Physics Research Quarterly Report, April-May-June, 1967.*

5. *Blueprints H-3-27001, Sheets 1 through 9.*

AN IMPROVED SHORT TIME APPROXIMATION FOR EVALUATING THE EGELSTAFF-SCHOFIELD SCATTERING LAW MODEL

C. W. Lindenmeier

As discussed in previous Physics Research Quarterly Reports, hereafter referred to as I and II,[1,2] experimental measurements of the scattering law for water appear to be fitted, with good accuracy, by Egelstaff-Schofield theory[3] using an analytical spectral function of the form

$$\rho(\beta) = \frac{1}{M}\,\delta(\beta) + \sum_i C_i\, g_i(\beta) \qquad (1)$$

where

$$g_i(\beta) = e^{-\delta_i/4}\,\beta \sinh \beta/2 \left[e^{-(\beta-\gamma_i)^2/4\delta_i} + e^{-(\beta+\gamma_i)^2/4\delta_i}\right] \div (2\sqrt{\pi\delta_i}\, D_i) \qquad (2)$$

$$D_i = \delta_i \cosh \frac{\gamma_i}{2} + \gamma_i \sinh \frac{\gamma_i}{2} \qquad (3)$$

$$\int_0^\infty g_i(\beta)\, d\beta = 1 \qquad (4)$$

and

$$\frac{1}{M} + \sum_i C_i = 1 \quad . \qquad (5)$$

If the spectral function is given by Equation (1), the width function

$$W(t) = \int_0^\infty \rho(\beta)\,(\cosh \beta/2 - \cos \beta t)\, d\beta$$

then has the analytical form:

$$W(t) = \frac{1}{M}\,(1/4 + t^2) - \sum_i Q_i(t) \qquad (6)$$

where

$$Q_i(t) = A_i - B_i \cos \gamma_i \, te^{-\delta_i t^2} \tag{7}$$

$$A_i = \frac{C_i \cosh \gamma_i/2}{D_i} \tag{8}$$

and

$$B_i = \frac{C_i \, e^{-\delta_i/4}}{D_i} \tag{9}$$

Based on Egelstaff-Schofield theory, the scattering law is given by

$$S(\alpha,\beta) = \frac{1}{2\pi} \int_{-\infty}^{\infty} dt \, e^{i\beta t} \, e^{-\alpha W(t)} \tag{10}$$

Evaluating the scattering law, Equation (10), still requires the numerical integration of a Fourier transform type integral. To generate scattering kernels in the form required by transport analysis, it is necessary to perform an integration over $S(\alpha,\beta)$ which requires evaluating $S(\alpha,\beta)$ many times. Hence, it is desirable to find methods which permit economical computer evaluations. Three methods have proved successful: direct fourier transformation, expansion in a power series in α, and expansion in an asymptotic series in α^{-1}.

The short time approximation finds application in evaluating the scattering law as a power series expansion in α, and as reported in I and II consisted of approximating the Q_i's as given by Equation (7) for the cases in which

$$\gamma_i << \beta$$

by expansion to second order about $t = 0$:

$$Q_i(t) \approx A_i - B_i\left(1 - \frac{\gamma_i^2}{2} + \delta_i\right)t^2 \tag{11}$$

Considerable improvement in accuracy can be obtained in the short time approximation by expanding $Q_i(t)$ about $i/2$ rather than about 0, thereby preserving the Placzek moments:[4]

$$Q_i(t) \approx C_i\left[\left(\tfrac{1}{2} - G_i/4\right) + i(1 - G_i)t + G_i t^2\right] \tag{12}$$

where

$$G_i = \left[\left(\gamma_i^2 + 2\delta_i + \delta_i^2\right) \cosh \gamma_i/2 + 2\delta_i\gamma_i \sinh \gamma_i/2\right] \div 2D_i \tag{13}$$

and we again use the above approximation when

$$\gamma_i << \beta \quad .$$

Treating at least two of the Q_i's exactly and proceeding as in I and II, we find for the j^{th} energy transfer region:

$$S(\alpha,\beta) \simeq \frac{1}{\pi} e^{-k\alpha} \int_{-\infty}^{\infty} \left[e^{i(|\beta|-\alpha s)t} \cdot e^{-\alpha J t^2} \, e^{\alpha L_1 e^{-\delta_1 t^2}} \cos \gamma_1 t \cdot e^{\alpha L_2 e^{-\alpha_2 t^2}} \cos \gamma_2 t \right] dt \quad (14)$$

where

$$K = 4/M + \sum_{i=1}^{j-1} R_i + \sum_{j}^{N} A_i$$

$$J = 1/M + \sum_{i=1}^{j-1} S_i$$

$$R_i = C_i(1/2 - G_i/4)$$

$$S_i = C_i(1 - G_i)$$

$$T_i = C_i G_i$$

Since the expansion described above destroys detailed balance, Equation (14) should be used for calculating down scattering only and upscattering should then be calculated using detailed balance.

Comparing results from Equation (14) with the results obtained from a direct Fourier transform that uses the exact W(t), we find in the region of $\beta = 20$ discrepancies of a few percent where the older expression, Equation (11), showed discrepancies as high as twenty percent.

References

1. *C. W. Lindenmeier. "Scattering Law for Water I," Physics Research Quarterly, January-March, 1962, HW-77311. General Electric Company, Richland, Washington.*

2. *C. W. Lindenmeier. "Scattering Law for Water II," Physics Research Quarterly, July-September, 1963, HW-79054. General Electric Company, Richland, Washington.*

3. *P. A. Engelstaff and P. Schofield. "On the Evaluation of the Thermal Neutron Scattering Law," Nuclear Science and Eng., vol. 12, pp. 260-270. 1962.*

4. *G. Plaxzek. Physical Review, vol. 86, p. 377. 1952.*

4.0 PLUTONIUM UTILIZATION STUDIES

PLUTONIUM UTILIZATION STUDIES

J. R. Worden

Studies are in progress to determine if plutonium enrichment can be used to improve performance of thermal, light water reactors. In principle, plutonium can be used to shape the spatial power distribution axially in the core by grading the enrichment without the cost penalty normally associated with using uranium for this purpose. It is of interest then to determine what incentives exist in improved reactor performance and efficiency if the axial power shape is optimized.

An initial study has been completed from which an optimized axial power distribution has been determined. Empirical correlations indicate that the heat removal potential of coolant decreases exponentially along a heated channel. Thus, a power distribution compatible with heat removal potential of the coolant will be peaked at the inlet end. This is accomplished to some extent in boiling light water reactors by judicious placement of control rods.

It must be emphasized that the present phase of the plutonium optimization studies indicates potential improvements in system performance only. The extent to which this potential can be realized will depend on a thorough analysis of power distribution during burnup, control requirements, and the fuel management scheme.

The reactor system considered in the present study is a 1000 MW_e BWR designed by General Electric.[1] The basic design features were reproduced using the thermal and hydraulics design code, REPP.[2] an axial power profile[1] typical of the hot channel in an equilibrium core at the beginning of a cycle (Figure 4.1) was used in a base case.

The power profile was then modified to correspond roughly to the shape of the limiting heat flux along the hot channel as determined from the base case.

A power profile that peaks 1/10 the distance downstream from the inlet end of the fuel and has a peak-to-average value of 1.9 (Figure 4.1) was used in the present study. If one allows some centerline melting of the fuel, nearly 20% fewer fuel rods are required with this power profile in the hot channel (Table 4.I, Case 2).

From this case it is concluded that any benefits from graded axial enrichment can be realized only if the limit on fuel centerline temperature is simultaneously relaxed. One way this can perhaps be realized is by fabricating low density fuel elements. Assuming the fuel will sinter leaving a central void, the maximum fuel temperature is reduced markedly (Table 4.I, Case 3).

The central problem then is one of maintaining this advantage, or at least some part of it, during burnup of the core. The present study indicates there is certainly incentive

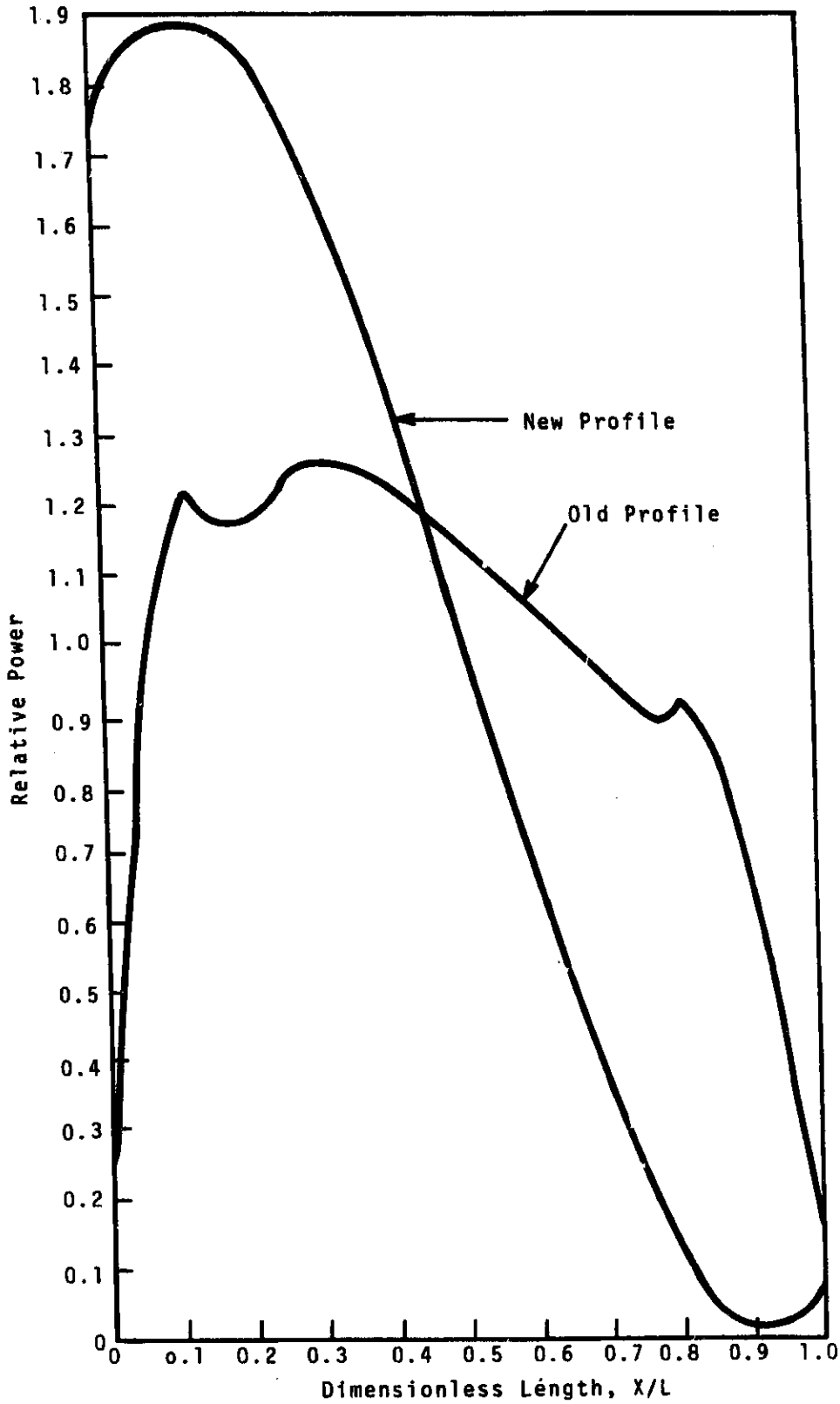

FIGURE 4.1. Comparison of a BWR Power Profile at Startup to a New Power Profile Optimized from Thermal Hydraulic Considerations

TABLE 4.I. 1000 M_e BWR Optimization Study

	Case 1 Base Case	Case 2 Base Case New Profile	Case 3 Low Density Fuels
Equivalent core diameter, in.	187.1	168.79	168.77
Reactor power, MW	3290	3290	3290
Maximum fuel temperature, °F	4380	4873	2691(a)
Fuel quantity, lb	345717	281357	151423
Fuel density ratio	0.93	0.93	0.50
Fuel rod OD, in.	0.562	0.562	0.562
Active fuel length, in.	144	144	144
Number of fuel rods	37436	30464	30498
Fuel rod pitch, in.	0.7382	0.7382	0.7377
Power peaking factor	1.3	1.9	1.9
Location PPF, X/L	0.32	0.1	0.1

(a) *The temperature shown resulted from a hand calculation and therefore is an approximate number. However, it does illustrate the effect of low density fuel on fuel centerline temperatures.*

for further studies of nuclear behavior including burnup, fuel management schemes and control requirements. These studies are presently in progress.

References

1. *1000 MW_e Boiling Water Reactor Plant Feasibility Study, Volume II, GEAP-4476. General Electric Company, Richland, Washington. February 14, 1964.*

2. *PUP Quarterly Report July, August, September 1966. "Boiling Water and Pressure Water Reactor PuO_2-UO_2 Fueling Study," Unpublished Report, Pacific Northwest Laboratory, Richland, Washington.*

OPTIMUM DENSITY FOR PLUTONIUM FUELS

D. E. Deonigi

The recycle of plutonium in light water reactors is a subject of great interest to the reactor industry. The efficient use of plutonium implies more than the simple substitution of plutonium for uranium enrichment in reactors designed for uranium fuel. The reactor physics behavior of plutonium is different from uranium in that it is desirable to have a higher H/U ratio for plutonium fuels and the fertile ^{240}Pu isotope has a larger capture cross section than ^{238}U. The optimum H/U ratio is a balance between decreasing plutonium inventory cost and a decreasing conversion ratio due to fewer ^{238}U resonance captures.

A previous report[1] considered three methods of optimizing the reactor for plutonium utilization; reducing fuel density, reducing fuel rod diameter, and increasing the lattice pitch. The results from rod

size studies indicated that the optimum diameter plutonium fuel rod was about equal to the uranium rod diameter in the latest uranium reactor designs; for example, Burlington. There is little incentive left for optimization based on rod size in the latest designs since further reductions in rod size will be more than offset by fabrication penalties.

It now appears that the lattice pitch improvements are also nearly offset by the increased capital cost required by the larger pressure vessel design.

The remaining concept, the reduction of fuel density, appeared at the time of the previous report to be less attractive. The optimum density would lower the fuel cycle costs by 0.1 mils/kW-hr or less from a reference case, whereas the reduced rod size and increased lattice would do better in most cases. However, with the higher H/U ratios of the latest reactor designs, all of these concepts become break-even cases.

A new effect has been studied recently: the effect of reduced fabrication costs (per unit volume) of lower density fuel rods. In the previous work the fabrication costs per unit volume were assumed to decrease to 80% of theoretical density and be constant below this. However, several techniques are available which may cause a step change in fabrication costs near 60% of theoretical density, and new techniques are being developed which may permit the use of these lower density fuels.

In Figure 4.2, the indifference relationship between fabrication cost and fuel density is shown for three fueling schemes: enriched uranium, plutonium enrichment in natural uranium, and plutonium enrichment in depleted uranium. Relative fabrication costs above the indifference curve result in higher fuel cycle costs, while those below the curve result in lower fuel cycle costs. The plutonium enrichment curves do not decline as rapidly with density as the enriched uranium curve leading to the possibility that reduced density plutonium fuels may be fabricated at costs which not only offset the plutonium fabrication penalty but also result in lower fuel cycle costs. For example, a PuO_2-UO_2 fuel element at 75% TD fabricated for 70% of the normal cost for UO_2 elements results in a fuel cycle cost reduction of about 0.1 mils/kW-hr.

Reference

1. *Economically Optimum Plutonium Lattices for Water Reactors*, BNWL-SA-738. *Pacific Northwest Laboratory, Richland, Washington.*

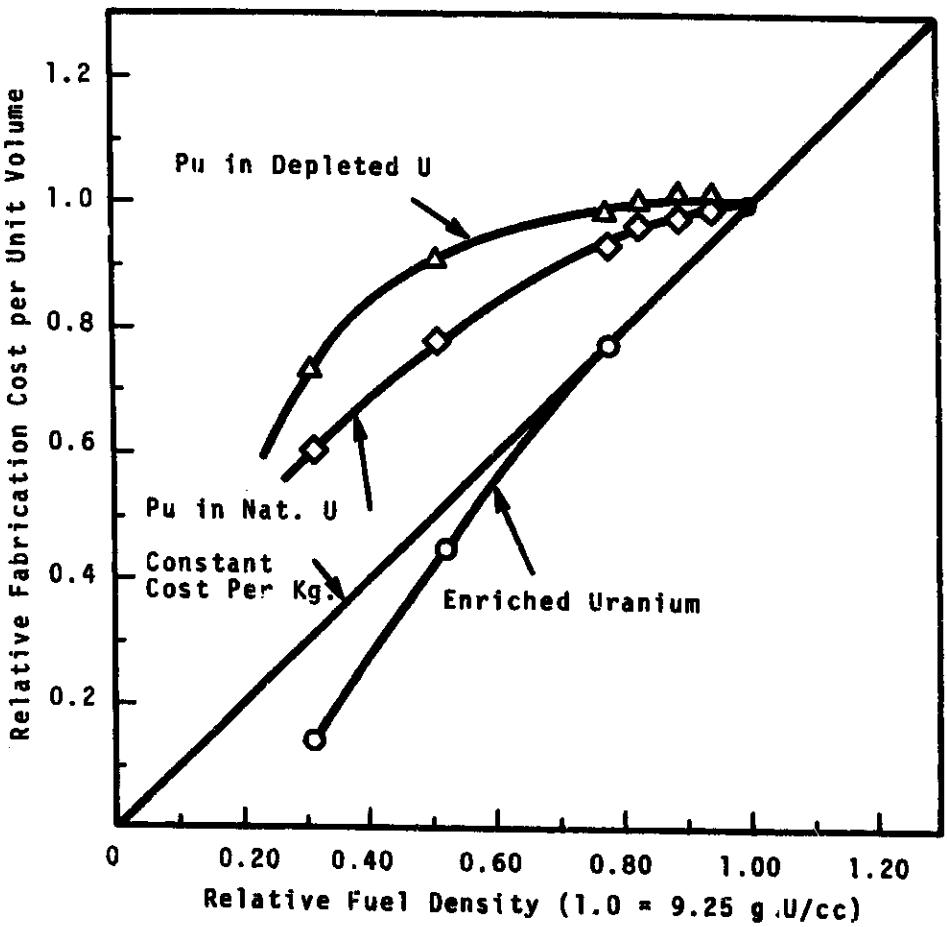

FIGURE 4... Indifference Fabrication Costs Related to Fuel Density for Three Fueling Schemes

5.0 PRTR OPERATION

IN-FLUX CORROSION OF ZIRCONIUM ALLOYS - A. B. Johnson Jr.

The PRTR has operated with two coolants, previously with pH-10 LiOH (D_2O) and currently at neutral pH.[1] Tests are in progress to evaluate and compare the corrosion rates of zirconium alloys in the two environments. In the lithiated environment corrosion rates were accelerated by the flux on Zircaloy-2 and Zircaloy-4 specimens exposed 209 days at a fuel rod position. A summary of the nature of the accelerated corrosion is as follows:

1) In-flux weight gains generally followed the flux profile.
2) Weight gains were lowest on specimens exposed as-etched; specimens prefilmed to pretransition and posttransition weight gains had comparable weight gains.
3) In-flux weight gains on Zircaloy-2 and Zircaloy-4 did not differ significantly.
4) Prefilming adversely affected in-flux corrosion and hydrogen pickups.

Examination of PRTR Zircaloy-2 process tubes also confirmed that accelerated flux-induced corrosion occurred in the lithiated PRTR coolant. Corrosion studies in the Engineering Test Reactor indicate that radiation damage is not the only factor necessary to accelerate the oxidation rate; the composition of the coolant appears to be important.

To evaluate Zircaloy corrosion in the neutral pH coolant, a new corrosion specimen assembly was inserted at a fuel rod position. Zircaloy-2 is the primary test alloy, but the assembly contains Zircaloy-2 and Zircaloy-4 specimens from the lots tested in the lithiated environment. The following surface conditions are being investigated: as-etched; prefilmed 3 days at 400 °C in 1500 psi steam; prefilmed 1 day at 300 °C in water followed by 2 days in 400 °C steam. The two-stage treatment is reported[2] to result in hydrogen pickups lower than those resulting from a single stage autoclave treatment at 400 °C.

An out-of-reactor control test is being conducted in an an autoclave operated at 260 °C in neutral pH deionized, deoxygenated water at 1050 psi.

References

1. *A. B. Johnson, Jr. In-Reactor Oxidation of Zirconium Alloys in pH-10 LiOH and pH-10 NH_4OH, BNWL-SA-822, March 1967. Paper No. 28, High Purity Water Symposium, NACE 23rd Annual Meeting, Los Angeles, California.*

2. *W. Debray, L. Stieding and V. Rosler. "Influence of Oxide-Layer Formation on the Hydrogen Pickup of Zircaloy," J. Electrochem. Tech., 4, No. 3-4 pp. 113-117. March-April 1966.*

SHUTDOWN RADIATION MEASUREMENTS

L. D. Perrigo

Systematic shutdown radiation measurements are made on the PRTR

to determine radioactivity buildup rates. Recent emphasis has been placed on comparing buildup rates in the PRTR primary system operating with a "neutral" pH coolant to those encountered during earlier reactor operating periods with pH-10 coolant.

Figure 5.1 shows typical radioactivity buildup data for the PRTR primary system from initial startup

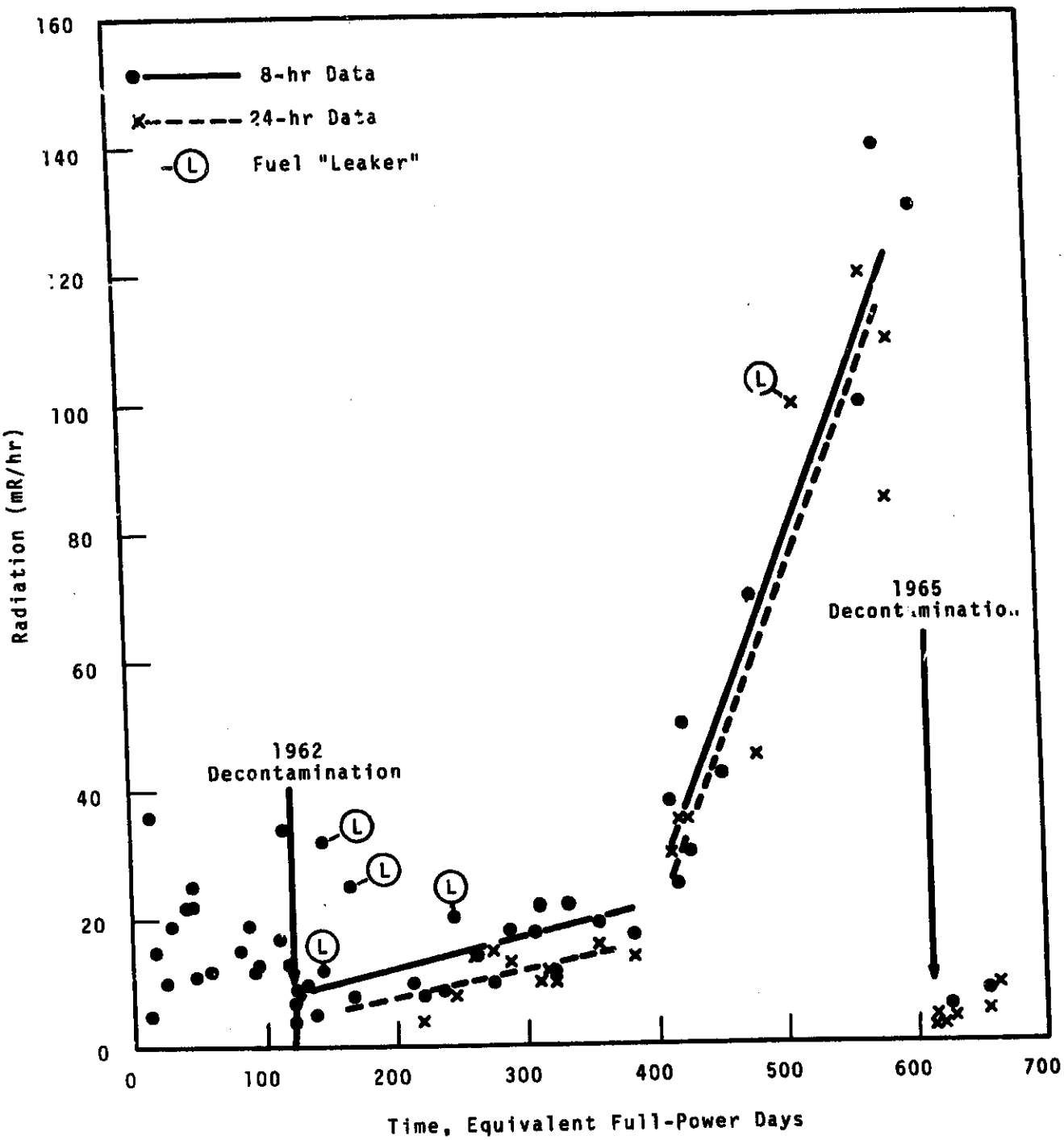

FIGURE 5.1. Radioactivity Buildup in the Volute of a PRTR Primary Pump

in 1961 to the present. Operation prior to 614 equivalent full power days (EFPD) was with pH-10 coolant; subsequent operation has been with "neutral" pH coolant. Of particular interest at the present are the two periods of operation following decontamination at 121 and 614 EFPD. Although it is too early to establish buildup rates for operation with the "neutral" pH coolant, examination of radiation data from the two post-decontamination periods show substantially the same levels of activity. The similarity in levels after about 50 EFPD of post-decontamination operation was found for all nine positions routinely monitored on the PRTR primary system. Currently there appears to be no enhanced radioactivity resulting from a change in coolant purity. However, definite trends for the buildup of radioactivity in a system operating with a "neutral" pH coolant must await additional reactor operation. Recent PRTR data has been normalized[1] to 70 MW (even though power levels are currently lower) so that current data may be compared with data acquired with earlier measurements.

References

1. *J. A. Ayres, L. D. Perrigo, and R. D. Weed. "Decontamination in a PWR," BNWL-SA-938, Pacific Northwest Laboratory, Richland, Washington. Published in* Nucleonics, *vol. 25, no. 4 pp. 58-62, 72. April 1967.*

FUELING VEHICLE COOLING

J. K. Anderson

The FERTF 8-rod fuel element has unusual cooling problems during charge-discharge because of the protective sleeve surrounding the fuel and the required low temperatures during the handling of defected elements. This protective sleeve tends to reduce air flow through the element during normal air cooling and shields the element from the emergency water cooling system. Therefore, analyses and experiments were performed to determine the adequacy of the normal air cooling system and the effectiveness of emergency water cooling systems, and to investigate alternative cooling methods. The analyses were based on an 8-rod element with a maximum specific power of 0.23 kW/ft at time of discharge. The results of these studies are as follows:

Air Cooling

Calculations showed that the normal air cooling would be adequate for cooling a non-defect 8-rod FERTF element in the fuel vehicle, but would not hold defected rods within the required temperature limits. Further calculations were performed to develop information which would allow the estimation of maximum fuel temperatures from measurements of bulk outlet temperature. These calculations were performed for fuel

elements with and without the basket tube liner (inner sleeve) installed and with the assembly enclosed by the discharge cask shroud. Two methods were used. In the first method, the fraction of the air flow passing outside the basket tube, between the basket tube and fuel ring, and inside the fuel ring were calculated for various total air flows. From these flow splits, maximum rod temperatures were calculated by assuming that the rate of heat flow out of a fuel rod was uniform around its circumference. In general, these calculations indicated that the highest temperature of a fuel rod would be inside the rod ring. Realistically, such a temperature imbalance around the rod circumference would tend to decrease the heat flux at the inner surface and drive more heat to the outer surface. Under some conditions, the calculated inner surface temperatures were higher than those which would exist if there were no cooling at the inside of the rod ring and all heat were being driven to the outside. Consequently, a second method of calculation was used to determine maximum fuel rod temperatures in which all heat was assumed to be driven to the outside. The results of these calculations were presented as plots of maximum surface temperature versus bulk outlet temperature.

Emergency Water Cooling of Nondefected Element

The emergency cooling system in the fueling vehicle provides water spray from nozzles at several axial and radial positions directly on the fuel rods in the normal 19-rod fuel element if forced air circulation is lost. However, the basket tube around the 8-rod element would prevent the spray from reaching the fuel rods. Estimates of maximum fuel temperatures following loss of air cooling were made by assuming that the present emergency water cooling system was used to spray water on the outside of the basket tube. In such a case, heat transfer from the fuel rods to the basket tube would be primarily by radiation. Without a basket tube liner, maximum fuel rod temperatures would probably cause fuel rods to rupture but would not produce any core or cladding melting. With a basket tube liner installed, the thermal resistance between the liner and the basket tube would cause higher fuel temperatures for this method of emergency cooling. The temperatures would depend on the closeness of the fit between the basket tube and liner but should be below the melting point of core or cladding materials.

Water Cooling With Vertical Downflow

As discussed above, the air cooling system would not limit the temperatures of defected fuel elements below the point at which absorbed water would be vaporized and would cause the expulsion of fission products. Also, the existing emergency water spray cooling system would not prevent excessive fuel temperatures in an 8-rod element. Therefore, an alternative cooling system was proposed. By this system, water

would be supplied by lines attached to the discharge hook at the top of the fuel element hanger. Calculations showed that a flow rate of only 0.5 gpm inside the basket tube would limit fuel temperatures below 212 °F if the water spread uniformly over all surfaces. However, at this flow rate, channeling of the flow and nonuniform distribution would probably exist. Consequently, several experiments were performed to investigate flow requirements.

1. An 8-rod fuel element was enclosed in a transparent plastic basket tube to allow observation of flow pattern. Experiments were conducted with water introduced from above through a 3/4 in. hose. The water stream fell parallel to the fuel element hanger and impinged on the top fuel element fittings at a flow rate of about 2.2 gpm. The water was observed to flow preferentially down fuel rods beneath the falling stream, and rods on the other side of the assembly were only partially wetted. The hose was then deflected so that the water stream was striking the hanger rod about 6 in. above the top of the fuel assembly. With this arrangement, the following observations were made:
   - At a flow rate of 2.2 gpm, all fuel rods were wetted by flowing streams.
   - At a flow rate of about 1 gpm, fuel rods beneath the hose were wetted over their full lengths. Fuel rods on the far side showed alternate wetting and drying of the top 3 to 4 in. with continuous wetting over the rest of their lengths.
   - At a flow rate of 0.27 gpm, fuel rods beneath the hose were wetted over their entire lengths. Observable surfaces of the fuel rods on the far side of the assembly were largely dry down to the position of the top retaining bands. Below this position, these rods were wetted over their entire surfaces.
   - At flow rates of 5 to 10 gpm, all fuel rod surfaces were covered with heavy layers of flowing water. Spaces between fuel rods and the basket tube were filled with a flowing air-water mixture.
   - The retaining bands around the fuel rod bundle appear to act as flow distribution devices, spreading the water film over the fuel surfaces.

   The flow rates referred to above are flow rates inside the basket tube.
2. Experiments in the fueling vehicle with water supplied from two lines at the top of the fuel hanger showed that a substantial fraction of the water was falling outside the basket tube where it could cool the fuel rods.
3. In order to utilize the cooling water more effectively, a new fuel element hanger was designed. This hanger includes a top chamber to receive the water and a hollow hanger to channel the water within a few inches of the top of the fuel rods. Flow patterns were observed with an 8-rod element, in

a transparent basket tube, suspended from the new hanger. These observations, made at total coolant flow rates of 2, 4, 6, and 8 gpm showed the following:

- At 2 and 4 gpm, persistent dry patches existed on the fuel rods. Under these conditions, adequacy of cooling is doubtful.
- At 6 gpm, flowing films of water were observed on all visible rod surfaces. These films would probably provide adequate cooling.
- At 8 gpm, heavy films of flowing water were observed on all visible fuel rod surfaces. In addition, streams of water flowed in the void spaced, contacting the fuel rods. These streams should quickly restore liquid flow over surfaces where temporary dry patches might form. At this flow rate, adequate cooling seems assured.

EMERGENCY COOLING OF FERTF

J. K. Anderson and A. M. Sutey

Studies were performed to re-evaluate the adequacy of the emergency cooling system in the PRTR Fuel Element Rupture Test Facility (FERTF) to prevent excessive fuel temperatures following various loss-of-coolant accidents. Under normal conditions, cooling water to the FERTF is provided by two positive displacement pumps. In the event of a piping rupture, emergency coolant can be supplied to either the recirculating pump inlet or the outlet piping from the pressure tube. Any piping rupture large enough to seriously interfere with coolant flow past the fuel would cause an immediate safety circuit trip. However, it would still be necessary to provide enough cooling to remove the fission product decay heat from the fuel element.

Two types of accidents are of primary concern. One is a large piping rupture in inlet piping to the pressure tube which contains the fuel. (If a rupture should occur downstream of the pressure tube, the pumps would continue to provide adequate flow past the fuel.) The second type of accident is a loss of normal pumping capability, perhaps through a piping break upstream of the check valve near the pump discharge, or through total loss of pumping power. If a large break occurs in the pressure tube inlet piping, water from the pumps would flow out the break and would not reach the fuel. In this case, it would be necessary to cool the fuel by backflow of steam or a steam-water mixture during the blowdown period while the system pressure was decreasing from the normal 1000 psig to less than 100 psig. (Emergency water is supplied to the outlet piping at a pressure of about 100 psig. Emergency water flow would vary from zero at a FERTF system pressure of 100 psig to about 60 gpm at a system pressure of 0 psig.)

In earlier studies, it had been assumed that blowdown flow rates would be adequate to cool the fuel elements at the pressure decreased to 100 psig and that thereafter, the

emergency water flow would provide adequate cooling. In the present study, however, it was noted that emergency coolant supplied to the outlet piping enters the FERTF system at a vertical run of pipe from the pressure pipe to a bank of regenerative heat exchangers. To reach the fuel, the emergency water must travel upward over the highest point in the cooling system. During the blowdown, large voids would be created in the heat exchangers, and the initial tendency would be for emergency water to flow downward into these voids. Thus, the emergency coolant might not reach the fuel for several minutes after its injection had begun. Conceivably, at planned power levels, fuel element temperatures could exceed the specified 1400 °F limit during this period.

In order to remove this uncertainty, it was recommended that the point of emergency water injection be changed to the top of the pressure tube. Thus, as soon as emergency water flow begins, all of the water will flow downward over the fuel element.

In the case of loss of normal pumping capability, circulation of water past the fuel would also be stopped. In this case, however, there would be no rupture path available for blowdown and depressurization to allow injection of emergency water. The system is equipped with a 1/2 in. drain line which is normally closed off by a valve. In an accident of this type, flow and pressure signals would automatically cause the valve to open and depressurize the system. Calculations indicated, however, that the capacity of the blowdown line might be inadequate to assure continuous cooling of the fuel during the period of depressurization and emergency water injection. The blowdown rate would depend greatly on the type of flow out of the line; liquid, two-phase, or vapor. The system is complicated, and the flow regime in the blowdown line cannot be estimated with assurance throughout the entire blowdown period.

Two possible solutions to this problem were suggested:

- Install a small (10 to 15 gpm) high pressure pump with an independent power supply for emergency water injection. This would allow injection to begin immediately and provide a continuous flow of water over the fuel and out the blowdown line.
- Replace or supplement the present blowdown valve with a larger valve. Blowdown times could be short enough that excessive fuel temperatures would not be reached before emergency water was provided by the present system.

Calculations showed that either of these suggested alternatives could be employed to assure adequate cooling of the fuel. Availability of pumps and valves is being investigated so that a choice can be made between these alternatives.

UPSTREAM BOILING BURNOUT

D. R. Dickinson

The burnout heat flux in heat transfer to boiling water usually

decreases with increasing enthalpy, and boiling burnout therefore usually occurs first at the downstream end of a uniformly heated channel. However, recent tests at PNL have demonstrated that under certain conditions burnout occurs at upstream locations. The present research program is being conducted to study further this phenomenon of upstream burnout to determine the conditions under which it occurs and the reason why it occurs.

From earlier tests, certain significant conclusions about the mechanism of upstream burnout were derived. At the conditions under which these tests were performed (mass velocity of 3 to 7 x 10^6 lb/hr ft^2, steam qualities at burnout greater than 10%, and a pressure of 1500 psia), an annular flow pattern probably existed in the test section. With this flow pattern, there is a film of liquid on the wall of the heated tube and a core of vapor with suspended water droplets in the center. When the tube is heated, water is evaporated from the surface film, and burnout occurs when evaporation has proceeded to the point where the film disappears and the heated surface is no longer wetted. In general, liquid water may be supplied to the heated surface at a given point by flow through the liquid film from the upstream end and/or by deposition of liquid drops. It was shown in the previous quarterly report that deposition is the most important mechanism under the conditions of these tests.

When upstream burnout occurs, the rate at which water drops are transported to the heated surface from the interior is equal to the burnout heat flux divided by the heat of vaporization. For upstream burnout to occur with a uniformly heated test section, this rate of transfer must be greater downstream than at burnout. It was suggested in the previous quarterly report that the drop size is reduced as the steam-water mixture moves downstream, and that the smaller drops are more easily transported to the surface because of their smaller inertia. Further analysis of test data during the past quarter has developed the following explanation.

Water drops suspended in the steam will be broken up by shear forces imposed by the turbulence of the vapor steam. This break up will be resisted by surface tension forces. Thus, the water drops will be reduced in size until these two forces come into equilibrium, or until the Weber number is reduced to some critical value. The shear force will be a function of the relative velocity between the drops and the vapor, and this difference will depend on the amount of turbulence. If it is assumed that this velocity is proportional to the average axial velocity of the mixture, V, then the average drop size should be approximately proportional to $\sigma/\rho_v V^2$, where σ is the surface tension and ρ_v vapor density.

The dimensionless ratio of the mass transfer coefficient for the

transport of water droplets to the surface to the average axial velocity, k/V, which is a measure of the efficiency of drop deposition, is plotted in the Figure 5.2 as a function of $\sigma/\rho_v V^2$. The data plotted represent conditions at upstream burnout for a uniformly heated tubular test section with an ID of 0.435 in. The data represent qualities at burnout from 10 to 70%. It was assumed here that at upstream burnout all the liquid is present as suspended drops, and that these have the same average axial velocity as the vapor. It will be noticed that data at mass velocities of 3, 5, and 7 x 10^6 lb/hr ft^2 and pressures of 1000 and 1500 psig all fall approximately on a single curve. (When plotted in the more conventional form of burnout heat flux versus local quality, these data gave widely separated curves.) The ratio k/V rises sharply as the drop size, $\sigma/\rho_v V^2$, is reduced.

Present data are not adequate to conclude whether this correlation results from a fundamental dependence on drop size, as suggested above, or is simply fortuitous. Additional tests, to be started soon, will be made to obtain data over a wider range of pressure, and hence of surface tension and vapor density.

PRTR PRESSURE TUBE EVALUATION

T. R. Ostrom

The PRTR pressure tubes were fabricated from Zircaloy-2 ingots by a forging-hot extrusion-tube reducing process. These tubes have a unique shape, one end is flanged and the other tapers to a reduced diameter. They also have a unique microstructure distribution of an annealed region between the taper and tube midlength, with the remainder being cold worked. The ability of these tubes to sustain PRTR system loads with ever increasing neutron exposure has been a subject of study and testing since reactor startup. Recently, studies have been concerned with the effect of hydrides on pressure tube fracture.

The effect of hydrides on the fracture process was studied by successively sectioning the tube wall of PRTR pressure tube specimens that were artificially flawed, then split by internal pressurization. A composite of sections through the crack in a tube containing 25 ppm and one containing 275 ppm hydrogen is illustrated in Figure 5.3. The specimen containing 25 ppm hydrogen has a porosity in the vicinity of the fracture surface that is not evident in the specimen containing 275 ppm hydrogen. The difference in behavior is illustrated more clearly in Sections A and B, Figure 5.4. In Section B, the hydrides and the cavities are dispersed and do not easily form a continuous path across the tube wall; whereas, in Section A, the hydrides and the cavities connect into a continuous part fracture with less energy dissipation.

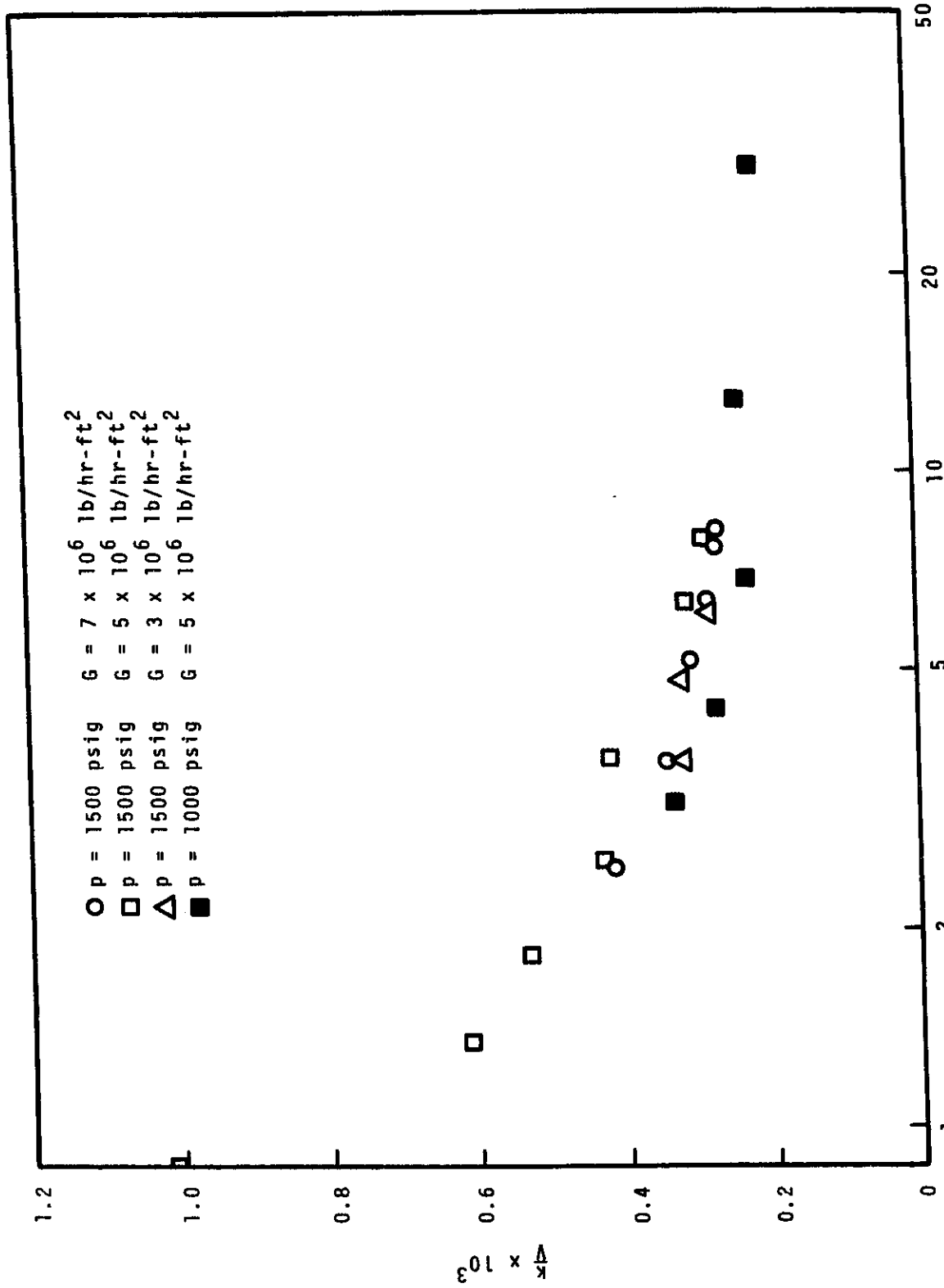

FIGURE 5.2. Transport of Water Droplets to Heated Surface in Upstream Burnout.

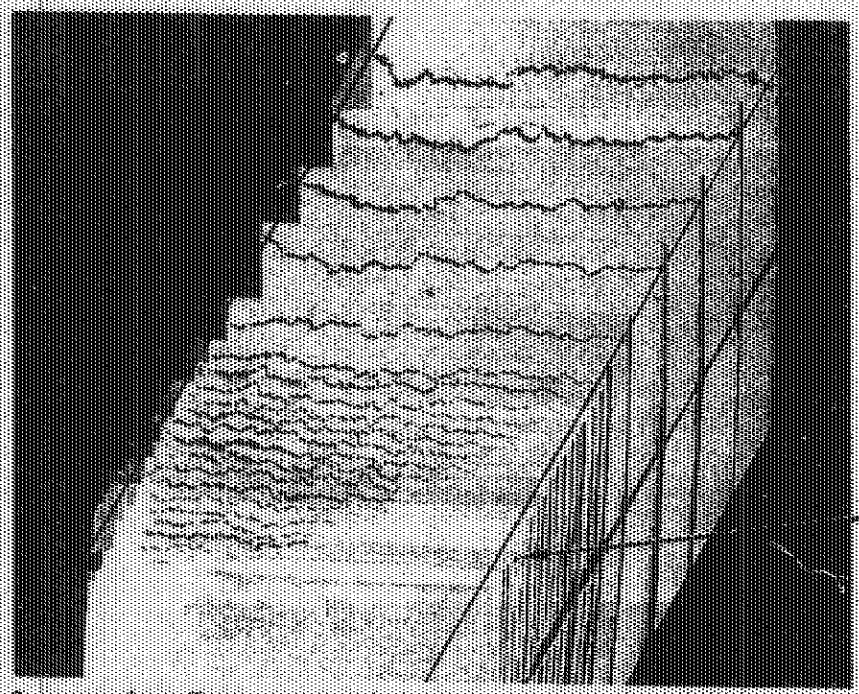

Successive Transverse Sections of Crack Tip Arrested by End Caps Original Tube Wall Thickness 0.156 inches

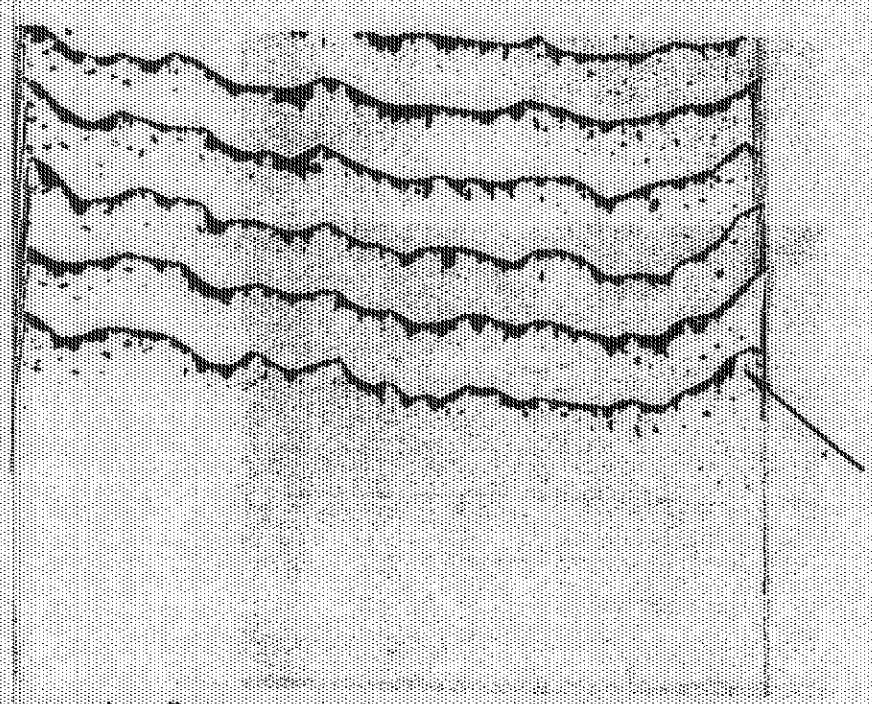

Successive Transverse Sections of Unstable Cracking Region Original Tube Thickness 0.275 inches

FIGURE 5.3. Composite of sections through a crack in a tube containing 275 ppm hydrogen and 25 ppm hydrogen.

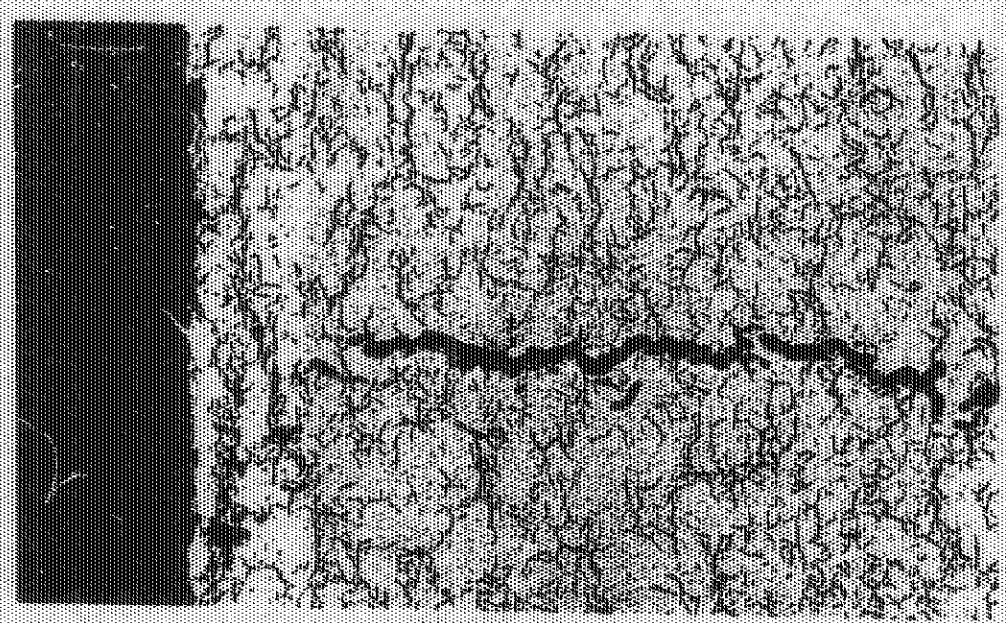

Section A
275 ppm H_2
100X Mag.

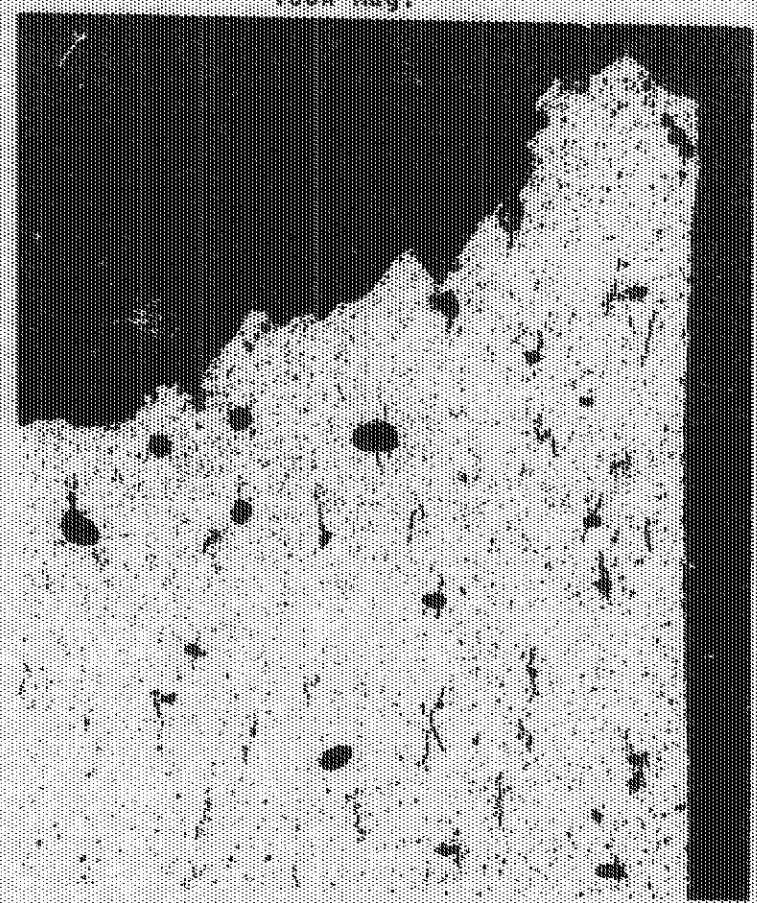

Section B
As Received Tubing 25 ppm H_2
100X Mag.

FIGURE 6.4. Sections A and B from Figure 6.3

OPERATING EXPERIENCE

J. R. Fishbaugher

Pertinent data for the quarter are as follows:

Production.....2162.78 MWd
Hours Critical.....1810.4 hr
Critical Efficiency..... 52.7%
Total Experimental Time Efficiency..... 62.9%
D_2O Losses
Indicated Stack Loss (8-23 to 11-17)..... 2813 lb
Physical Inventory (8-23 to 11-17)..... 4289 lb
Helium Loss.....351,701 scf

The plutonium Recycle Test Reactor operated at a maximum power level of 55 MW during September, October, and November. Reactor operation continued to be limited by the 5% rod power difference reported in July. Total production since the start of the batch core experiment is 5226 MWd or 26.1% of the batch core goal exposure. The 55 fuel element core has accumulated 4278 MWd.

Operating performance for the PRTR is shown in Figure 5.5. The PRTR operation was interrupted by 42 shutdowns of which 25 were intentional and 17 were scrams. A brief description of the major outages occurring during the report period follows:

September 10 - Shut down from 110.3 hr on schedule to perform the first interim critical test of the 55 fuel element batch core. Planned maintenance work and other test work required an additional 178.2 outage hr.

September 25 - Shut down for 218.6 hr to locate and correct D_2O leaks in the HX-5 heat exchanger. Leaks occurred in two tubes serving process channels 1251 and 1457. The tubes were blanked and the heat exchanger returned to service. Efforts were made to determine the exact location of the leaks.

October 16 - Shut down for 102.3 hr after the top rupture disc in the top and bottom shield coolant system broke. The break was caused when the expansion tank overflow control valve failed. The outage was continued to replace a broken shaft on boiler feedwater pump #4.

October 27 - Shut down for 25.0 hr to correct high D_2O losses. Replaced the bowl gasket on primary pump #3 and seal welded the flange on P-11 check valve.

November 12 - Shut down for 116.1 hr after the high pressure helium compressors failed to keep up with helium demand. The reactor remained shut down to restore the Fuel Element Rupture Test Facility to service and for scheduled repairs.

November 19 - The reactor was shut down for 25.6 hr to correct internal leakage through the DOV vent valve (H-99) at the inlet to the heat exchanger HX-1.

November 29 - Shut down for 54.8 hr to repair the FERTF loop main coolant pumps.

Other operating and equipment experience is as follows:

The FERTF was removed from service in September to conduct the interim critical tests. The FERTF was reactivated in November with redundant piping and circuitry for light water injection and test section blowdown. A commercially fabricated, 19-rod, 2 wt% PuO_2–UO_2 was charged into the in-reactor loop of the facility and

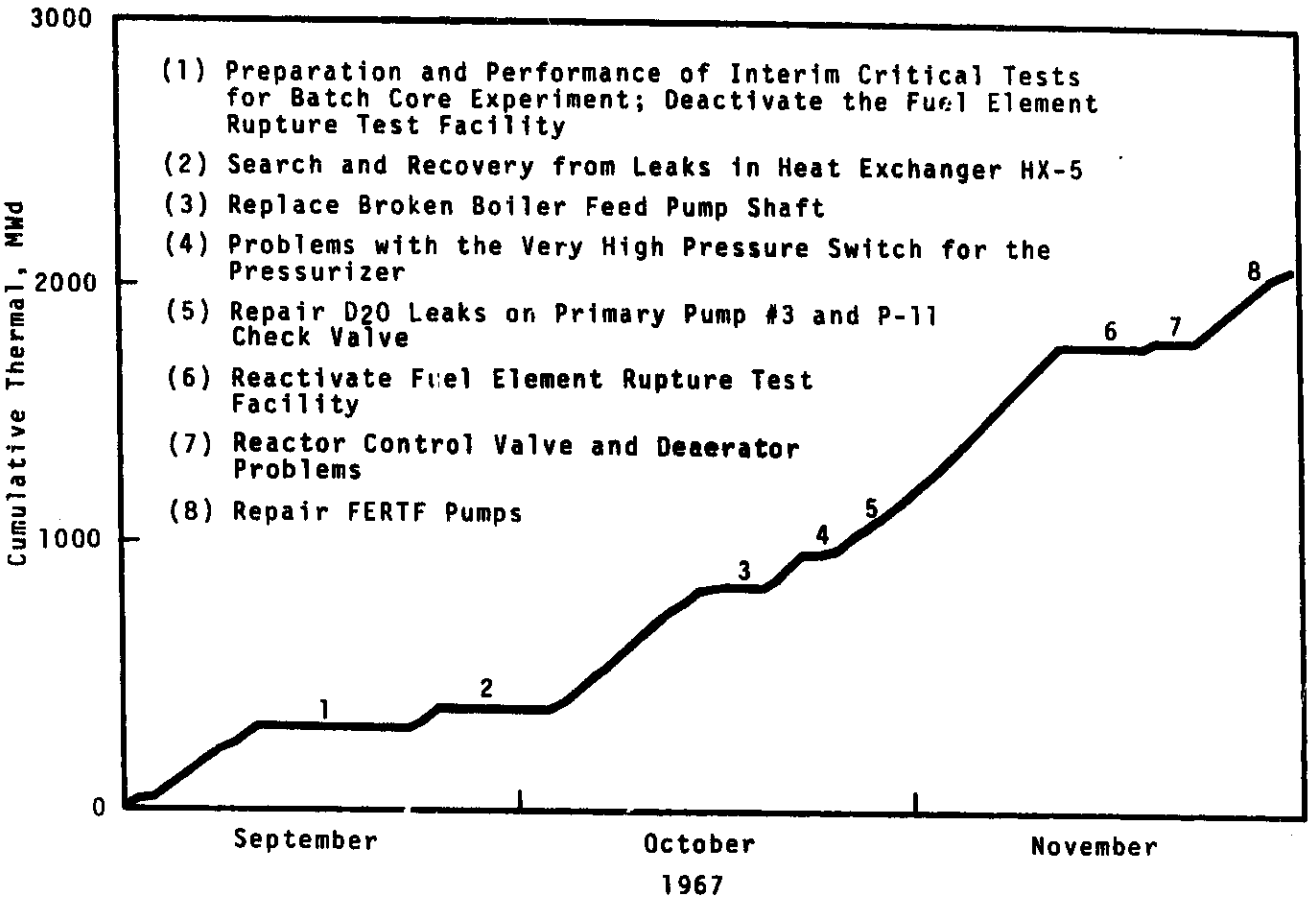

FIGURE 5.5. PRTR Operating Experience

operation was restricted to maximum coolant temperatures of 160 °F. Higher than usual oxygen concentration in the coolant required several periods of single-pass coolant operation. Several pieces of silver metal were removed from FERTF valves RL-1 and 130, and one small piece was removed from between the wire wrap and a rod on the fuel element. Coolant pump cylinder linings are the primary source of this material. Surveillance for ^{110}Ag activity has begun. First samples show the presence of this isotope at low levels in water and resin samples from this system. The loop piping was flushed to remove any other pieces of metal that might have been in the main coolant stream.

Corrosion surveillance X-rays were made of selected locations on FERTF piping and equipment. These X-rays did not reveal any pitting, visible cracks, or other damage. However, visual inspection revealed three locations in the FERTF equipment cell where vibration was causing significant wear on branches from the main piping.

During October 24 and 25, 1967 the reactor was shut down ten times and the cause was traced to the very

high pressure trips. One of the two switches had drifted and was tripping at 1100 psig, or 60 psig below the normal set pressure. With the primary coolant cold, the pressure control span was 1050 to 1090 psig; but when hot, the pressure would occasionally reach a higher value, hence most of the pressure trips occurred during heat-up. A design change was initiated to provide annunciation when either of the two high pressure switches are tripped.

At different times during the past six months, moderator temperature spikes of about 6 °F have been observed during reactor operation. Early in September, it was noticed that a sudden moderator temperature change was experienced when the moderator level was raised to the evaluation of the overflow orifices, 99.4 in. A small reactivity transient accompanied the temperature spike, and therefore, the reactor was operated 5 MW below the limiting power level while the problem was investigated. Investigation showed that the top layer of D_2O in the calandria was hotter than the balance of the D_2O, and that when this top layer would flow over the orifices, the moderator outlet temperature would increase approximately 6 °F. The temperature of the moderator water in the calandria would decrease slightly, causing a reactivity transient. This transient resulted in a 1 to 2 MW power change. To resolve this problem, the moderator high level alarm has been set to sound at 99 in., and normal reactor operation is limited to a moderator level range below the upper row of overflow orifices.

A significant recent equipment problem at the PRTR was the leaks in two tubes of the primary treatment heat exchanger, HX-5. Wear from rubbing against a support baffle resulted in failure of a tube in 1963, and it is probable that wear was the cause of the two present leaks. However, the exact cause of these leaks has not been determined because of the extreme difficulty of access to either the inside or outside of the leaking tubes within the tube bundle. An investigation of the HX-5 replacement has begun.

On October 31, 1967, deaerator low-low level annuciator was received and PW-85 open momentarily. Lowering the deaerator pressure cleared the alarm and the valve closed. The low-low level alarm was associated with the deaerator pressure and temperature and was not caused by actual lowering of the deaerator pressure and temperature and was not caused by actual lowering of the deaerator water level. Similar events were experienced four more times over the next 10 days. On November 20, 1967, the reactor was shut down to correct deaerator pressure and boiler feedwater temperature control problems. Corrective action included the following:

1. The steam pressure control valve, S-31, was disassembled and a new seat and plug were installed.

2. The vacuum relief valve was disassembled and new internal parts installed.
3. The temperature probe was calibrated.
4. Liquid level and pressure control instruments were overhauled.

On November 12, 1967, after the high pressure helium compressors failed to keep up with the helium demand, the reactor was shut down. The compressors had been working harder than normal because of the increased leakage through the pressurizer overpressure control valve, H-80A. Previous experience had shown that both H-80 and 80A leaked through when either valve was closed, and if both valves were closed there was almost no leakage. The two overpressure control valves, H-80 and 80A, which are piped in series, were connected to operate in parallel from the same control air signal. Since this change was made, the HPHC operating time has been sharply reduced.

Radiation levels in all PRTR systems continued to be lower than expected. Extended periods of operation in the past three months resulted in only slight increases in radioactivity in the helium core blanket gas system and in the primary and reflector cooling systems. These small increases indicate that little if any fuel or fission products from the 1965 FERTF fuel rupture were being transported out of the reactor flux region into these systems. Gamma activity from ^{60}Co was predominant in the oxide layer that was removed from a primary nozzle cap spider in May.

The particle filters in the moderator system showed increased radioactivity, but only slight increases were evident in the rest of the moderator system. Gamma radioactivity from ^{60}Co, ^{51}Cr, and ^{144}Ce was present in samples taken from these filters in June.

Seven process tubes were examined during this period; a total of 40 during the calendar year. No significant changes were observed since their previous examination.

The PRTR had no significant corrosion or crud deposition problems. The corrosion and crud surveillance programs are continuing with specific measurements and inspections made on a regular schedule. The helium system and all cooling systems are covered by these surveillance programs.

Major corrosion surveillance items for the moderator system included aluminum coupons which showed negligible corrosion when suspended in the calandria and a corrosion probe which showed a corrosion rate less than 0.01 mils per month in the outlet line from the moderator pumps. The primary system contained stainless steel and zircaloy corrosion coupons in a bypass loop at full system temperature and pressure. Inspections and measurements from these coupons indicated that no significant corrosion occurred.

Corrosion was monitored in the various reactor shield cooling systems with continuously measured

probes. These carbon steel probes indicated a corrosion rate of less than 0.01 mils per month in the top and bottom shield system (deionized water pH 10.0 with NH_4OH), while the indicated rates were 0.1 to 0.25 mils per month in the biological and thermal shield systems cooled with process water.

Corrosion was held to a minimum in the PRTR secondary cooling system by deaeration and a phosphate-sludge conditioning treatment. Measurements from carbon steel coupons installed inside the shell of the steam generator, HX-1, as well as direct visual and selected X-ray examination inside the shell, showed a minimum amount of uniform corrosion and negligible pitting attack. A recent inspection of the recently installed deaerator cone showed it to be in excellent condition.

A plug of charred organic material was removed from a 12-in. vertical length at the end of the line used to feed sodium phosphate and organic sludge conditioner to the secondary water inside the steam generator (HX-1). This line has been returned to service. (The feedwater system had been operated temporarily with addition of phosphate to the main boiled feedwater line outside the steam generator.) Ultrasonic measurement of the boiler feedwater header at this addition point indicated that no corrosion damage had occurred.

PROCESS TECHNOLOGY

J. R. Fishbaugher

The irradiation status of the fuel elements in the PRTR on November 30 is tabulated below.

Interim Critical Tests

The interim critical tests for the first burnup step of the batch core experiment were completed in September at a batch core exposure of 3369 MWd. The results showed that the reactivity of the core decreased from an initial excess reactivity of 262 to 228 mk. The extrapolated batch core life is 22,300 MWd.

Moderator level coefficient measurements could not be made by positive period methods because

	Type of Fuel Element	No.	Peak FE Exposure, MWd	Accumulated Exposure, MWd
	Batch Core Fuel Elements	71	112.0 ($3360\frac{MWd}{Ton\ U}$)	4787.6
(new)	UO_2–2 wt% PuO_2			
(old)	UO_2–2 wt% PuO_2	3	205.1 ($6153\frac{MWd}{Ton}$)	438.2
	UO_2–1 wt% PuO_2	3	428.o ($8560\frac{MWd}{Ton\ U}$)	1082.2
	UO_2–0.5 wt% PuO_2	3	553.8 ($11,076\frac{MWd}{Ton\ U}$)	1477.2
	UO_2	1	478.1 ($9562\frac{MWd}{Ton\ U}$)	478.1

of temperature effects in the irradiated fuel. Minor procedure changes have been made for subsequent tests.

PRTR Test 72-1: Irradiation of Zircaloy Corrosion Coupons

An assembly of Zircaloy-2 and -4 corrosion samples was installed on fuel element 6512 in place of a fuel rod in September. The element is being irradiated in PRTR fringe channel 1154 for a planned exposure of 200 or more operating days.

PRTR Test 108: Irradiation of EBWR Cluster

Underwater examination of the EBWR fuel element revealed that one of the two pins that connect the lifting bail to the fuel element basket had dropped out. Irradiation was discontinued until permanent repairs can be made. The fuel element had been in the PRTR since January 26, 1965 and had received 60 MWd of exposure.

PRTR Test 116: Testing of the Pneumatic Facility

Sample exposures and flux measurements were completed in October for the PRTR pneumatic facility. The controlling PRTR operating standard was prepared in November and the facility is ready for routine use.

PRTR Test 124: Fission Gas Pressure Measurement in HPD Fuel Elements During Irradiation

The fission gas pressure measuring elements continue to perform satisfactorily. One hundred four pressure and temperature measurements were made on each of the two test rods in fuel element 6519 located in process channel 1245. The maximum pressure observed was 18 psig and the maximum temperature was 532 °F. Electrical continuity problems continue to limit the number of valid readings obtained from the test rods in fuel element 6520 located in process channel 1548. Thirty-eight pressure readings and 53 temperature readings were obtained for rod #8 while 78 pressure and 62 temperature readings were obtained for rod #7. The maximum pressure observed was 80.5 psig and the maximum temperature was 525 °F observed in rod #7 while the reactor was operating at 51 MW.

PRTR Test 132: Primary Solids Removal

Visual surveillance of crud deposition on fuel elements is a continuing program, with as many as seven elements examined at intervals of 2 to 8 weeks. Thin crud deposits were visible on bands, wires, and some portions of fuel element

rod surfaces. The apparent amount of crud remained essentially constant for the past 3 months. Two very small samples of crud were obtained directly from rod surfaces in November and are being analyzed.

Additional crud surveillance and control is maintained on the primary system with operation of 40 μ and either 10- or 5-μ pore size filters located in three reactor channels. Changes in flow in these channels were effective in signaling the occurrence of crud releases (as occurs following a reactor scram). Large samples of crud were recently obtained from these filters and are undergoing detailed analysis for particle size and identification. A major crud constituent has been identified as magnetic iron oxide. Several small crud samples were also obtained during reactor operation, and they indicated that crud levels in the primary coolant were about 0.1 ppm. Nearly all of the radioactivity in the samples was due to ^{60}Co.

PRTR Test 136: Determination of Maximum Allowable Fuel Rod Specific Power

The purpose of this test is to increase the fuel rod specific power in steps until the fuel centerline temperature limit of 2790 °C (onset of melting) is reached. Efforts on this test were devoted to an investigative study of the previously reported event wherein evidence of fuel melting was found after an irradiation that reached a maximum of 20.2 kW/ft.

A major effort was devoted to the determination of whether there are "real" power differences between the PRTR Ring One process tubes. Measurement of the centering of the process tubes within their shroud tubes was obtained for five of the six Ring One tubes. The results contributed little to the resolution of the question.

Two special fuel bands were irradiated on each of three Ring One fuel elements. The bands were removed and gamma scanned to indicate, from preliminary results, about 2 to 3% difference in tube power.

PRTR Test 140: Calibration RTD's at Ascending Power Levels

The purpose of this test is to calibrate the process tube outlet RTD's at various reactor power levels such that an extrapolation of the process tube differential temperature versus reactor power level will pass through zero delta temperature at zero reactor power. This test also changes from a single RTD to an average of four RTD's for measurement of the process tube inlet temperature.

All padding resistors on the tube outlet RTd's were removed and a successful calibration of differential temperature versus reactor power at several power levels was obtained. New padding resistors were installed as necessary on the central 54 process tubes. Subsequent calibrations indicate that a definite improvement in differential temperature measurements has

resulted and that all major calibration anomolies have been eliminated.

The change from a single RTD to an average of four RTD's for measurement of the process tube inlet temperature has increased the indicated differential temperature by 2 °F.

Work has begun on a computer program that will accept PRTR tube scanner data as input and provide the following output:

1. A plot of tube differential temperature versus reactor power for each process tube.
2. A plot of process tube flow versus the angular position around the lower ring header at which the process tube jumper joins the header.
3. A listing of tube powers by ring as well as the deviation of each tube power about the average for the ring in which the tube is located.

It is planned to run this program during cold startups following scheduled outages to determine calibration errors in the process tube instrumentation.

PRTR Test 142: Irradiation of Pelleted Fuel Elements in Main Core

Following a successful irradiation of a pelleted high power density fuel element in the FERTF, irradiation of this type of element in the main core was begun in September.

6.0 PUBLICATIONS AND PRESENTATIONS

PUBLICATIONS

B. H. Duane. Maximum Likelihood Nonlinear Correlated Fields (BNW Program LIKELY), BNWL-390. Pacific Northwest Laboratory, Richland, Washington, September 1967.

W. A. Reardon and D. E. Christensen. "Depleted Plutonium-Aluminum Alloy Fuel, Nucl. Sci. & Eng. vol 30, no. 2, pp. 222-232. November 1967.

D. R. Skeen and L. J. Page. The Battelle Version of the THERMOS Code, BNWL-516. Pacific Northwest Laboratory, Richland, Washington, September 1967.

D. R. Skeen. The Modified ABH Methods for Tempest, BNWL-515. Pacific Northwest Laboratory.

R. B. Smith. Some Measurements of the Neutron Scattering Law for Light Water at 95 °C, BNWL-345, Pacific Northwest Laboratory, Richland, Washington. August 1967.

PRESENTATIONS

C. H. Bean, R. E. Sharp, and W. J. Bailey. "The EBWR Plutonium Recycle Demonstration Experiment," BNWL-SA-1199, Presented at and to be included in the published proceedings of the IMD-AIME, 1967 Nuclear Metallurgy Symposium on Plutonium Fuels Technology, October 4-6, 1967.

F. G. Dawson, P. H. Kier (ANL, S. Goldsmith, and R. C. Liikala. "EBWR Plutonium Demonstration Experiments," Trans. Am. Nucl. Soc., vol 10, no. 2, pp. 500. 1967.

M. D. Freshley, T. B. Burley, and S. Goldsmith. "Plutonium Fuels Irradiation in PRTR-Present Status," Trans. Am. Nucl. Soc., vol 10, no. 2, p 518. November 1967.

M. D. Freshley and S. Goldsmith. "Operating Experience with Plutonium Fuels in PRTR," Presented at the 1967 AIME Nuclear Metallurgy Symposium on Plutonium Fuels Technology, October 4-6, Phoenix, Arizona.

J. W. Kutcher, R. E. Harris, and R. I. Smith. "Power Tests with the UO_2–2 wt% PuO_2 Batch Core in the PRTR," Trans. Am. Nucl. Soc., vol. 10, no. 2, pp. 517-518. 1967.

R. I. Smith, E. C. Davis, Jr., and L. D. Williams. "Critical Experiments with Phoenix Fuel in a MTR Mockup," Trans. Am. Nucl. Soc., vol. 10, no. 2, pp. 537. 1967.

R. C. Smith and L. G. Faust. "High Exposure Plutonium Studies - Radiation Levels and Power Nuclide Content," Trans. Am. Nucl. Soc., vol 10, no. 2, p. 519. November 1967.

V. O. Uotinen. "Temperature Coefficients of PuO_2-UO_2-H_2O Lattices," Trans. Am. Nucl. Soc., vol 10, no. 2, pp. 564-565. 1967.